HEAT GENERATION CAPABILITIES OF AN EXTERNAL GEAR PUMP AND NEEDLE VALVE

By

GEORGE B. GIBSON

Bachelor of Science

Texas Technological College

Lubbock, Texas

1962

Submitted to the faculty of the Graduate School of
the Oklahoma State University
in partial fulfillment of the requirements
for the degree of
MASTER OF SCIENCE
May, 1963

HEAT GENERATION CAPABILITIES OF AN EXTERNAL

GEAR PUMP AND NEEDLE VALVE

Thesis Approved:

Gerald D. Parker

Thesis Adviser

J. R. Mickelt

Dean of the Graduate School

PREFACE

This thesis represents an experimental study of the heat generation capabilities of an external gear pump and needle valve using the petroleum-base Mil-H-5606 hydraulic oil as the fluid media. The effect of air entrainment upon these heating capabilities was an additional consideration. This study represents a portion of the Boeing Hydraulics Research Project sponsored by the Boeing Airplane Company of Wichita, Kansas.

I wish to thank Dr. J. D. Parker for his continual help in the preparation of this thesis and throughout my graduate study. I also wish to acknowledge the assistance of the Mechanical Engineering staff, especially George Cooper, John McCandless, and L. S. Benjamin.

Finally, I will always be grateful for the continued encouragement and patient understanding of my family throughout my university career.

TABLE OF CONTENTS

LIST OF TABLES

LIST OF FIGURES

LIST OF PLATES

CHAPTER I

INTRODUCTION

The problems of hydraulic system overheating are definitely not new, but with the development and application of higher performance fluid power systems the problems have become increasingly significant. In past years most systems had relatively low flow rates and pressure drops; thus, system overheating was not an area of great concern. However, the rapid technological advancements of recent years, particularly in the aircraft, missile, and space-vehicle industries, have considerably altered this viewpoint regarding fluid power systems.

The present trend in the development of fluid power systems is toward higher output and smaller over-all package size. To be more specific, this implies increased mass flow rates, higher pressure drops, and reduced weight and surface area. In such high performance systems, overheating problems can manifest themselves in many areas. Excessive temperatures can critically affect system contamination and reliability, pump cavitation and life, foaming and oil deterioration, and reservoir pressurization requirements (1).

In general the heat generated within a hydraulic system is a direct result of viscous drag and system throttling, whereby the mechanical energy introduced into the system by the pump is converted to thermal energy. This conversion of energy occurs throughout the system, especially in components such as pumps, motors, and relief

valves. Thus, the "heat generation capability" of a particular component refers to its capability of converting a portion of the mechanical energy imparted to it into thermal energy. However, not all heat is generated within the system itself. The system environment may also be a major contributor in certain applications. A simple illustration of environmental influence is the heat input to a hydraulic pump mounted within the jet engine housing of an aircraft. Large amounts of heat could be conducted through the pump mounts and casing, while heat transfer could occur through radiation as a result of the high temperature surroundings. Similarly, convective heat transfer would be possible due to the large mass of air moving through the hot engine and past the pump.

Another problem closely connected with system overheating is air entrainment within the fluid itself. Again, the problem areas of system reliability, pump cavitation, pump life, oil deterioration, and reservoir pressurization are affected.

The objectives of this thesis are: first, to determine and analyze the heat generation capabilities of two basic hydraulic components--the gear pump and the needle valve--and, secondly, to determine the effect of air entrained within the fluid upon these heat generation capabilities.

CHAPTER II

PREVIOUS INVESTIGATIONS

The development and application of high performance hydraulic systems and the associated overheating problems have become significant in only the last few years. The research done on the thermal considerations of hydraulic components is therefore relatively limited. Even those articles that deal with the overheating problem specifically tend to be of a qualitative rather than quantitative nature, preferring to discuss in rather general terms the causes and effects of overheating, component selection, and heat exchanger design. Seldom are there included any fundamental relationships or design data which the engineer may use to analyze and design properly a fluid power system from a thermal viewpoint. Similar statements may be made concerning the effect of air in hydraulic systems.

Wittren (2) discusses hydraulic system overheating only in general terms and suggests several techniques to reduce heat generation within the system itself. Much of his discussion deals with the proper selection of components such as pumps, motors, actuators, fluid lines, and control valves. Useful design information is given in his discussion of optimum reservoir shapes and internal circulation methods. Spherical, cylindrical, and rectangular shaped reservoirs were studied with the latter having the better cooling capacity. Placing baffles within the reservoir itself or putting indentations in

the reservoir walls was found to increase the heat-transfer rate by introducing turbulence into the oil circulation. Oil-to-water coolers were stated as being more compact and less subject to fouling than the oil-to-air heat exchanger although the latter was considered the more practical in the upper range of operating temperatures near 200° F.

Douglas (3) divided the component heat generation problem into the following classifications: auxiliary pumps, power pumps, pipes, directional valves and fittings, and throttling devices which he defined as any device causing a restriction greater than that normally caused by piping. Actual experimental data was included on heat generation within these five classifications. Heat generation per 100 psi for various efficiencies was plotted versus flow rates for both the auxiliary and power pumps. Viscous heat generation within piping was plotted against flow rate for various pipe diameters with the fluid being an oil of 200 SSU viscosity. Throttling devices, along with the directional valves and fittings, were equated to a corresponding pipe length, and the heating effect was determined from that information already developed for piping losses.

Containing experimental work very similar to that of Douglas was an engineering report published by Racine Hydraulics and Machinery, Incorporated (4). Again, the heat generation problem was divided into specific areas: external heated sources, volume control valves, pressure control valves, pumps and fluid motors, piping, and directional control valves. Variable displacement pumps as well as fixed displacement pumps and motors were included in the heating analysis. Instead of relating pressure and volume control valves to an equivalent pipe

length as did Douglas, the report directly illustrated the relationship of heat generation to differential pressure for various flow rates.

The study of hydraulic system overheating by Magnus (1) was purely analytical. He related a temperature increase to a differential pressure with component efficiency and fluid properties as parameters. Introduced was a term Magnus designated as "bypass ratio" in which he took into account the effect of recirculating the bypass portion of fluid of a relief valve on the system temperature. Magnus also felt that the conservative approach to the thermal design of a system was to consider that all pump input power was converted to heat by the system and must eventually be rejected as heat. In high performance systems heat exchangers are generally required for adequate heat dissipation as the convection, conduction, and radiation heat-transfer rates are often insufficient to maintain the desired operating temperatures.

Associated with the problem of system overheating is that of air entrainment within a fluid power system, yet no concentrated effort has been made to determine the effect of air on system performance from a thermodynamic viewpoint. Questions concerned with the nature of the compression process of the air, the exchange of energy between the air and surrounding oil, and the effect upon component efficiency are often brought forth but seldom answered. Instead, most of the work has concerned itself with the problems of solubility and cavitation.

In studying fluid effects on system performance, LeRoy and Leslie (5) mentioned the dissolved-air problem. Data concerning the solubility of air in various liquids under equilibrium conditions are included. The hydraulic oil Mil-H-5606 was found to have the highest

solubility of the liquids tested. This particular oil was found to contain 10% air by volume under test conditions of 32°F. and one atmosphere of pressure. No information was included on the factors affecting the rate of solution of gases in fluids.

MacKenzie and Smith (6) performed tests on petroleum base and water base fluids by mixing air and a measured amount of fluid and holding the mixture under pressure on the air side of a piston accumulator. Upon completion of a test, the undissolved air was released from the accumulator and the remaining oil-air mixture was placed into a flask. Further processing determined the amount of air dissolved in the oil. Most of the tests were run over a period of 24 hours; however, one was run for 4 months at 2000 psi indicating 461 milliliters of air to 1000 milliliters of fluid.

Firth (7), in studying the effect of entrained air on fluid bulk modulus, found that the addition of air to oil noticeably decreased the bulk modulus. Several tests were run on an oil-air mixture for various amounts of entrained air. Oil containing no air was found to decrease in volume 1% at a pressure of 2000 psi, while the same oil containing 10% air (by volume) indicated a reduction in volume of 11% at the same pressure level. A similar study was made by Smith, Peeler, and Bernd (8).

The effect of air entrainment upon cavitation can be indirectly related to component heat generation through efficiency. In an investigation of hydraulic noise Louthan (9) found that pump inlet pressure waves were violently increased with air dissolved or entrained in the fluid. In discussing the relationship between oil-air mixtures and hydraulic noise, Louthan defined several degrees of association of

the two substances:

1. Entrained air in large bubbles (diameter greater than 0.330 inches) in which the air and oil are essentially separate. This condition of having the air coarsely and unevenly distributed causes extreme pump cavitation.
2. Entrained but dispersed air with no sizable bubbles. This is normally the accepted state of the pump inlet obtainable by careful tank design and pressurization to minimize bubble growth between the tank and pump. Cavitation is considerably reduced.
3. Oil saturated with dissolved air only. This state is difficult to obtain with rapid circulation of a limited quantity of oil.
4. An unsaturated solution of air in oil. Such a condition is generally restricted to the high pressure portion of the system.

To keep the dissolved air from separating out, Louthan suggested using a pressurized pump inlet. Although his analysis concerns itself primarily with hydraulic noise and cavitation, the implications relative to system heating are evident. The presence of air within the system and the occurrence of cavitation effectively reduce the efficiency of a hydraulic pump resulting in a greater conversion of mechanical energy to thermal energy. Not only is the actual amount of oil pumped considerably reduced, but the cavitation phenomena produces an undue amount of wear on the individual pump parts resulting in shorter component life and poorer mechanical efficiency.

In studying cavitation in reciprocating and rotary pumps, Pigott (10) introduced air into a spur gear pump having a glass front through which high-speed photographs of the pumping process were taken. The

photographs indicated that small bubbles present at the pump inlet were centrifuged into large bubbles located in the roots of the gear teeth, and these large bubbles were not materially reabsorbed on the discharge side. However, the centrifuging was found to be minor when pumping a heavy crude, and the bubbles remained fine and were largely absorbed on discharge.

Schanzlin (11) commented on the heating effect resulting from the compression of entrained air and made additional mention of the centrifuging process previously spoken of in Pigott's study. Schanzlin's work is further discussed in Chapter III.

CHAPTER III

ANALYTICAL CONSIDERATIONS

As previously mentioned Magnus (1) states that the conservative approach to the thermal design of a system is to consider that all the pump input power is converted to heat by the various system components and must eventually be rejected as heat. In essence this is a restatement of the First Law of Thermodynamics which states that in a closed system executing a cycle the net work input is proportional to the net heat output (12). Written quantitatively, the First Law states

$$\oint dW = J \oint dQ \tag{1}$$

where

$\oint dW$ = work input during the cycle,

$\oint dQ$ = heat output during the cycle,

J = proportionality constant, and

$\oint$ = the cyclic integral.

In terms of the rates at which work is done and heat is transferred across the boundary of the system, Equation 1 can be written as

$$\oint \dot{W} = J \oint \dot{Q} \tag{2}$$

where

$\dot{W}$ = power input, and

$d\dot{Q}$ = rate of heat transfer.

The typical hydraulic system illustrated in Figure 1 is a direct application of Equation 1 and Equation 2. The pump introduces a given amount of mechanical energy into the system, and this energy is used to provide useful work such as turning a shaft or is dissipated in the form of thermal energy at various stations in the system. The First Law as stated above applies only to cyclic processes; however, the application of the First Law to non-cyclic processes yields

$$\dot{Q} - \dot{W} = \Delta\dot{E} \tag{3}$$

where

$\Delta\dot{E}$ = rate of change of the system energy.

Equation 3 is often considered an alternate way of expressing the First Law. Applying Equation 3 to the system of Figure 1 necessitates the increase in the energy of the system if the heat-transfer rates are insufficient to maintain cyclic operation. Such an increase in energy usually manifests itself as a rise in system temperature. The temperature rise continues until the temperature difference between the system and the environment is sufficiently large to enable the heat transfer rate to equal the input of mechanical energy. Heat exchangers are required if it is desired to maintain operating temperatures below the equilibrium temperature.

Of interest in the investigation are the capabilities of the individual components, primarily the gear pump and the needle valve, to convert mechanical energy to thermal energy. Gear pumps are generally separated into two broad categories: external gear pumps and internal gear pumps. The following analysis will largely concern

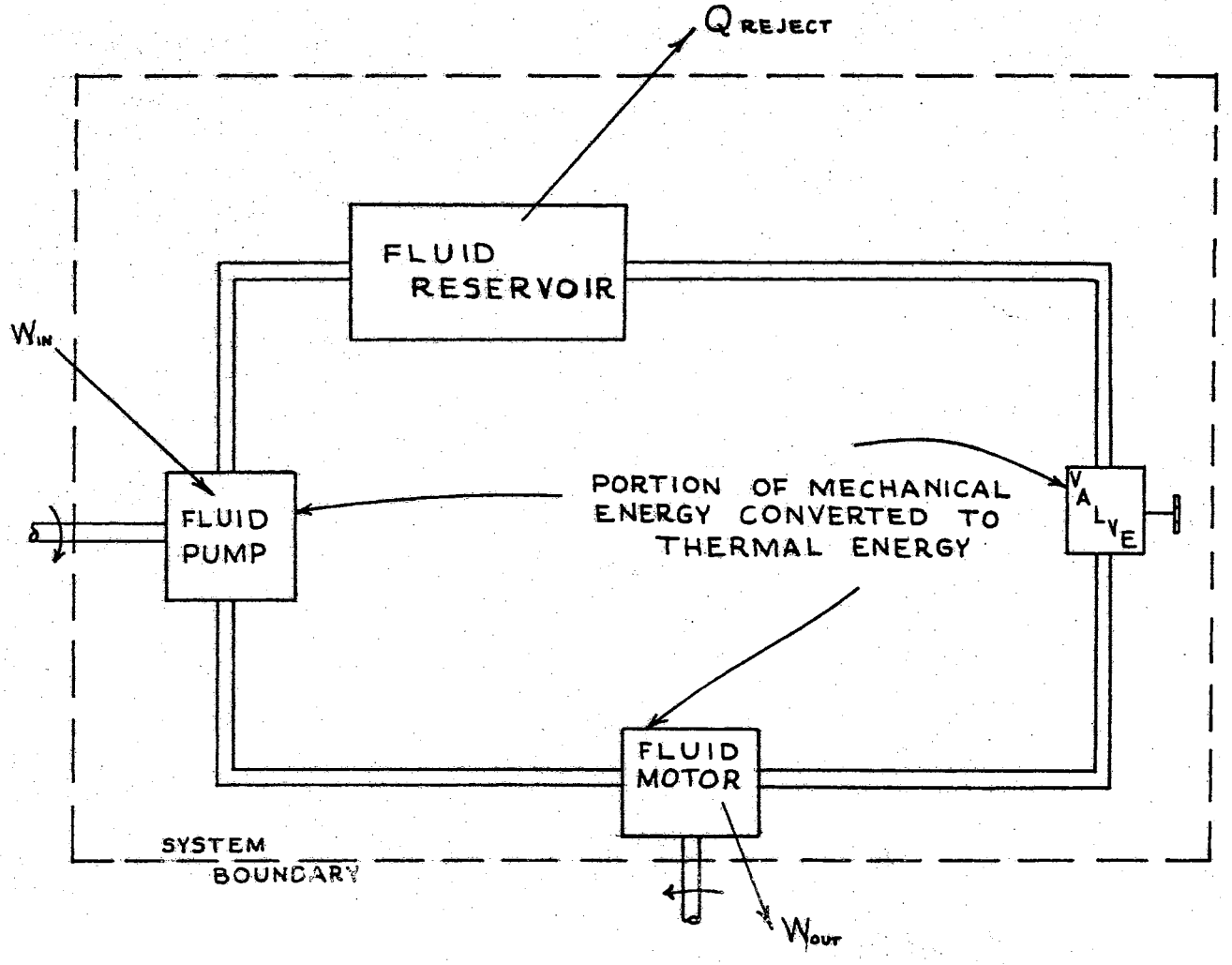

Figure 1. Application of First Law to Typical Hydraulic System

itself with the standard, external, spur gear pump as shown in Figure 2. However, the relationships developed are applicable to the pumping process in general and are not restricted solely to gear pumps.

In the external gear pump the gears are suitably housed to give very small clearances on both sides and around the periphery of the gears. Oil entering the pump is trapped between the rotating teeth and the housing and is carried around the periphery of the revolving gears to the discharge side. When the teeth reach the meshing position, the oil is forced to enter the pressure lines of the system.

An open flow system through which fluid passes under steady-flow conditions is called a steady-flow system, and the energy of the open-system remains constant as long as steady-flow conditions prevail (12). An energy balance applied to a steady-flow system, such as that of Figure 3, states

[Net amount of energy to system as heat or work for a given time interval] + [Stored energy of mass entering system for the same time interval] - [Stored energy of mass leaving system for the same time interval] = 0 (4)

Written symbolically, Equation 4 appears as

$$\mathring{Q} - \mathring{W} + \mathring{m}p_1v_1 - \mathring{m}p_2v_2 + \mathring{E}_1 - \mathring{E}_2 = 0 \tag{5}$$

where

$\mathring{Q}$ = net amount of heat added to the system for a given time interval,

$\mathring{W}$ = net amount of work, excluding flow work, done by the system for the same time interval,

$\mathring{m}p_1v_1$ = amount of flow work on the system by the entering fluid for the interval,

$\mathring{m}p_2v_2$ = amount of flow work done by system or fluid leaving,

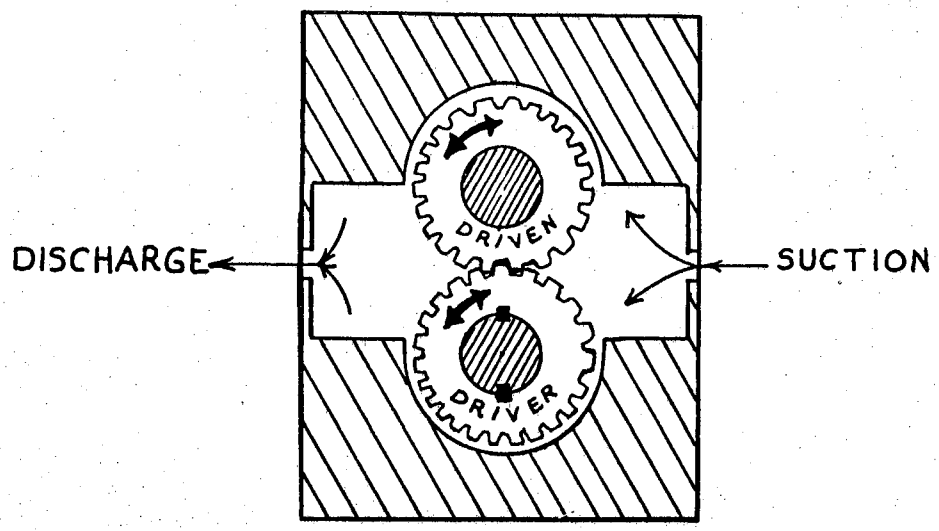

Figure 2. Standard External Spur Gear Pump

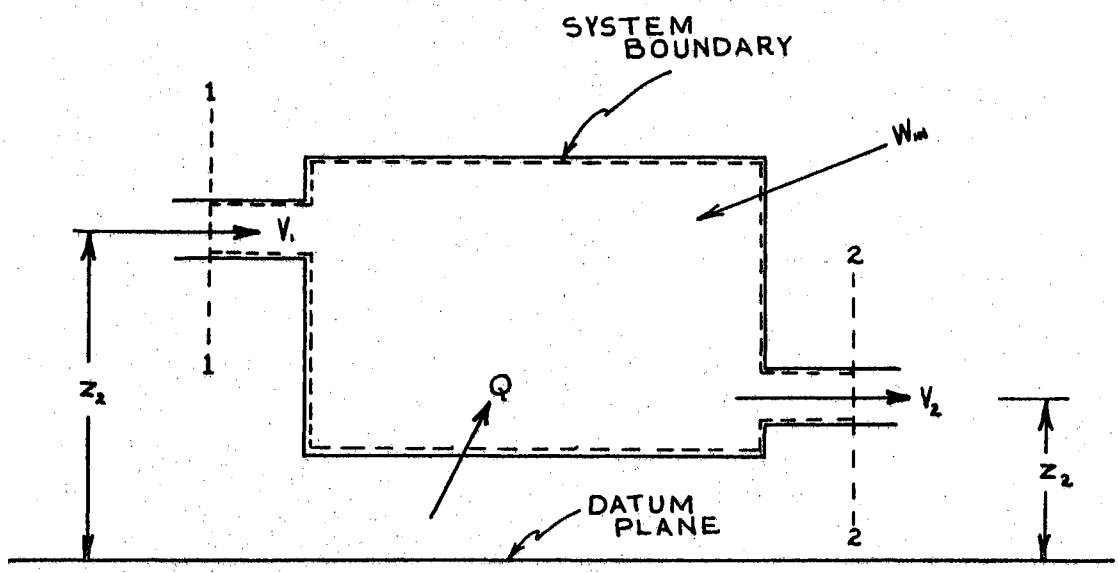

Figure 3. General Steady-Flow System

$\dot{m}$ = mass rate of fluid flow,

p = pressure,

v = specific volume,

$\dot{E}_1$ = stored energy rate of fluid entering the system,

$\dot{E}_2$ = stored energy rate of fluid leaving the system.

The energy term (neglecting the effects of electricity, magnetism, and surface tension may be written as

$$\dot{E} = \dot{m}(u + \frac{V^2}{2g_c} + \frac{g}{g_c} z) \tag{6}$$

where

u = internal energy,

V = average velocity of the fluid,

z = elevation above an arbitrary datum,

g = gravitational acceleration.

Substituting Equation 6 into Equation 5, collecting terms, and rewriting yields

$$\dot{Q} + \dot{W}_{in} = \dot{m}(u_2 - u_1) + \dot{m}(p_2v_2 - p_1v_1) + \dot{m}(\frac{V_2^2 - V_1^2}{2g_c}) + \dot{m}\frac{g}{g_c}(z_2 - z_1). \tag{7}$$

In the thermal analysis of the pump, the kinetic and potential energy terms are negligible and, therefore, are disregarded. Also, it is assumed that adiabatic conditions prevail. By recalling that

$$h = u + pv \tag{8}$$

where

h = enthalpy,

and remembering the previous assumptions, Equation 7 can be written as

$$\dot{W}_{in} = \dot{m}(h_2 - h_1) = \dot{m}(u_2 - u_1) + \dot{m}(p_2v_2 - p_1v_1). \tag{9}$$

The enthalpy for the liquid varies as a function of both pressure and temperature; therefore, the change in enthalpy in Equation 9 can be expressed as

$$\Delta h = \Delta h_p + \Delta h_t \tag{10}$$

where

Δh_p = enthalpy change at constant pressure.

Δh_t = enthalpy change at constant temperature.

The specific heat at constant pressure is defined as

$$C_p = \left(\frac{\partial h}{\partial t}\right)_p . \tag{11}$$

Therefore, it can be stated that

$$(h_2 - h_1)_p = \int C_p dt = C_p(t_2 - t_1) \tag{12}$$

where

C_p is considered to remain constant with respect to temperature.

In the determination of the change in enthalpy at constant temperature, the relation

$$\left(\frac{\partial h}{\partial p}\right)_t = v - t\left(\frac{\partial v}{\partial t}\right)_p \tag{13}$$

is useful. Integration with respect to pressure produces

$$(h_2 - h_1)_t = v(p_2 - p_1) - t\left(\frac{\partial v}{\partial t}\right)_p (p_2 - p_1). \tag{14}$$

The $t\left(\frac{\partial v}{\partial t}\right)(p_2 - p_1)$ term is small and can be neglected (Appendix A). Therefore, the power input can be expressed as

$$\dot{W}_{in} = \dot{m}C_p(t_2 - t_1) + \dot{m}v(p_2 - p_1). \tag{15}$$

Analysis of the energy equation states that the pump work done on a mass of incompressible fluid in a reversible and adiabatic process during a given time interval is

$$\dot{W}_{in} = \dot{m}v(p_2 - p_1) . \tag{16}$$

Again, the kinetic and potential energy terms are neglected. The power input denoted by Equation 16 is the ideal amount required. If the overall pump efficiency is represented by η_o, the actual power input to the system is

$$\dot{W}_{in} = \frac{\dot{m}v(p_2 - p_1)}{\eta_o} . \tag{17}$$

Substituting the above relationship into Equation 15 and solving for temperature change across the pump results in

$$t_2 - t_1 = \frac{v(p_2 - p_1)}{c_p}\left(\frac{1 - \eta_o}{\eta_o}\right). \tag{18}$$

In terms of specific gravity, Equation 18 becomes

$$t_2 - t_1 = \frac{(p_2 - p_1)}{62.4\ c_p \gamma}\left(\frac{1 - \eta_o}{\eta_o}\right) \tag{19}$$

where

γ = specific gravity,

$62.4 \frac{lb_m}{ft^3}$ = density of water.

Thus, for a given pressure differential and constant fluid properties the thermal rise across a pump increases as the efficiency decreases.

The actual effect of entrained air on the heat generation capabilities of a gear pump is difficult to describe analytically for little is known concerning the energy interchange between the compressed liquid and air. Schanzlin (11) states that the temperature of the compressed air bubbles is somewhere between that achieved by isentropic compression and that by isothermal compression. Actually, the temperature of the bubbles is governed by the rate of air solubility, rate of compression, and heat absorption by the fluid. For compression occurring over a substantial time interval, the process would approach an isothermal condition; however, a rapid compression much like that taking place in the pump would approach the isentropic process. Regardless of the nature of the compression, Schlanzin found that the compressed air increased the reservoir oil temperatures as much as 25% of its original value in certain applications, and these elevated temperatures became sufficient to damage pump parts and oxidize the adjacent oil.

In describing the pumping process on the oil-air mixture, it is assumed that the work accomplished is done on the air and the oil separately, and that the individual processes are performed isentropically.

Thus,

$$\dot{W}_t = \dot{m}_o \int_{p_1}^{p_2} v\,dp + \dot{m}_a \int_{p_1}^{p_2} v\,dp \tag{20}$$

where

$\dot{W}_t$ = ideal pump input power,

$\dot{m}_o$ = mass flow rate of oil,

$\dot{m}_a$ = mass flow rate of air.

The specific volume term of the oil is considered constant and may be removed from the integral; however, the specific volume and pressure of the air are related by the assumed isentropic relationship

$$pv^k = C \tag{21}$$

where

C = constant, and

k = ratio of the specific heat at constant pressure to the specific heat at constant volume.

Isentropic compression was assumed as this would result in the largest temperature increase and heating effect. Solving Equation 21 for the specific volume and substituting in Equation 20 yields

$$\dot{W}_t = \dot{m}_o v_o \int_{p_1}^{p_2} dp + \dot{m}_a \int_{p_1}^{p_2} \frac{C^{1/k}}{p^{1/k}}\,dp \,. \tag{22}$$

Introduction of the efficiency term, integration, and simplification results in

$$\dot{W}_{act} = \frac{\dot{m}_o v_o (p_2 - p_1)}{\eta_o} + \frac{\dot{m}_a k}{\eta_o (k - 1)} \left(\frac{p_2}{\rho_2} - \frac{p_1}{\rho_1} \right) \tag{23}$$

where

$\dot{W}_{act}$ = actual power input to the oil-air mixture

ρ = density of the air.

In terms of the temperature difference, the actual power input to the pump can be expressed as

$$\dot{W}_{act} = \dot{m}_o c_{po} (t_2 - t_1) + \dot{m}_o v_o (p_2 - p_1) + \dot{m}_a c_{pa} (t_3 - t_1) \tag{24}$$

where the final temperature of the air due to compression, t_3, is different from the final oil temperature, t_2.

Equating Equation 23 and Equation 24 and dividing by $\dot{m}_o$ yields

$$\frac{v_o (p_2 - p_1)}{\eta_o} + \frac{\dot{m}_a}{\dot{m}_o} \frac{k}{\eta_o (k-1)} \left(\frac{p_2}{\rho_2} - \frac{p_1}{\rho_1} \right) = c_{po} (t_2 - t_1) + \tag{25}$$

$$v_o (p_2 - p_1) + \frac{\dot{m}_a}{\dot{m}_o} c_{pa} (t_3 - t_1).$$

Several comments can be made in regard to Equation 25. First, the term $\frac{\dot{m}_a}{\dot{m}_o}$ is generally an exceedingly small number; therefore, the quantities in which $\frac{\dot{m}_a}{\dot{m}_o}$ are included can be neglected with very little error. Sample calculations in Appendix A illustrate this point. Secondly, Equation 25 can be reduced to Equation 19 upon

neglecting the terms multiplied by $\frac{\dot{m}_a}{\dot{m}_o}$. Third, the effect of air within the system can be directly linked with the efficiency term. The volumetric efficiency will decrease with increasing amounts of entrained air, and a greater temperature rise across the pump is associated with this reduction in efficiency. A portion of the pump work originally used to raise the oil to a desired pressure level is now being expended in compressing the air. Thus, more work is required to bring the system up to its operating pressure. This inefficiency within the pump is manifested as a greater temperature increase due to the greater change of mechanical energy to thermal energy.

The previous discussion has been concerned with the temperature differential resulting from the pumping process, yet it must be remembered that within the pump itself even higher temperatures and pressures can be developed than those evident at the discharge. Pigott (10) found that entrained air produced a centrifuging process in gear pumps whereby small bubbles present at the pump suction were centrifuged into large bubbles locating themselves in the roots of the gear teeth. Thus, local compression of the air and oil upon gear meshing produced local pressures and temperatures of magnitudes much higher than actually observed. Such local compression processes can help explain system failures and oil deterioration, while the actual overall bulk temperature differential would indicate safe operation.

Figure 4 illustrates the temperature differential developed across a pump for various pressure differentials, as determined by

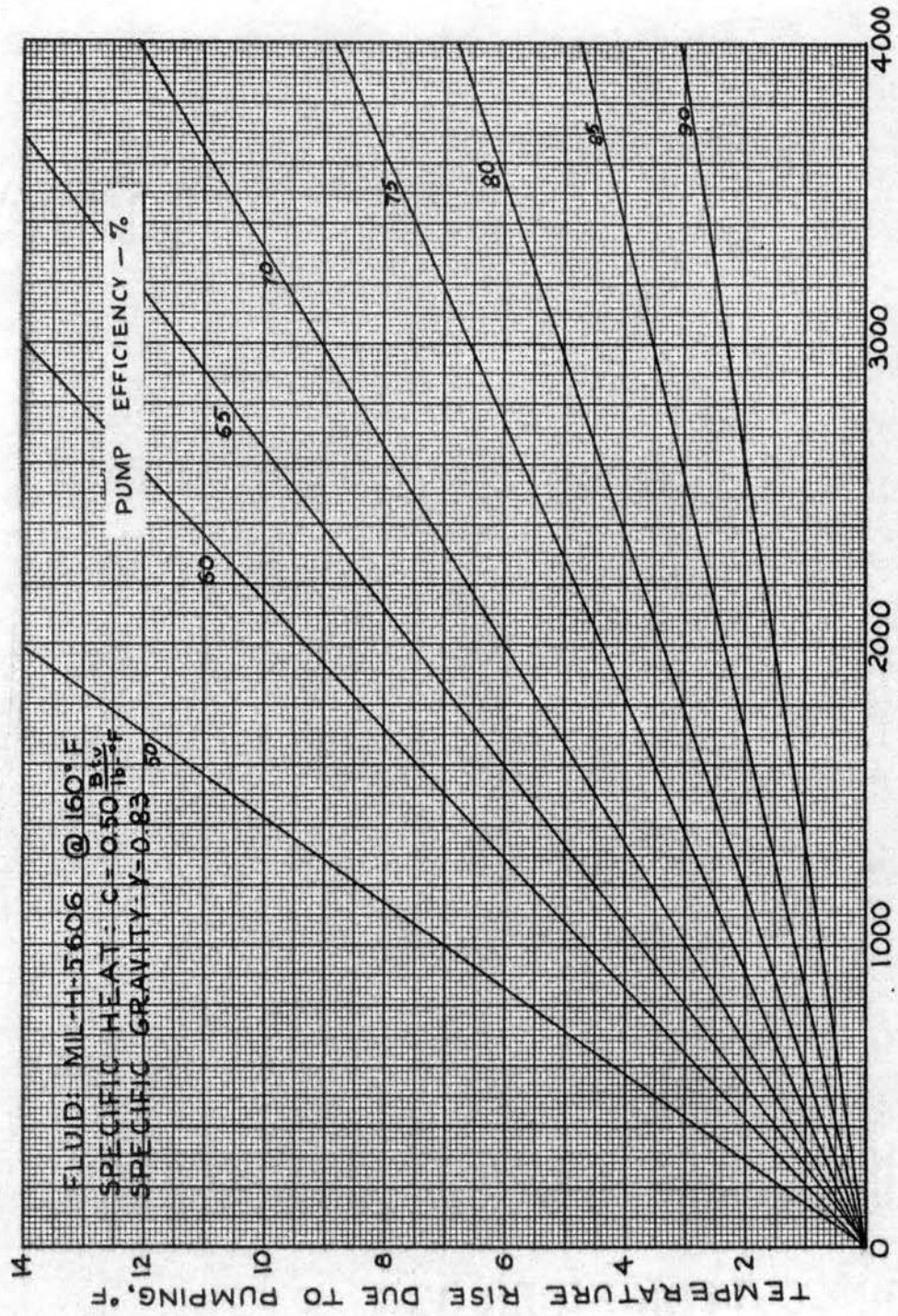

Figure 4. Theoretical Temperature Rise Due to Pumping

Equation 19. The fluid considered is Mil-H-5606 with a specific heat of 0.50 $\frac{\text{Btu}}{16 - {}^{\circ}\text{F}}$, and a specific gravity of 0.83 at 160° F (1).

The temperature rise resulting from control valve and system throttling can also be determined by considering Equation 15. Since it is assumed that no heat or work cross the boundary and that the kinetic and potential energy terms are negligible or zero, the relationship reduces to

$$C_p(t_2 - t_1) = v(p_1 - p_2) \quad . \tag{26}$$

Solving for the temperature change and introducing specific gravity term results in

$$t_2 - t_1 = \frac{(p_1 - p_2)}{62.4\ c_p \gamma} \quad . \tag{27}$$

Thus, the temperature rise due to valve throttling is directly proportional to the pressure drop considering constant fluid properties. If air is considered, then

$$\dot{m}_o c_{po}(t_2 - t_1) + \dot{m}_a c_{pa}(t_3 - t_1) = \dot{m}_o v(p_1 - p_2) \quad . \tag{28}$$

Dividing Equation 28 by $m_o c_{po}$ yields

$$t_2 - t_1 + \frac{\dot{m}_a c_{pa}}{\dot{m}_o c_{po}}(t_3 - t_1) = \frac{v}{c}(p_1 - p_2) \tag{29}$$

Again, the $\frac{\dot{m}_a}{\dot{m}_o}$ term is so small that the term introduced by a

consideration of the air may be neglected. This may be seen from the sample calculation included in Appendix A. If an adiabatic expansion of the air through the valve is assumed, a temperature drop occurs. Actually, the temperature lies somewhere between that temperature resulting from an isentropic expansion and that resulting from an isothermal process. Neglecting the air in the system reduces Equation 29 to the form of Equation 27. The temperature rise due to the throttling process of a valve is shown in Figure 5 for Mil-H-5606 oil having the same properties as previously stated.

Although the effect of recirculating fluid spilling over a relief valve back to the pump inlet was not experimentally determined in this investigation, mention should be made of this phenomena. Magnus made use of the term "bypass ratio", which he defined as

$$BR = \frac{\mathring{m}_4}{\mathring{m}_3} \tag{30}$$

where

BR = bypass ratio,

$\mathring{m}_3$ = system mass flow for a given time interval, and

$\mathring{m}_4$ = bypass mass flow for the same time interval.

Considering the system of Figure 6, it may be said

$$\mathring{m}_2 c_p t_2 = \mathring{m}_4 c_p t_4 + \mathring{m}_1 c_p t_1 \tag{31}$$

where

$\mathring{m}_2 = \mathring{m}_1 + \mathring{m}_4$, and

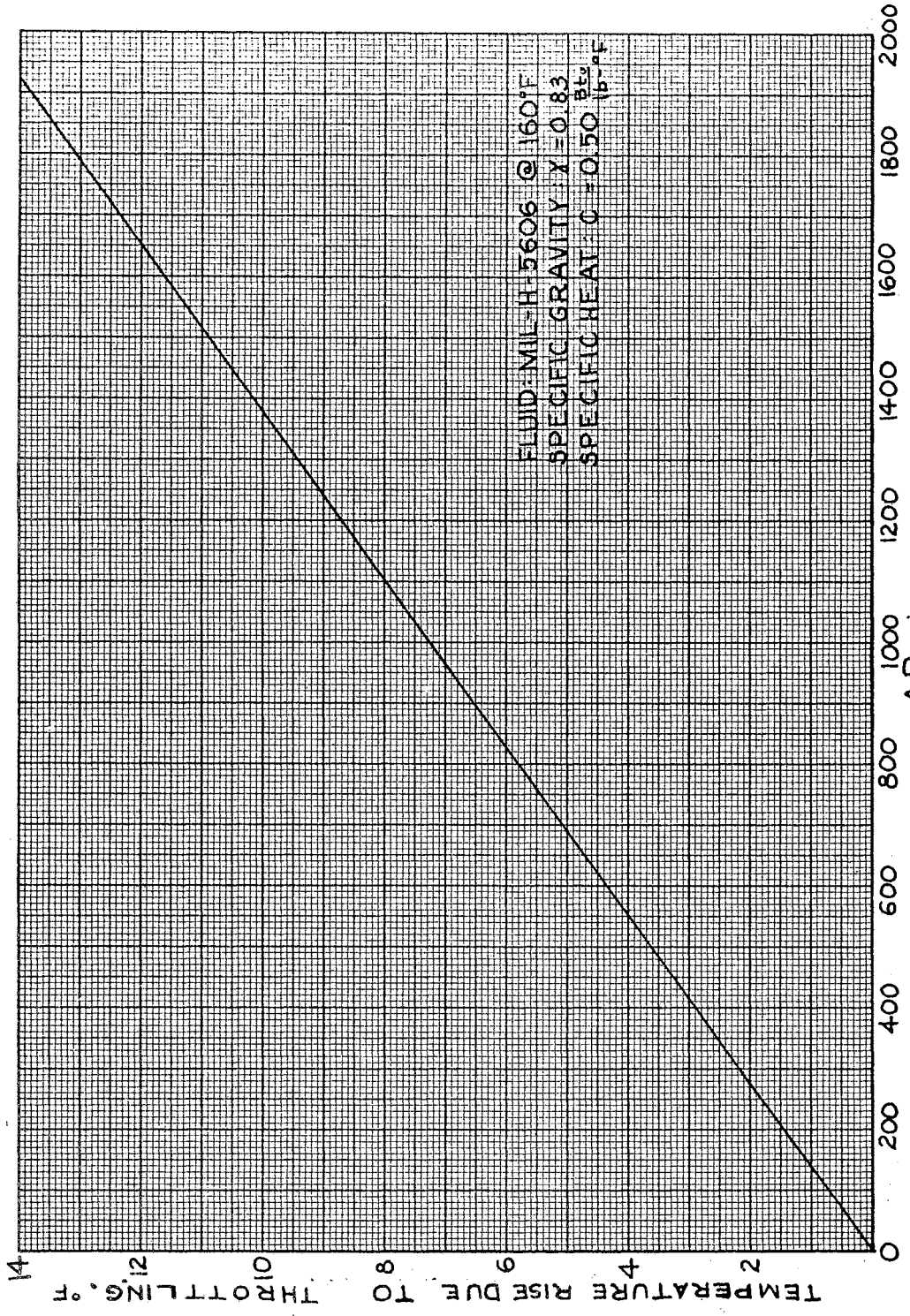

Figure 5. Temperature Rise Due to Throttling Process of a Valve

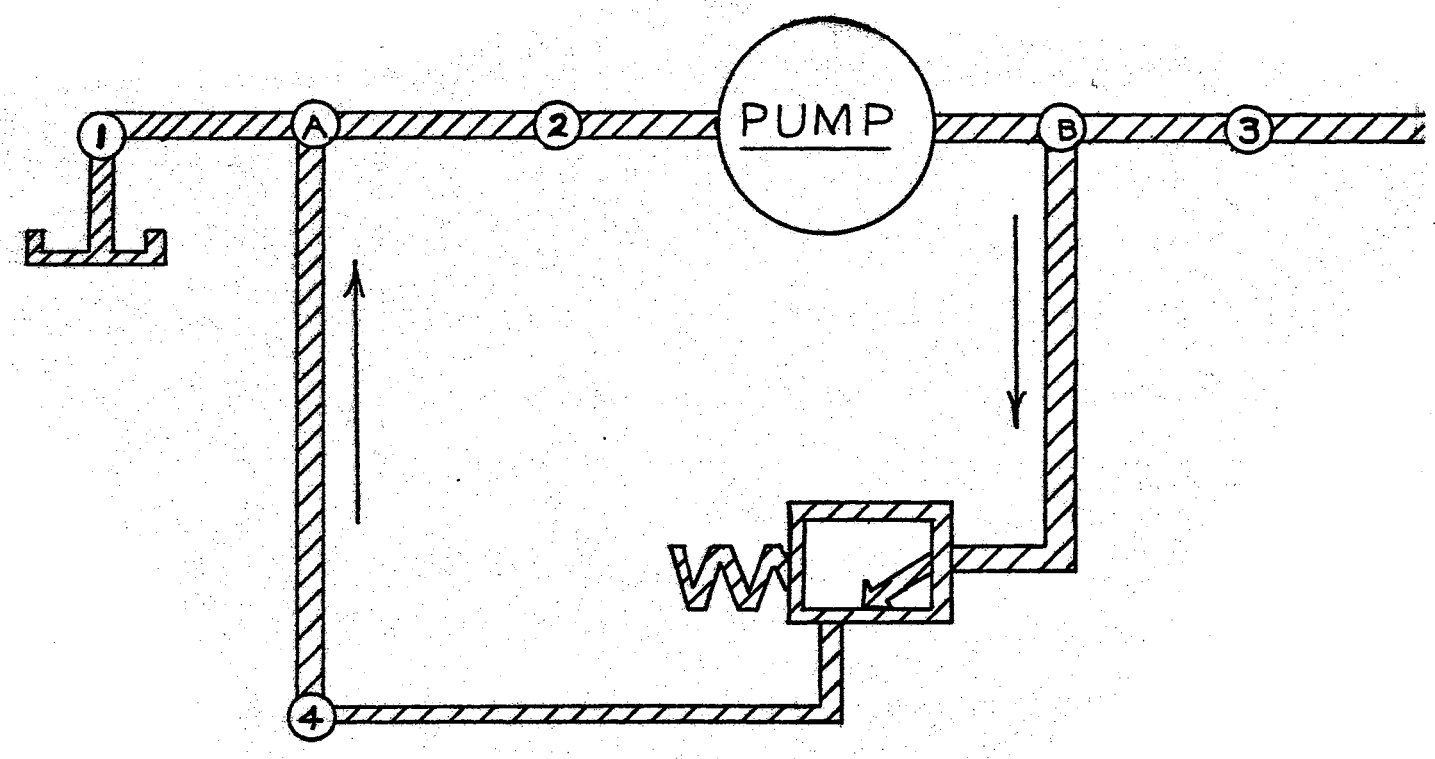

Figure 6. System Pump and Recirculating Relief Valve

$$m_1 = m_3 .$$

Removing c_p from Equation 31 and substituting for $\dot{m}_2$ and $\dot{m}_1$ results in

$$(\dot{m}_1 + \dot{m}_4)t_2 = \dot{m}_4 t_4 + \dot{m}_1 t_1 \tag{32}$$

which can be reduced to

$$t_2 - t_1 = \frac{\dot{m}_4}{\dot{m}_3}(t_4 - t_2) = BR\left[(t_4 - t_3) + (t_3 - t_2)\right] . \tag{33}$$

Equation 19 and Equation 27 applied to the system of Figure 6 and substituted into Equation 33 yield

$$t_2 - t_1 = BR\left[\frac{(p_3 - p_4)}{62.4 \gamma c_p} + \frac{(p_3 - p_2)}{62.4 \gamma c_p}\left(\frac{1 - \eta_o}{\eta_o}\right)\right] . \tag{34}$$

However, since p_2 equals p_4, Equation 34 becomes

$$t_2 - t_1 = BR\left[\frac{(p_3 - p_2)}{62.4 \gamma c_p \eta_o}\right] . \tag{35}$$

Thus, Equation 35 indicates the temperature rise at pump inlet due to recirculating a portion of the high pressure fluid through a relief valve.

Since the pump inlet temperature increases due to recirculation of the fluid, the pump outlet temperature must also rise. Adding the temperature rise across the pump to the elevated pump inlet temperature obtains the outlet temperature; quantitatively, this states that

$$t_3 - t_1 = (t_3 - t_2) + (t_2 - t_1) = \frac{(p_3 - p_2)}{62.4\gamma c}\left(\frac{1 - \eta_o}{\eta_o}\right) + BR\left[\frac{(p_3 - p_2)}{62.4\gamma c_p \eta_o}\right] \quad (36)$$

which may be simplified to

$$t_3 - t_1 = \frac{(p_3 - p_2)}{62.4\gamma c_p}\left[\frac{BR + 1 - \eta_o}{\eta_o}\right] . \quad (37)$$

Figure 7 illustrates pump inlet temperature rise as a function of the "bypass ratio" for Mil-H-5606 (1).

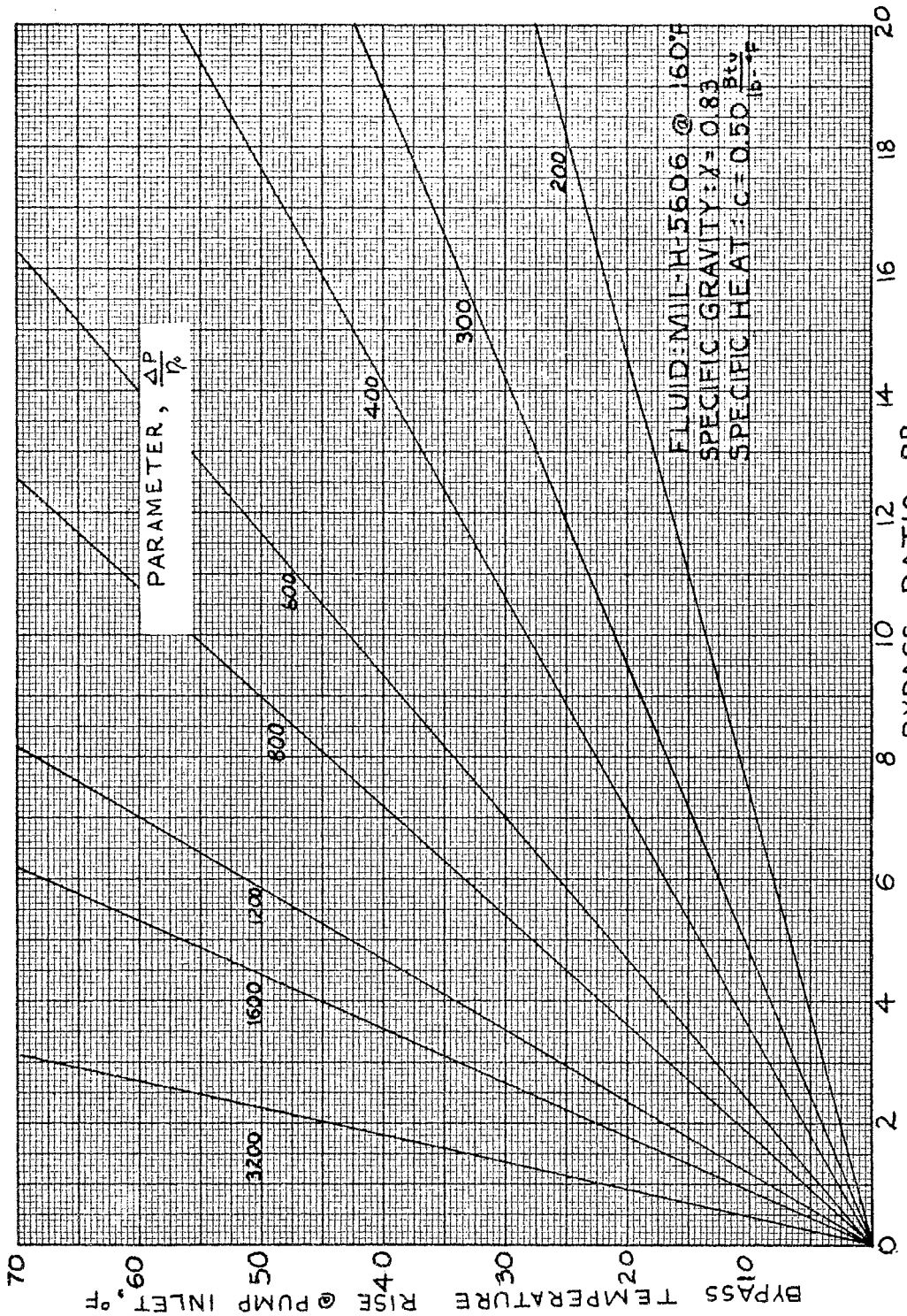

Figure 7. Temperature Rise at Pump Inlet Due to Recirculating a Portion of the Fluid

CHAPTER IV

EXPERIMENTAL APPARATUS AND PROCEDURE

The hydraulic power stand designed for the Boeing Hydraulic Circuit research project was modified in order to determine the heat generation capabilities of the basic pump and valve. The power stand was capable of system pressures up to 2000 psi and a maximum flow rate of 13.8 gpm. Pressure control was possible through the use of a pilot-operated pressure relief valve. System flow rates were governed through a volume control valve; however, proper settings of the afore-mentioned relief valve and the tested throttling valve performed essentially the same function. Desired flow rates were best obtained through correct adjustment of each of the three valves simultaneously. Temperature control of the circulating oil, the general purpose Mil-H-5606 petroleum base hydraulic oil common in most aircraft systems today, was exercised by the utilization of an oil-water heat exchanger within the system. The power stand itself is shown in Plate I, while the schematic is shown in Figure 8.

As noted in Equation 19, the efficiency term is of vital importance in determining the thermal rise across a pump. The overall pump efficiency was determined through measuring motor input, approximating motor efficiency, and measuring pump output rather than a dynamometer test on the pump alone. The reasons for determining the efficiency in such a

PLATE I. HYDRAULIC POWER STAND

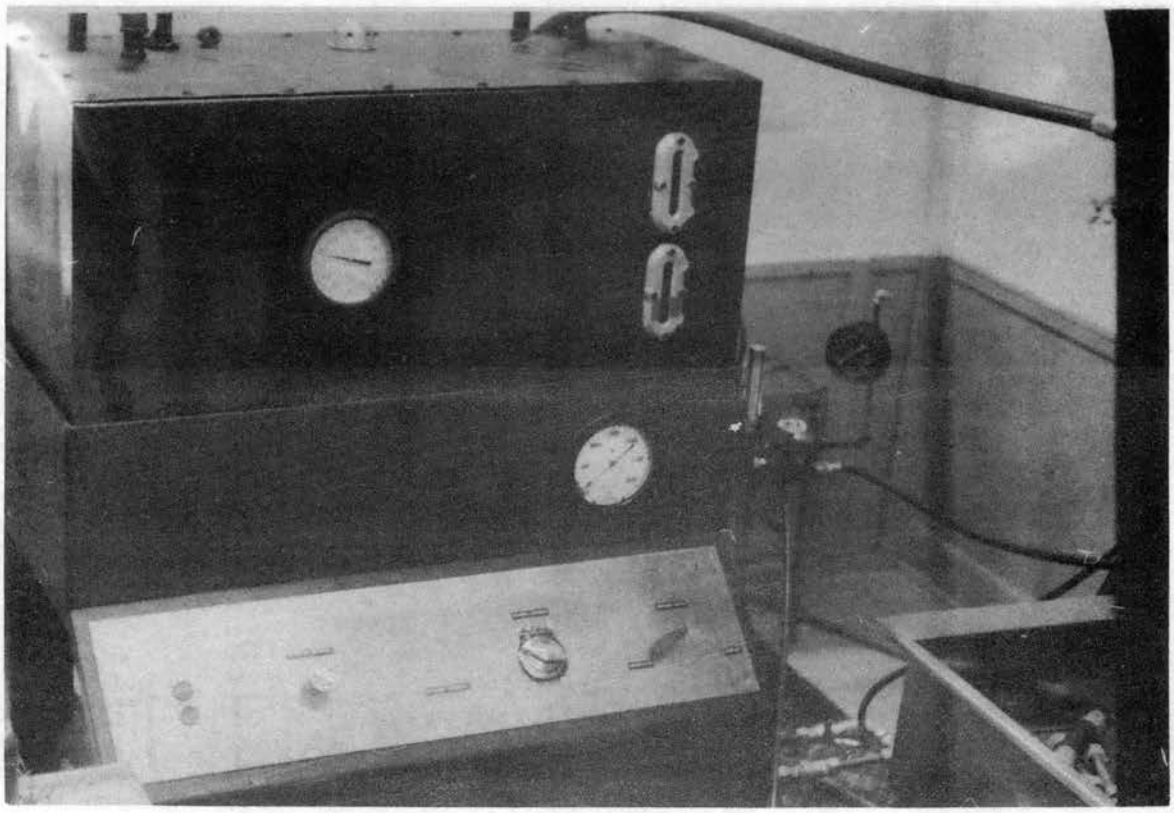

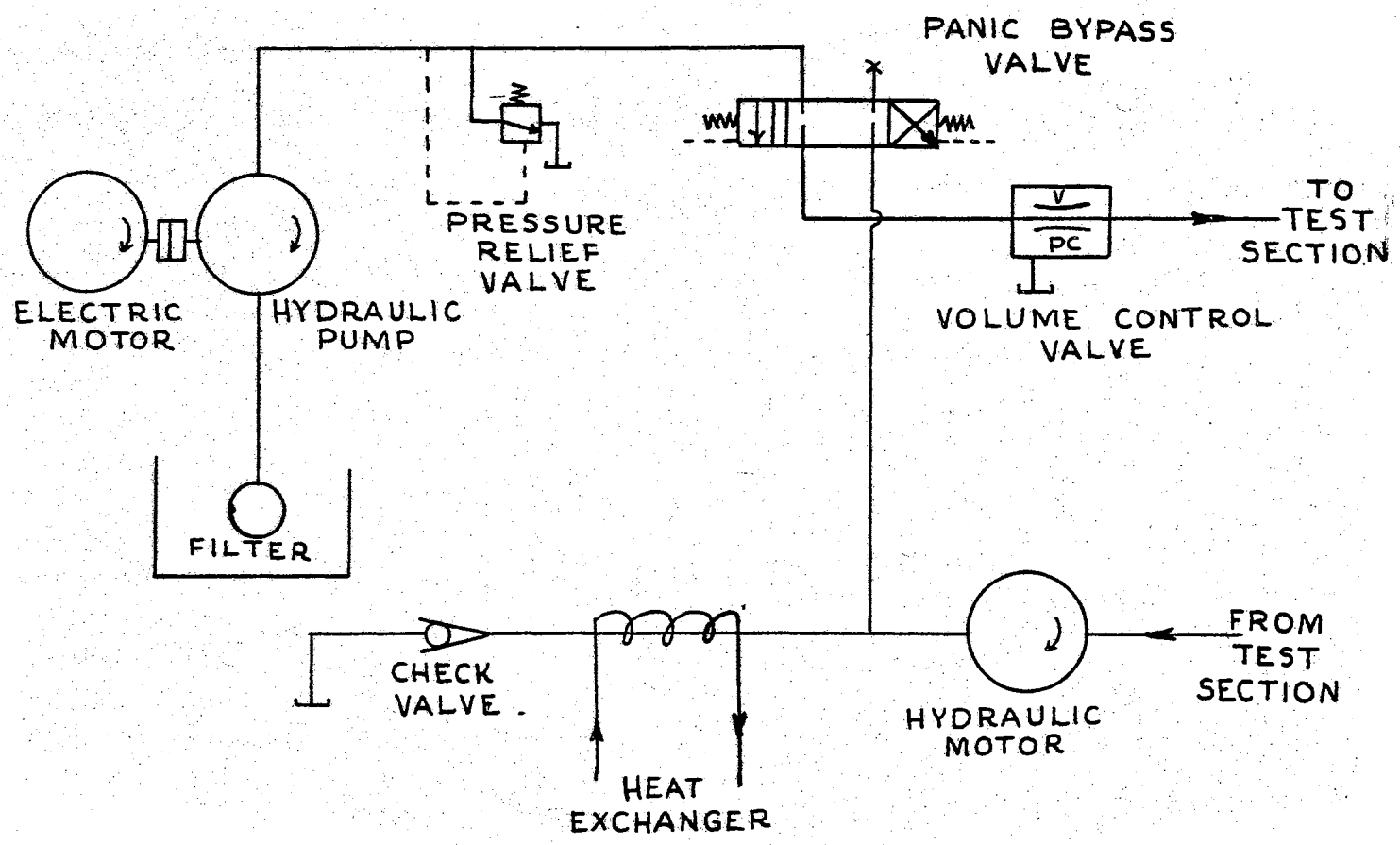

Figure 8. Power Stand Schematic

manner were:

(1) inadequate dynamometer facilities within the laboratory to accurately determine pump characteristics, and

(2) removal of pump from the system would have interrupted associated research.

Input power to the 3-phase induction motor was determined by using a Weston Industrial Analyzer, shown in Plate II. Line current, line voltage, and power factor in each of the three phases were determined as well as the total kilowatt input. The kilowatt reading was used, although input power could have been found using the relationship

$$P = \sqrt{3}\ EI \cos \theta \tag{38}$$

where

P = input power in watts,

E = line voltage in volts,

I = line current in amperes, and

$\cos \theta$ = power factor.

The $\sqrt{3}$ term is included as line voltages and currents were measured instead of phase voltages and currents. Several power readings were determined using Equation 38, and the results obtained compared relatively well with the wattmeter readings. However, considerable needle movement on the voltmeter, ammeter, and power factor meter made accurate readings difficult to obtain. The wattmeter indicated relatively constant values at each data point.

Actual motor output was somewhat more difficult to determine. Since the particular motor used is no longer manufactured, there

PLATE II. INDUSTRIAL ANALYZER

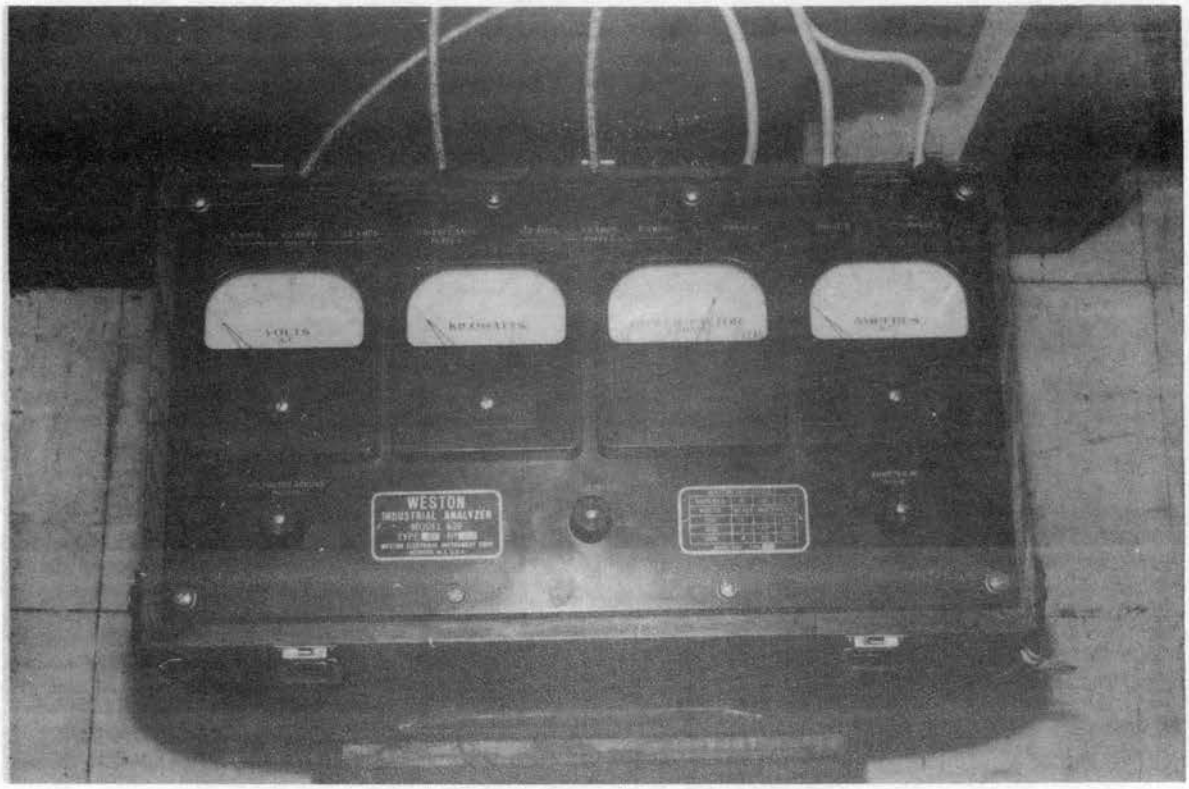

were no performance curves readily available. However, efficiency ratings at three load conditions were obtained from the manufacturer's representative in Tulsa, Oklahoma.

1/2 Load	3/4 Load	Full Load
82%	85%	86%

These three points compare favorably with the operating characteristics of a three phase, 60-cycle, 230 volt, 10 hp. induction motor as illustrated by Gray and Wallace (13). These characteristics, as shown in Figure 9 , were used to determine the operating efficiencies and horsepower output of the actual motor in use. Input power to the gear pump, which is also the output power of the electric motor, is given by the relationship

$$\eta_E \cdot HP_M = HP_{OM} = HP_{ip} \tag{39}$$

where

η_E = efficiency of the electric motor,

HP_M = input power to motor in hp.,

HP_{OM} = output power of motor in hp.,

HP_{ip} = input power to pump in hp.

The heat generation capabilities of the test pump, the Cessna gear pump shown in Plate III, were evaluated under essentially steady-state, adiabatic conditions. Once these conditions were obtained, temperature and flow measurements were made for various differential pressures across the pump--both with and without air injection into the oil.

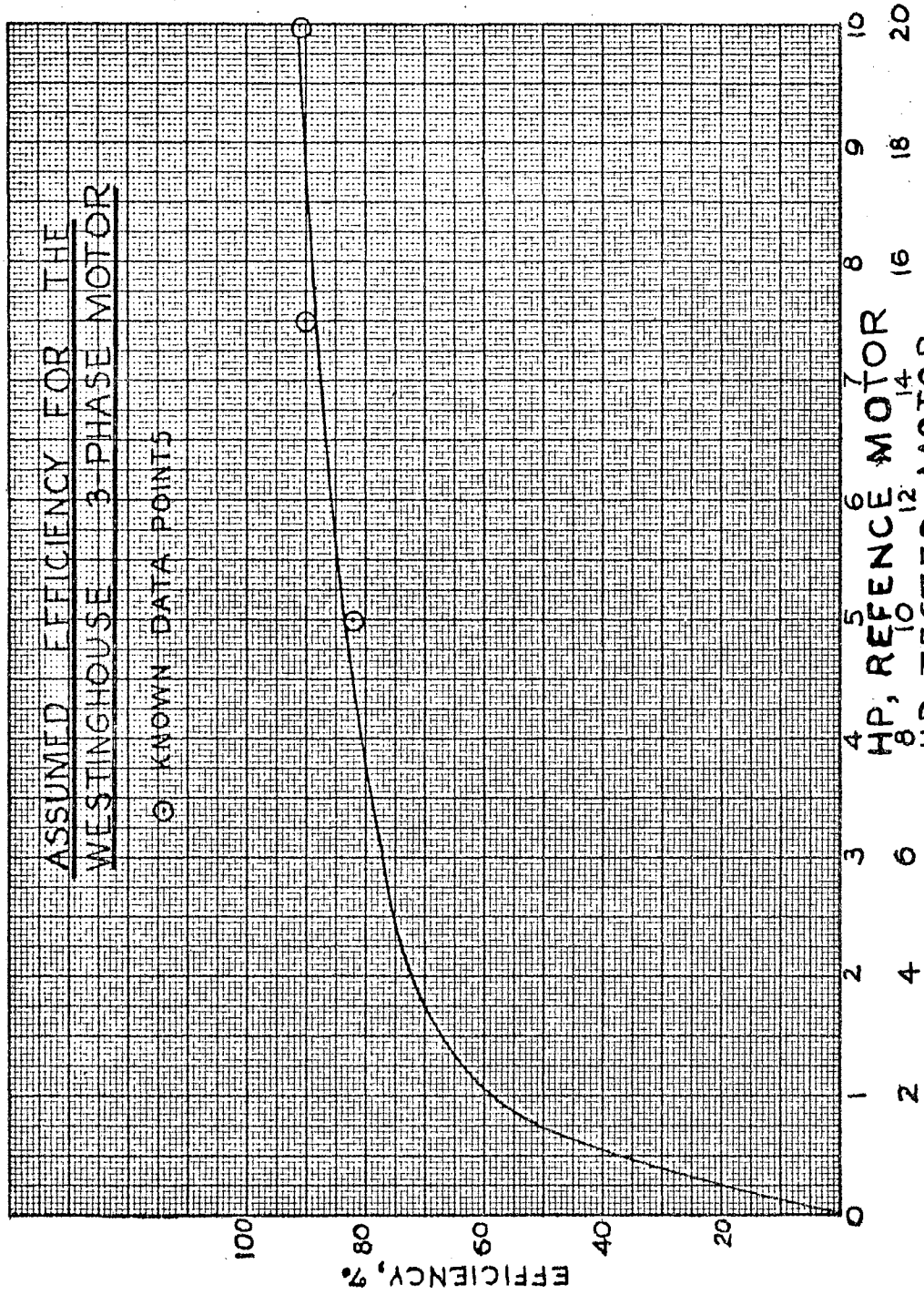

Figure 9. Assumed Electric Motor Efficiency Curve

PLATE III. EXTERNAL GEAR PUMP

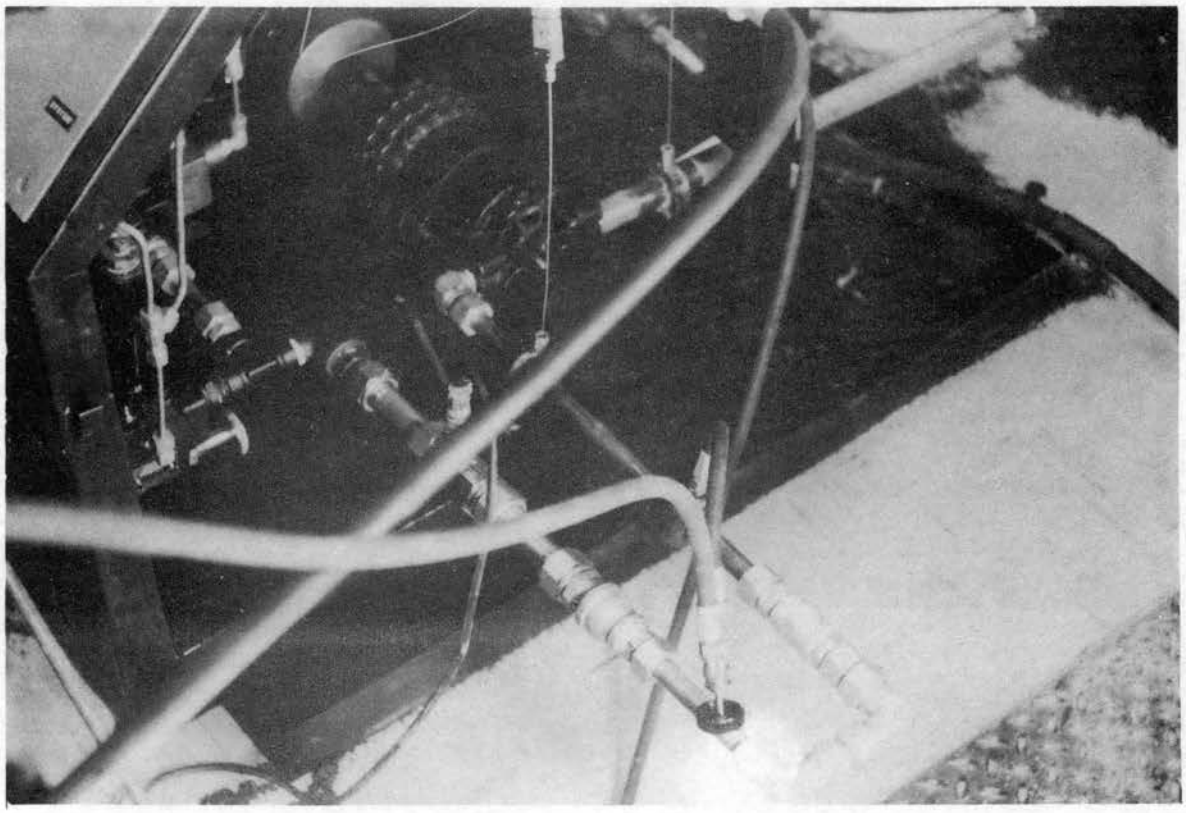

Steady-state conditions were maintained by adjusting the water flow rate to the heat exchanger until the reservoir temperature remained constant as indicated by the reservoir temperature probe. A constant pump inlet temperature reading was an additional check for steady-state operation, which became difficult to establish once pressure differentials of 500 psi were reached. The injection of air into the system made the problem of steady-state operation even more difficult due to the decreased pump efficiency. In both cases, the difficulty was a direct result of an inadequate supply of coolant water by which the reservoir test temperature was controlled.

In order to obtain adiabatic conditions, the pump and the suction and discharge lines were insulated by a molded fiberglass material. The insulation was composed of extremely fine diameter blown glass fiber bonded together with a phenolic resin. The valve and its piping were insulated by mixing an asbestos steam-joint cement with water and allowing the mixture to solidify. The insulated pump and valve test sections are shown in Plates IV and V, respectively.

Suction and discharge pressures for the pump, along with the upstream and downstream pressures across the needle valve, were measured according to the recommended practices set forth by the Society of Automotive Engineers (14). Piezometer rings were used as pressure pick-up connections to eliminate the inherent errors in standard tees. The suction and upstream piezometer rings were installed a distance of at least 4 inside diameters upstream of any connection or probe. Likewise, the discharge and downstream connections were placed at least 15 diameters downstream of any

PLATE IV. INSULATED PUMP TEST SECTION

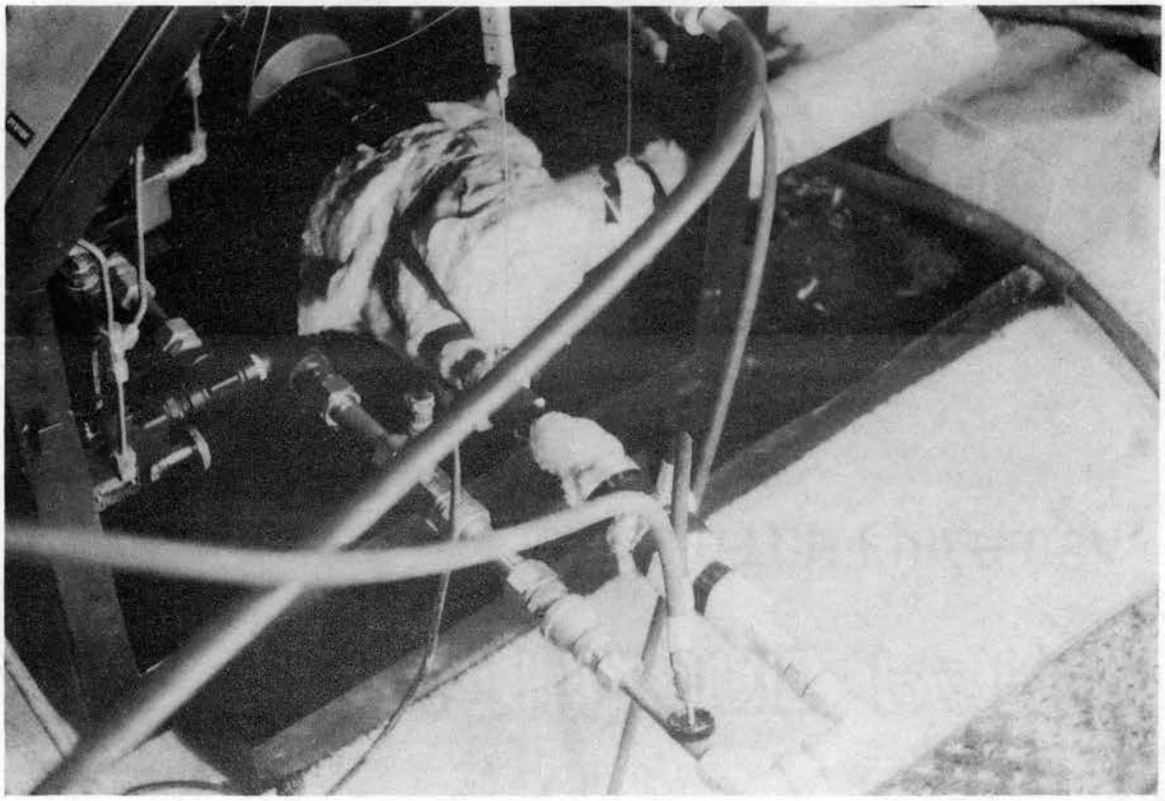

PLATE V. INSULATED VALVE TEST SECTION

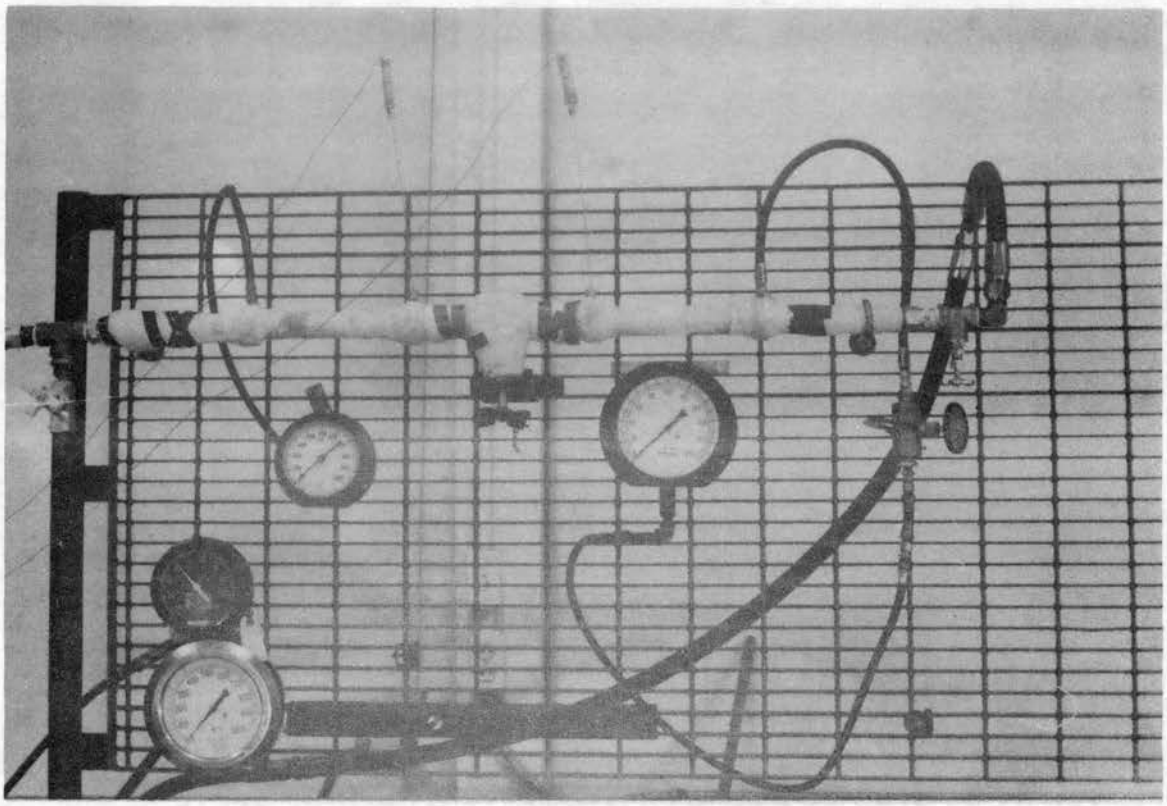

connection or probe. The pressure taps were then connected to their indicators. Calibration curves for the pressure indication system are included in the Appendix B. The 3/4 inch elbow at the pump outlet port was found to have the pressure drop of 3 feet of pipe (3). This pressure drop was considered negligible, and the differential pressure across the pump was taken as the actual difference of the values appearing on the gauges.

Minneapolis-Honeywell, Type J, Iron-Constantan thermocouples were used to measure the temperature differentials across the pump and valve. These thermocouple probes, shown in Plates IV and V, were placed with the sensing tip in the center of the flow passage in order to measure the oil bulk temperature. A typical installation is shown in Figure 10. In order to facilitate temperature measurement, a thermocouple switch was used in conjunction with the millivolt potentiometer. Once the potentiometer was balanced, the desired temperature was determined by merely turning the switch to the corresponding station and nulling the thermal emf. The millivolt potentiometer, ice bath, and thermocouple switch are seen in Plate VI, while a schematic of the thermocouple circuitry is shown in Figure 11. Thermocouple calibration plots are found in Appendix B.

The actual flow rate through the pump was measured by a variable reluctance turbine meter. A propeller located in the flow passage rotated at a rate proportional to the amount of fluid passing. The wheel motion is sensed by a reluctance-type pickup coil, and a corresponding voltage pulse is produced at the output terminals (15). The pulses were counted on a frequency meter, fed into an amplifier, and counted again by an EPUT meter which gave a more accurate count than the frequency counter. The turbine meter is shown along with the

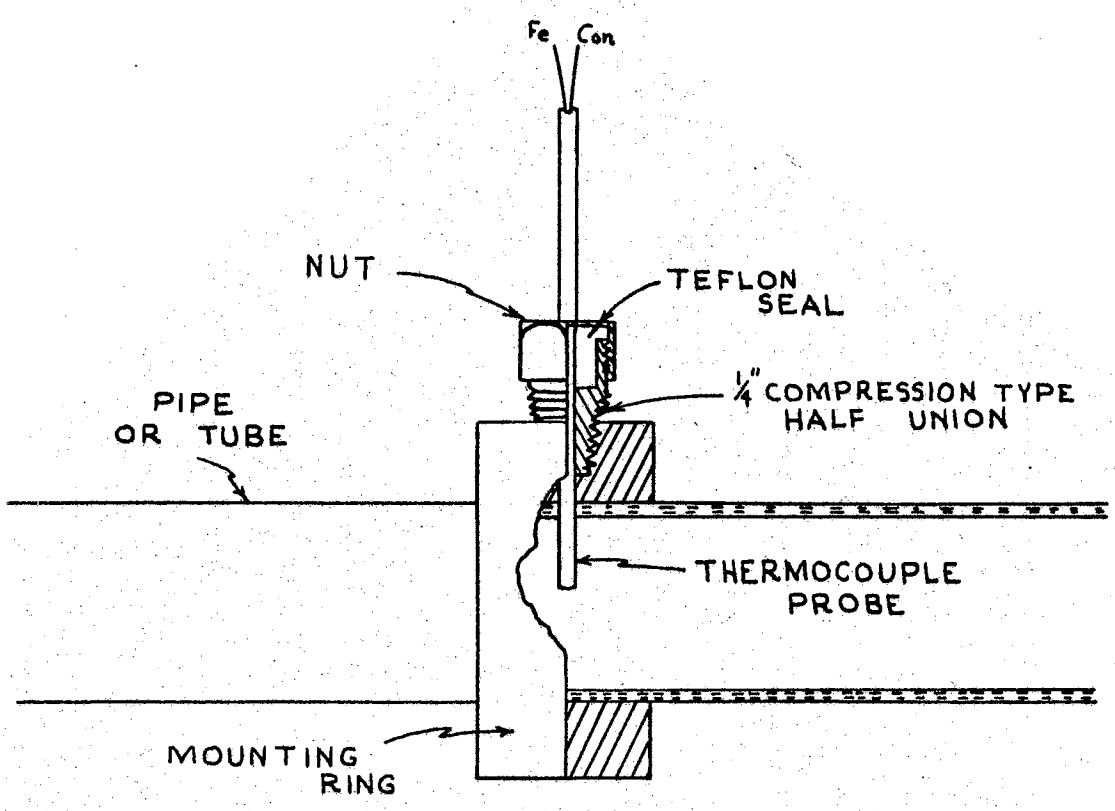

Figure 10. Typical Thermocouple Installation

PLATE VI. MILLIVOLT POTENTIOMETER, THERMOCOUPLE SWITCH, ICE BATH

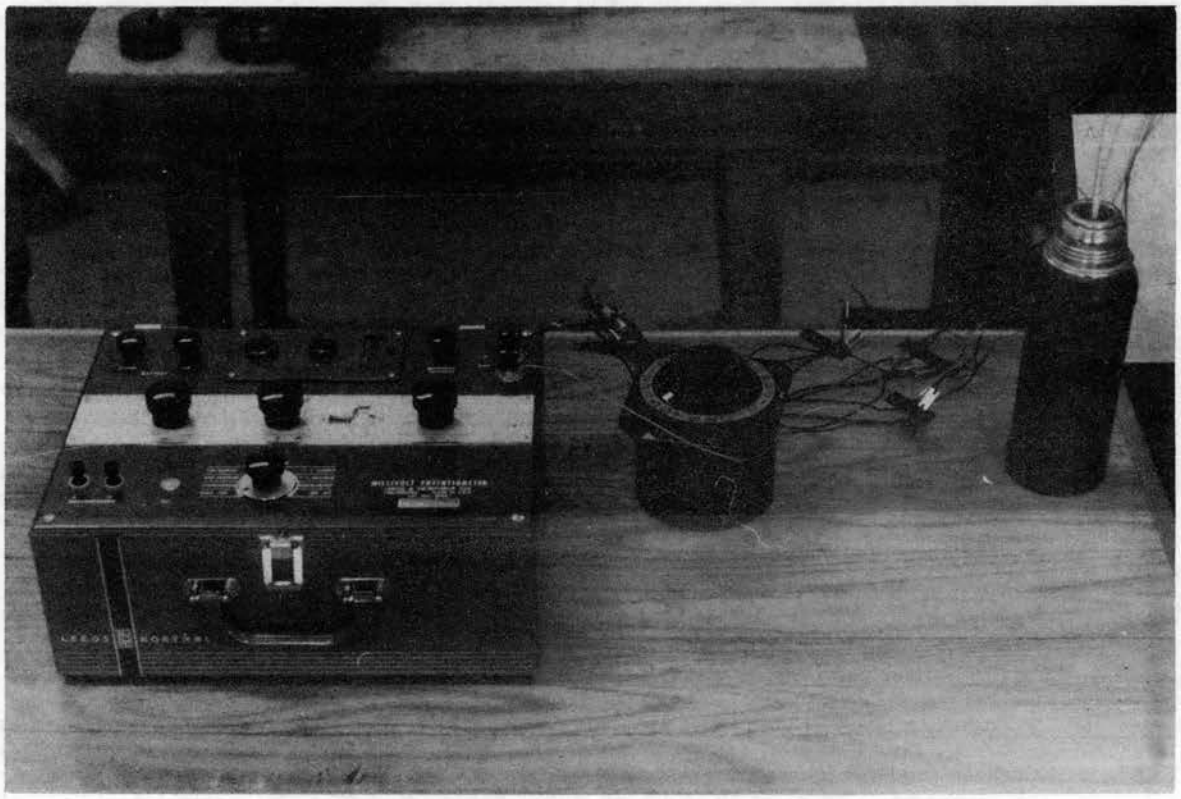

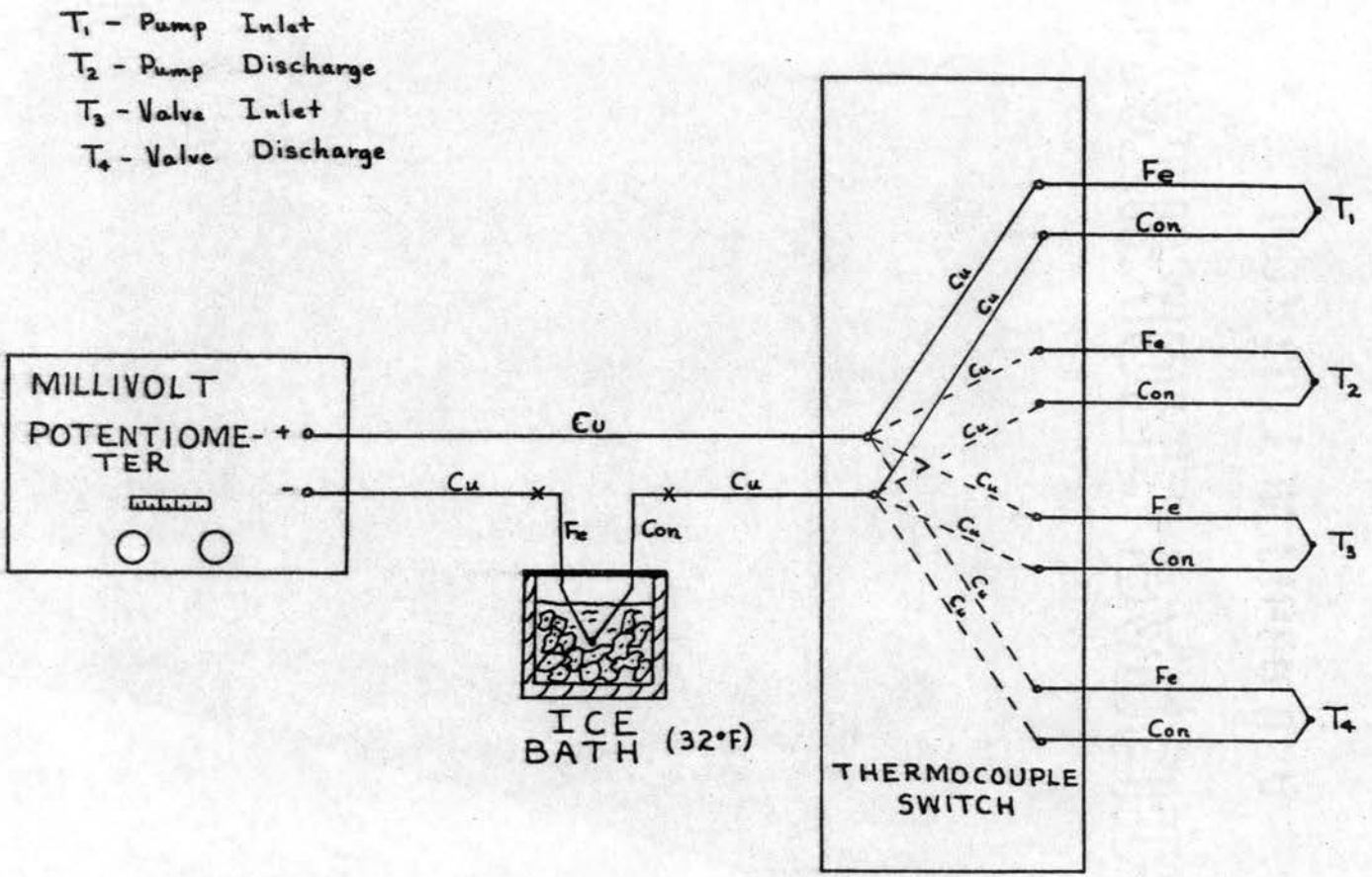

Figure 11. Thermocouple Switching Circuitry

frequency counter, amplifier, and EPUT meter in Plate VII. The calibration data are found in Appendix B.

The ideal pump flow rate was determined by measuring the speed of the motor and/or the pump by using a hand tachometer and multiplying this value by the pump displacement, which is 1.70 $^{in^3}/_{rev}$ as stated by the pump manufacturer. The flow rate through the test valve was determined by measuring the speed of the hydraulic motor shown in Plate VIII. A calibration of flow rate versus hydraulic motor rpm appears in Appendix B.

Air was injected into the system on the suction side of the pump by the method indicated in Plate IX. Laboratory supply air of approximately 95 psig was connected to the pressure regulator which reduced the pressure to the desired level of 2 to 4 psig. The two-position air valve permitted either the injection of this low pressure air or atmospheric air depending upon the position of the lever. The amount of air injection was controlled by the small needle valve mounted on the plexiglass tubing, while the small rotameter capable of measuring from 0 to 10 $^{ft^3}/_{hr}$ determined the actual air flow. The large rotameter was originally used, but it was not sensitive enough to measure accurately such low flow rates. Again, calibration information may be found in Appendix B.

Several problems were encountered with the initial injection of air into the suction side of the pump. Originally, a check valve was used in place of the needle valve. Since the suction line had a vacuum of 2"-3" Hg, the check valve alternately opened and closed letting in amounts of air in the order of 10-12 $^{ft^3}/_{hr}$. These amounts

PLATE VII. TURBINE METER, FREQUENCY COUNTER, AMPLIFIER, EPUT METER

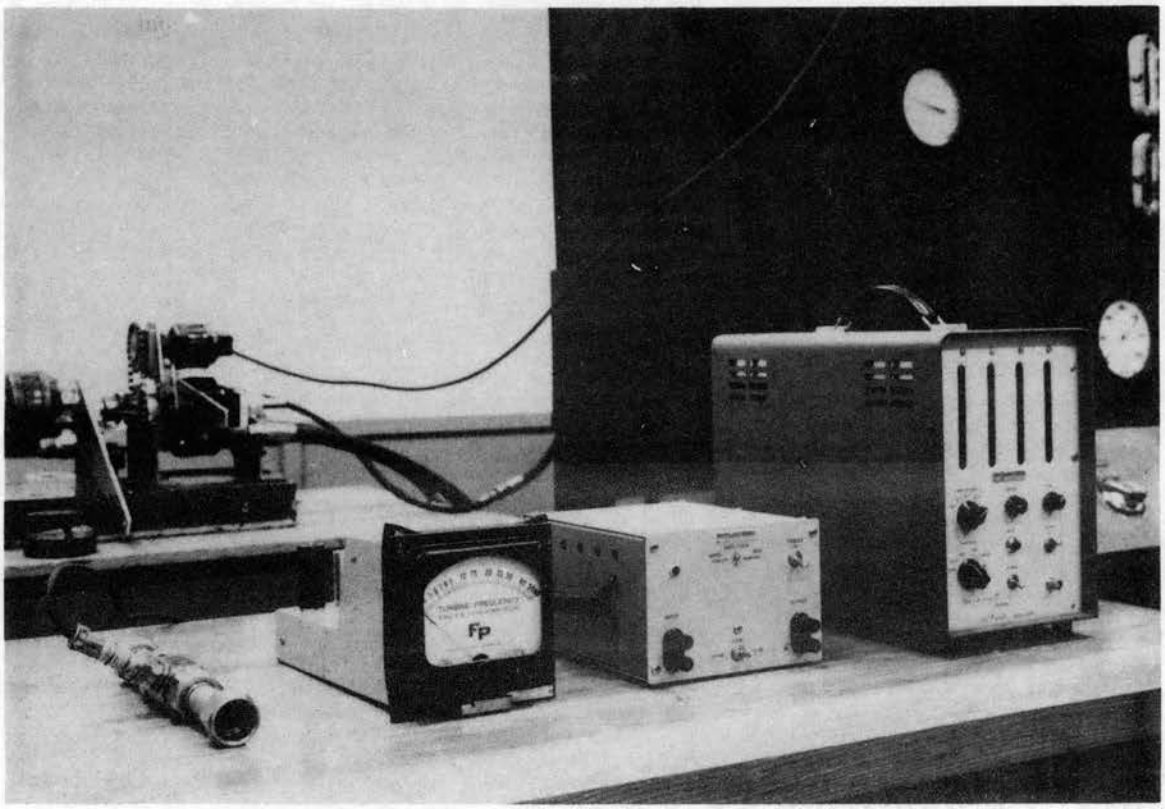

PLATE VIII. HYDRAULIC MOTOR

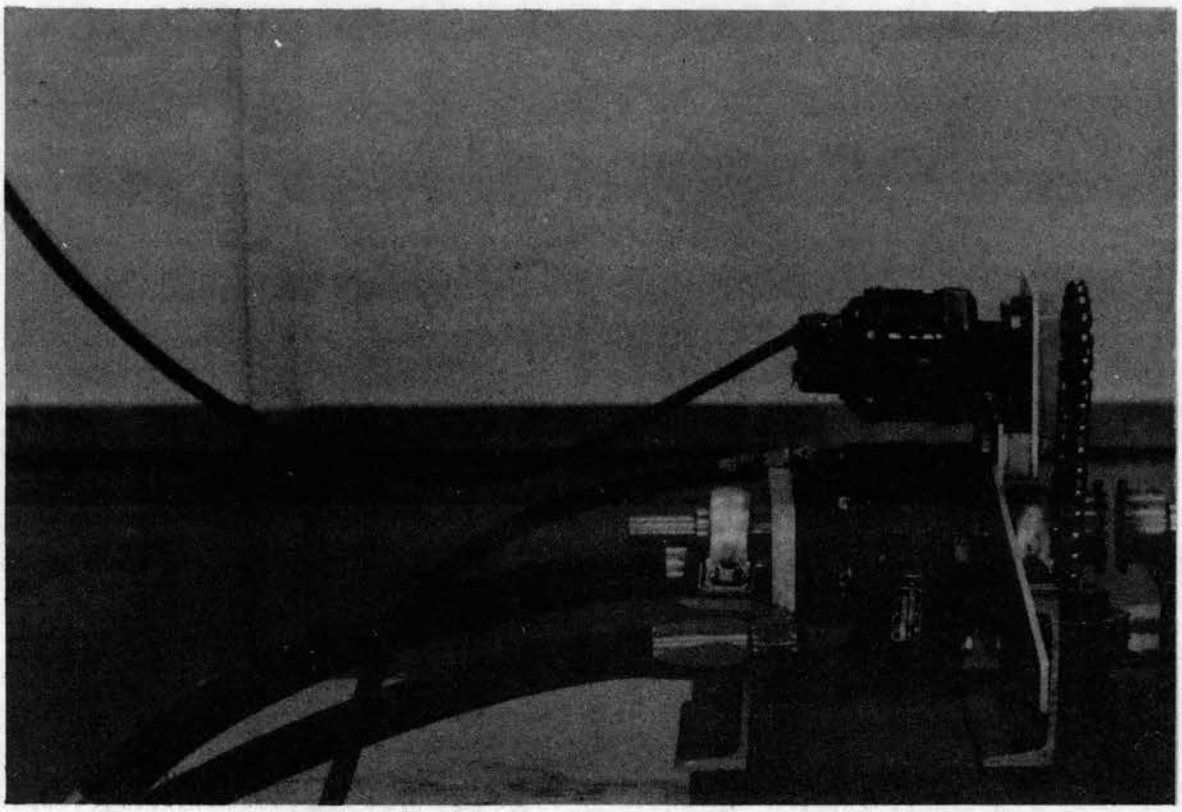

PLATE IX. AIR INJECTION SYSTEM

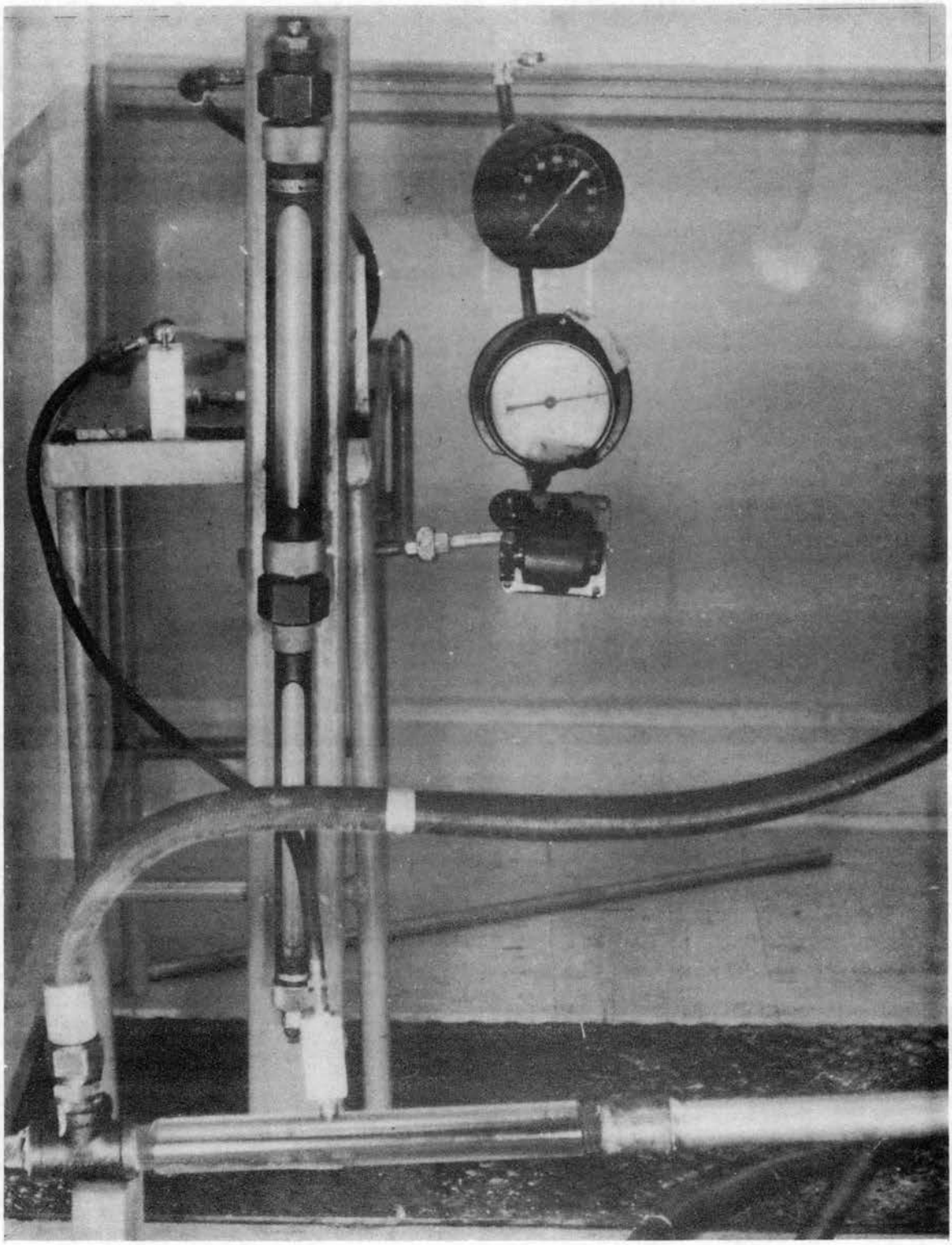

produced severe cavitation within the pump itself, and correct system operation could not be achieved. In addition to extreme vibrations and noise, violent pressure fluctuations across the pump and throughout the system were observed. The problem was removed by replacing the check valve by the needle valve which permitted a much finer metering of the air. Cavitation of the pump was not severe until air flow rates of 6 ft^3/hr were exceeded.

In making a test run, the following procedure was established:

1. The ice bath was prepared by placing crushed ice into a Dewar flask previously shown in Plate VI. Additional ice was added during the run whenever needed to maintain a reference temperature of 32° F.
2. The reference thermocouple was placed into the ice bath with the sensing tip well surrounded by ice. The additional thermocouple circuitry was also checked, as the small lead wires were easily broken.
3. The millivolt potentiometer was then balanced to insure correct emf readings.
4. The power stand was turned on with the fluid bypassed into the reservoir for a short time while power stand operation was checked.
5. The fluid was then switched into the test section, and the pressure and flow rate adjusted to the desired values.
6. The flow of water through the heat exchanger was then adjusted to obtain the desired reservoir temperature, usually in the range of 72°-74° F.

7. Various pressure differentials across the pump and valve were set for a given flow rate. Common settings across the pump were 300, 400, 500, 600, 700, and 800 psi in that order.
8. Once steady-state conditions prevailed at each of the settings, pressure, flow, temperature, and electrical power measurements were taken. Potentiometer balancing after each setting was performed as a check.

The test procedure was essentially identical with or without air injection into the system, the only difference being periodic checks to insure a constant air flow was being maintained for a given run.

CHAPTER V

EXPERIMENTAL RESULTS

The experimental test results of the basic pump and valve are shown in Figures 12 through 37, inclusively. In Figures 12 through 21 the temperature increases due to pumping are shown for various pressure differentials across the pump. Figures 22 through 24 show the volumetric and overall efficiencies as a function of the pressure differential. The thermal increases across the needle valve due to throttling are shown in Figures 25 through 37.

The theoretical temperature changes across a pump and valve were calculated according to Equations 19 and 27, respectively. The specific gravity and specific heat of the Mil-H-5606 hydraulic oil were evaluated at the mean temperature existing across the component; that is, the fluid properties would be evaluated at 75° F. for fluid entering a pump at 73° and exiting at 77°. These properties, as a function of temperature, are shown in Appendix C and were taken from data compiled in the Boeing Document T3-1292 (16).

For clarity, pump test runs in which no air was injected are preceded by the letter P in the figures, while tests including air entrainment are designated by PA. The individual valve tests follow the same notation with the letter V replacing the letter P.

It was assumed that no air was initially entrained within the oil. This assumption appears valid when considering the reservoir

design and the flow requirements of the system. The baffled reservoir helped prevent system aeration by restricting the return oil surge into the tank. An additional design feature tending to prevent aeration was the submersion of the return line in the oil, thus allowing no splashing to occur. At maximum operating conditions the system flow rate did not surpass 13.5 gallons per minute, and the reservoir oil capacity was maintained at approximately 57.8 gallons. Therefore, the oil was allowed to remain in the reservoir for an average time of 4.28 minutes before being recycled through the system. Any air contained within the oil should have been removed in this time interval.

Runs P-1 through P-5, shown in Figures 12 through 16, indicate that there is definitely a heating of the oil due to the pumping process. However, the heating effect is shown to be considerably more than that indicated by the theoretical calculations. As can be seen, the repeatability of the data is good. Test runs PA-1 through PA-5, shown in Figures 17 through 21, indicate that entrained air within the system increases the temperature rise across a pump for a given pressure differential above that occurring with no air entrainment. Again, the heating effect is considerably higher than theoretically expected. However, several possible explanations for these discrepancies exist.

In determining the theoretical temperature increase due to pumping to a desired pressure level, Equation 19 was used. For a given pressure differential, the temperature change is dependent upon three variables--specific gravity, specific heat, and overall pump efficiency. Since fluid data was taken from that provided in the afore-mentioned

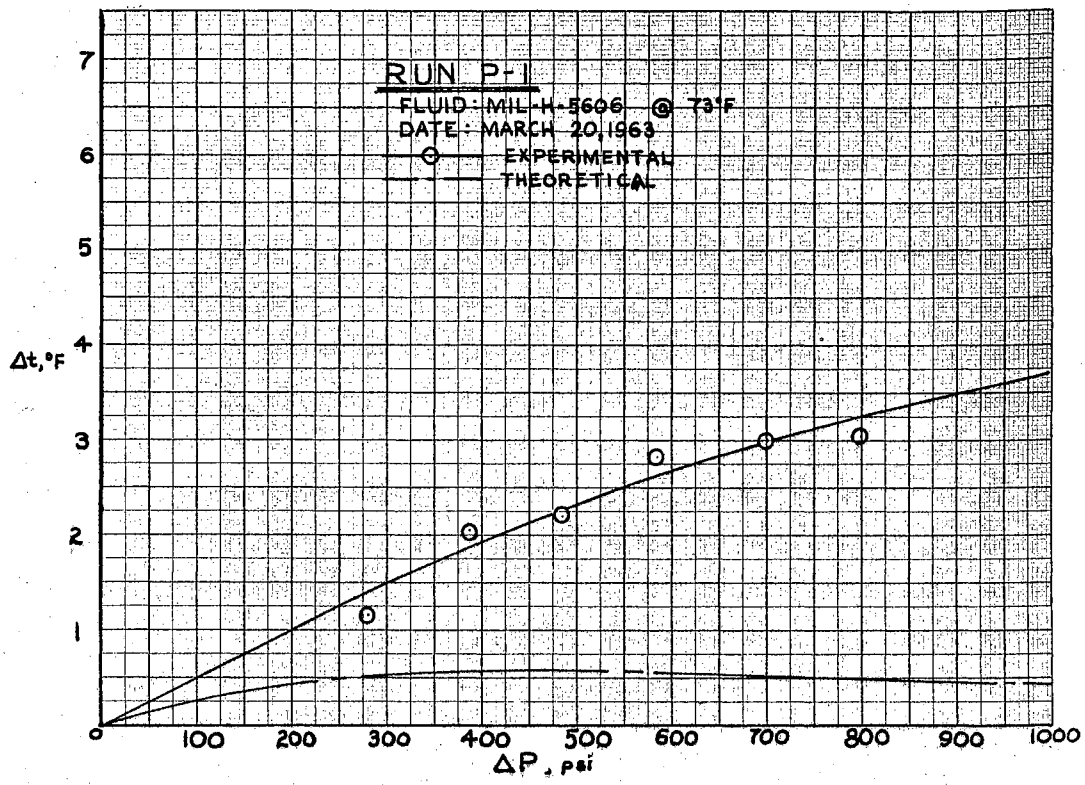

Figure 12. Run P-1

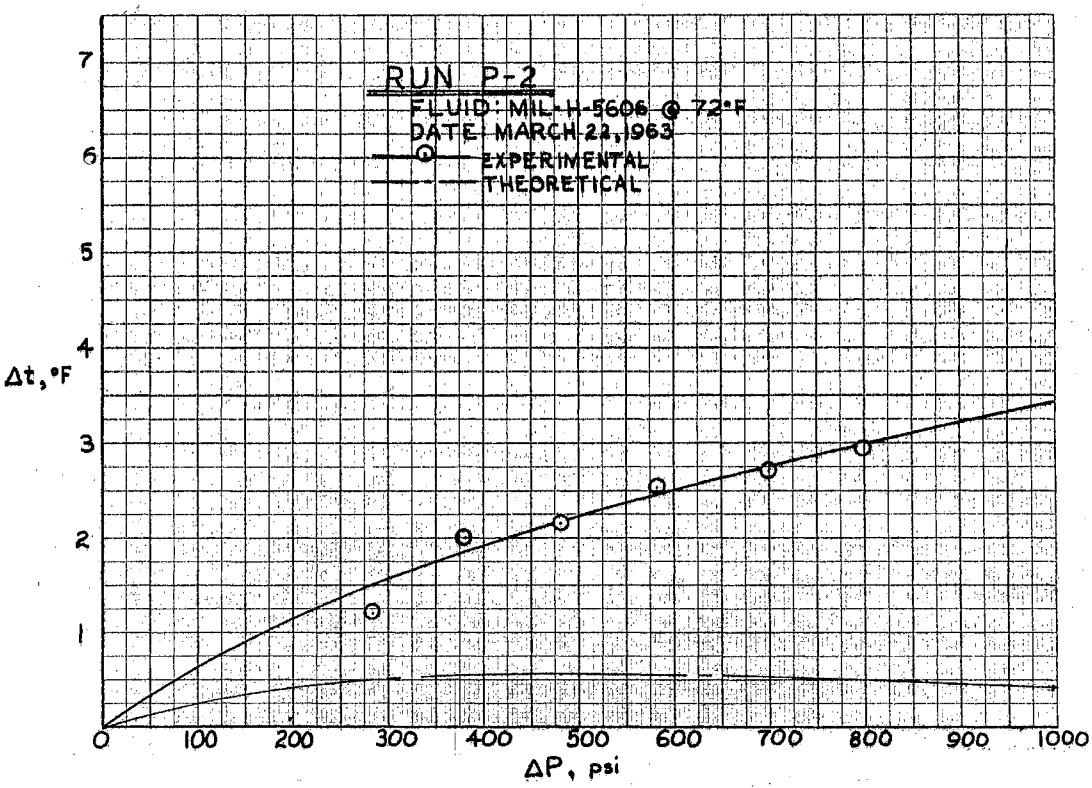

Figure 13. Run P-2

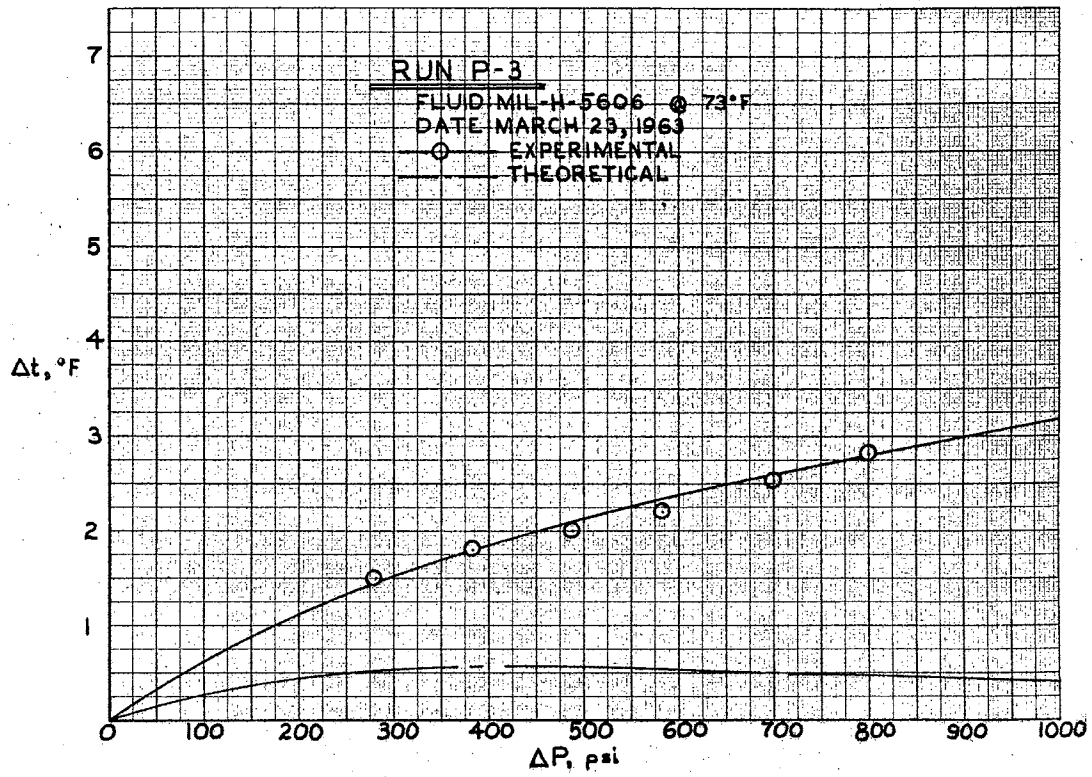

Figure 14. Run P-3

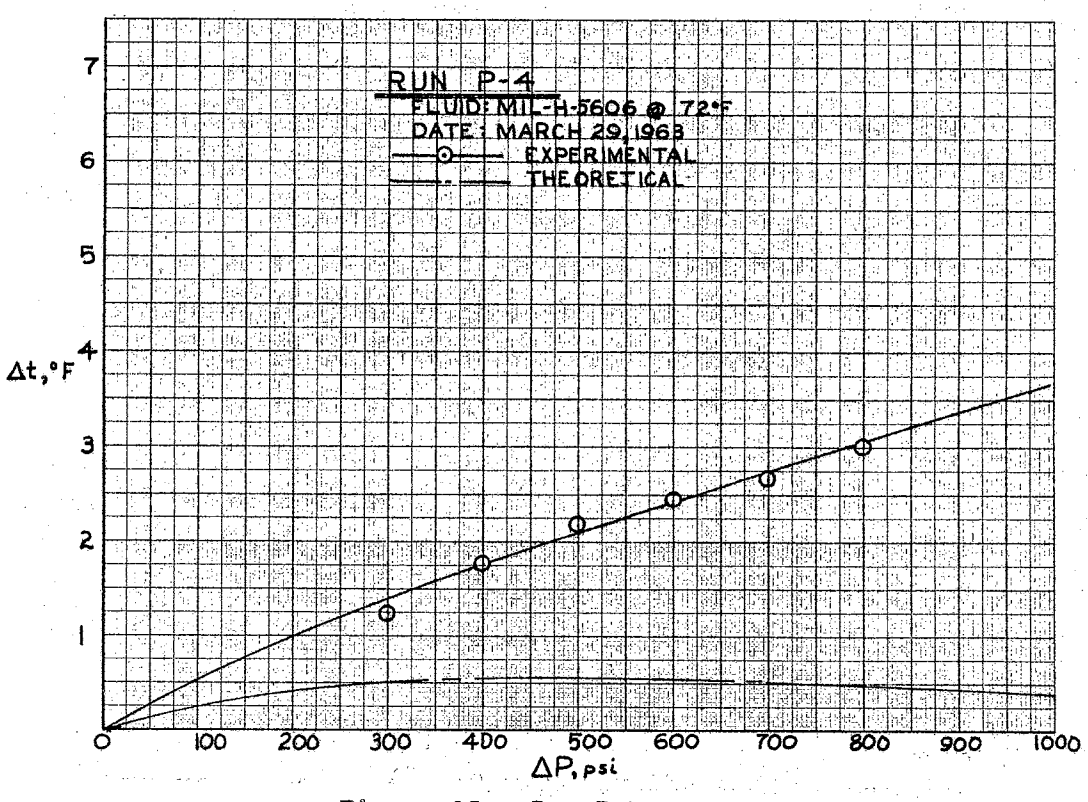

Figure 15. Run P-4

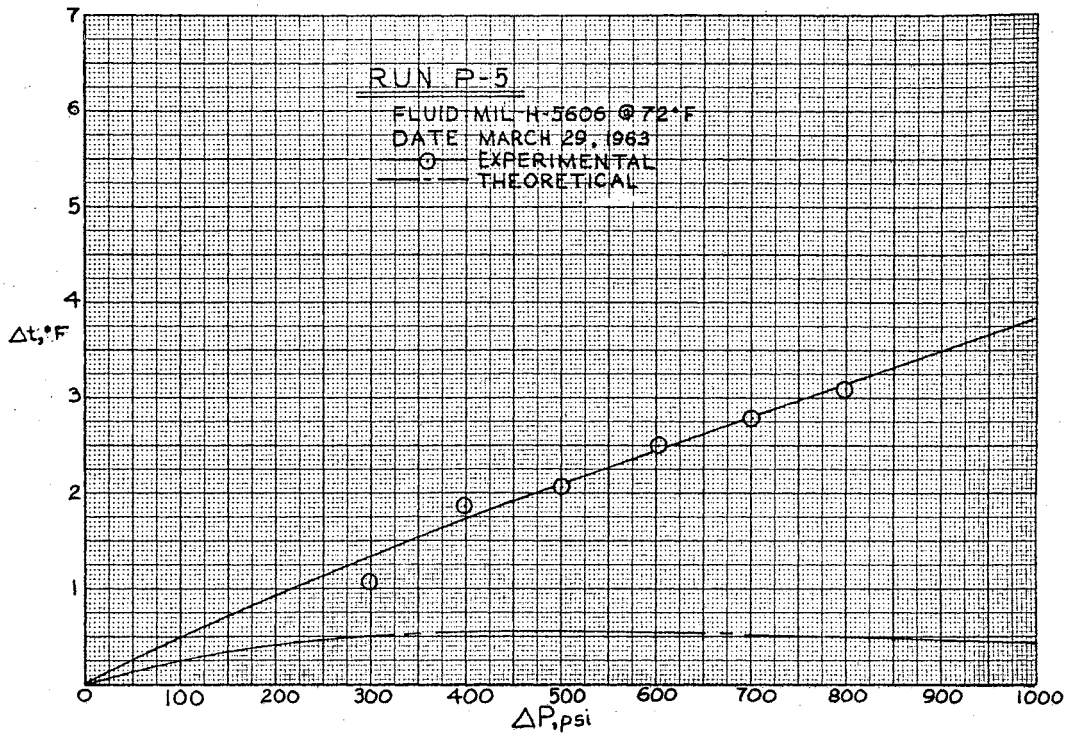

Figure 16. Run P-5

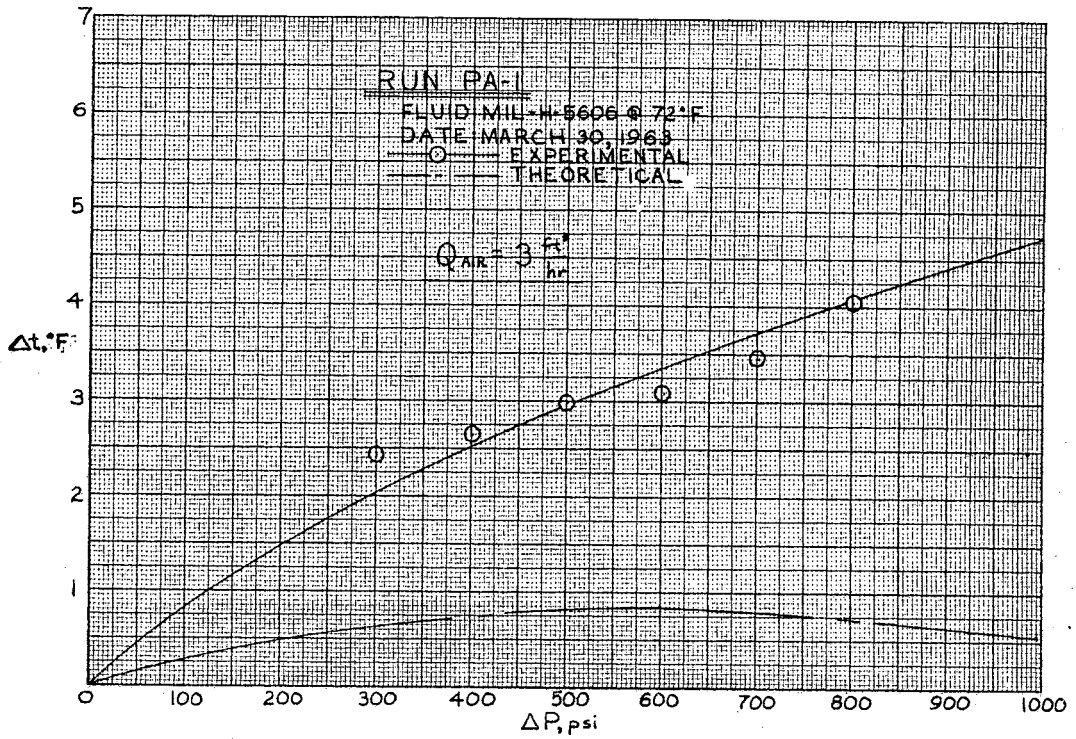

Figure 17. Run PA-1

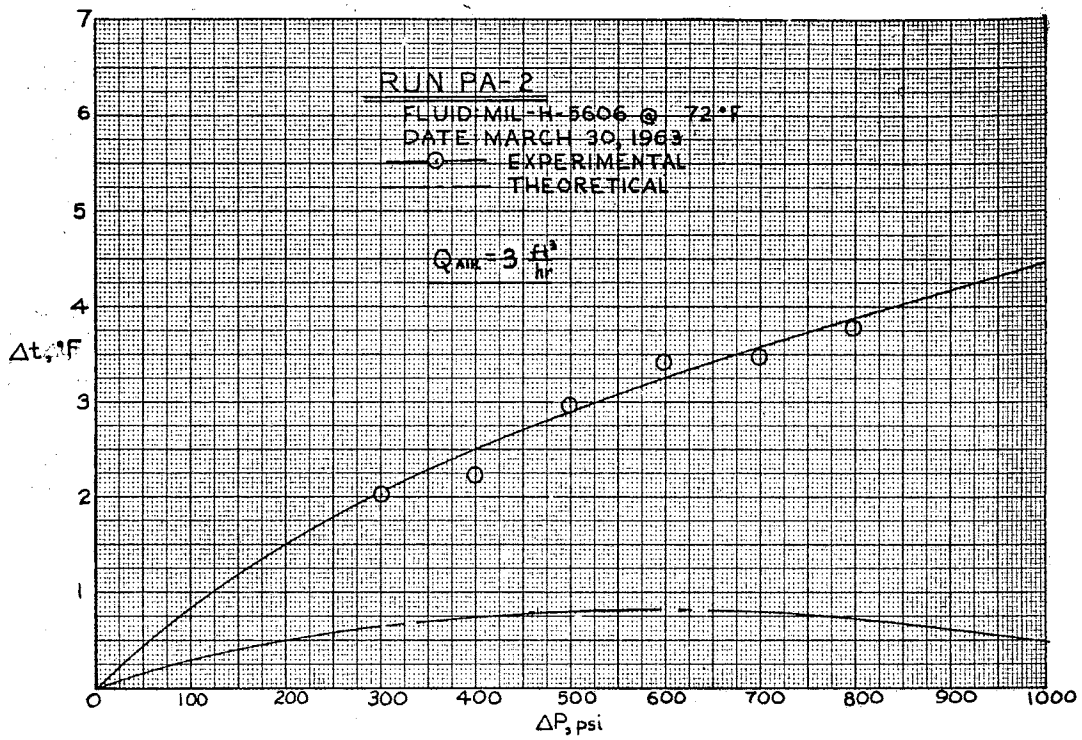

Figure 18. PA-2

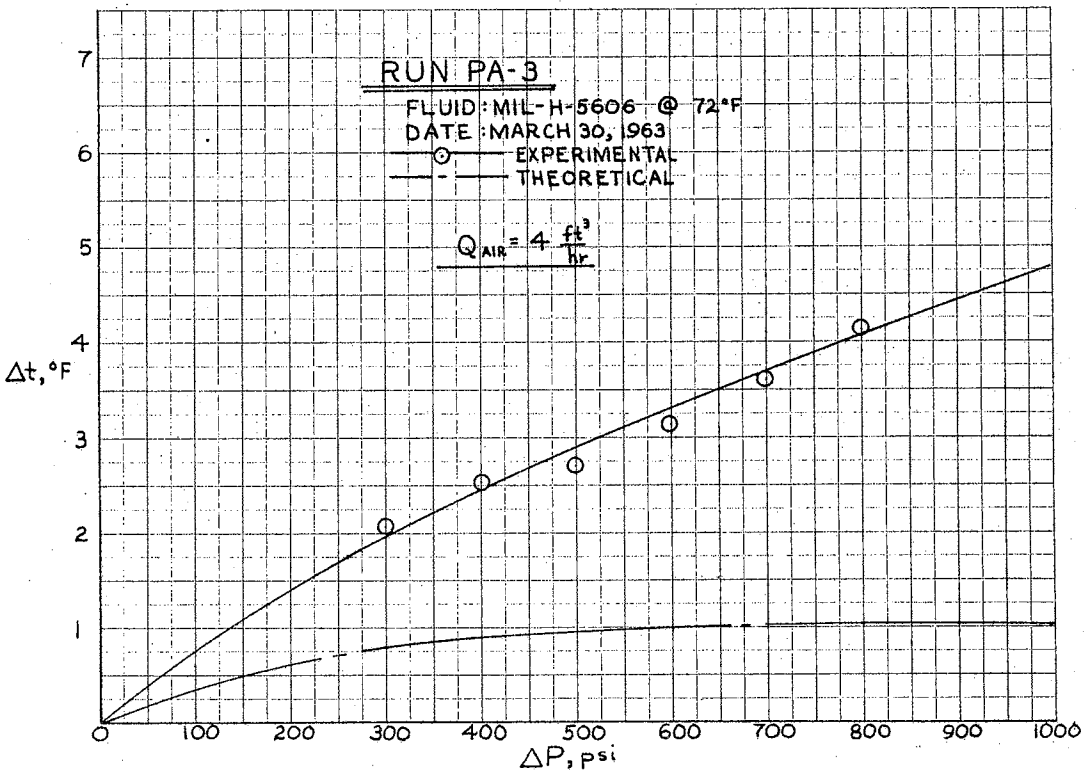

Figure 19. Run PA-3

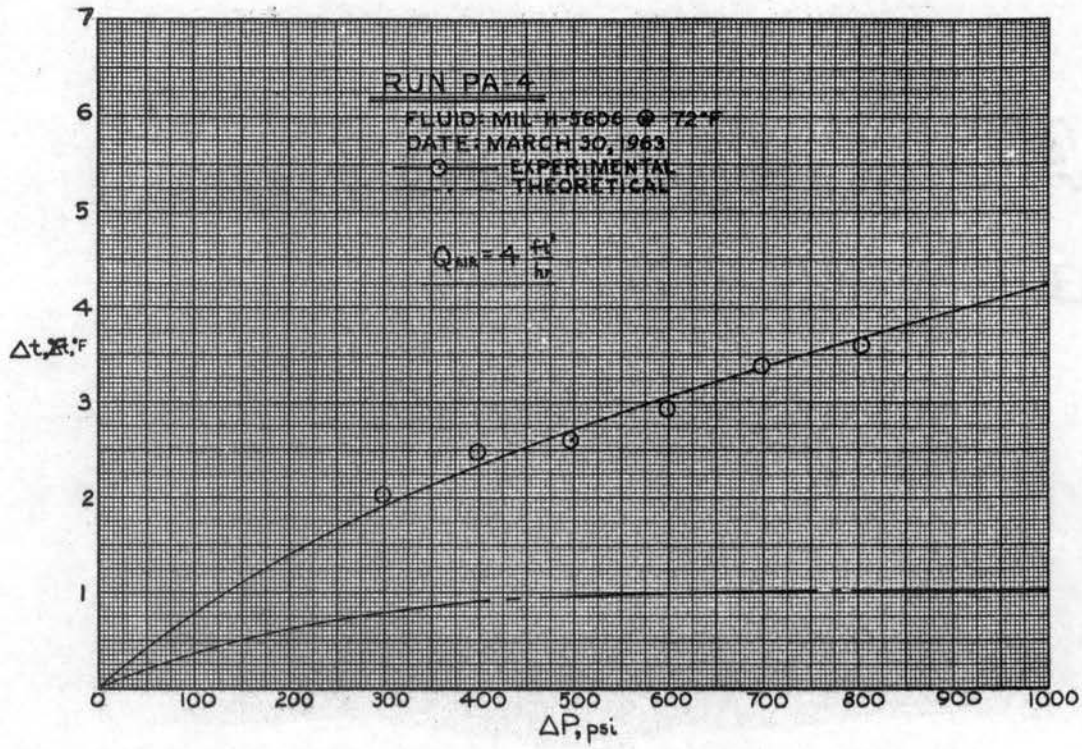

Figure 20. Run PA-4

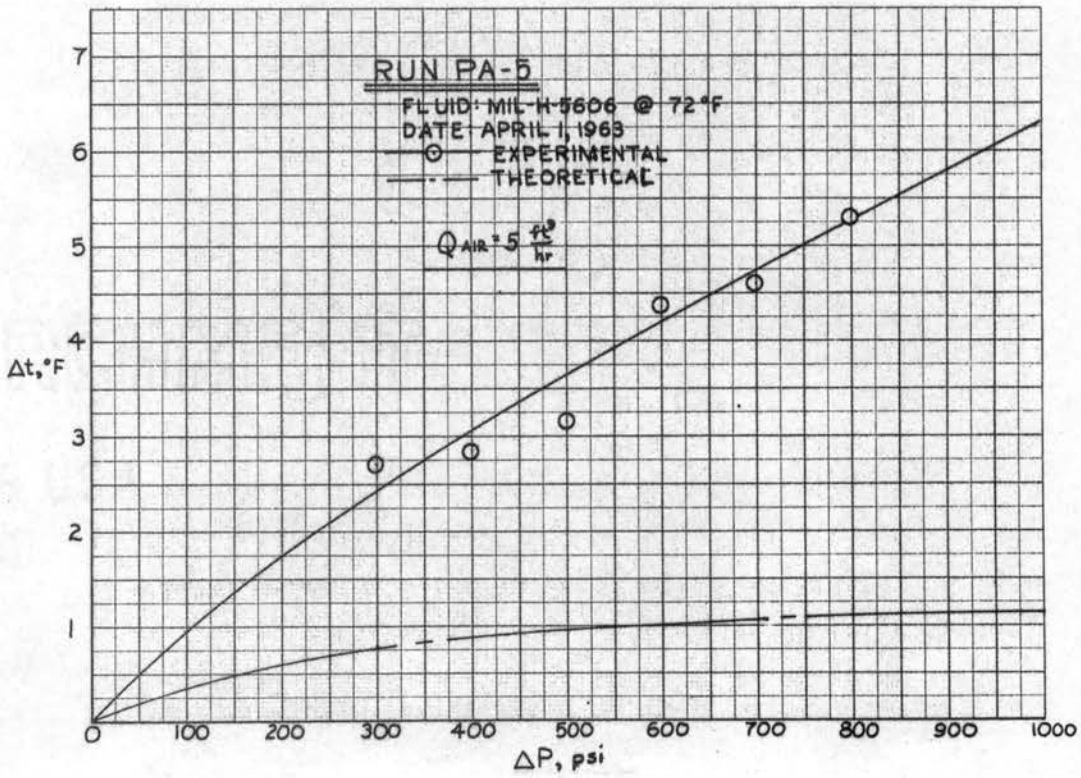

Figure 21. Run PA-5

Boeing report and not from specimens of the oil used in the actual testing, the values of the specific gravity and specific heat are possibly in error. Although it is doubtful that the fluid properties of the test fluid are exactly those used in the calculations, the true values probably differ very little as the oil was not subjected to degenerative tests.

The efficiencies used in the theoretical calculations were determined by the relationship

$$\eta_o = \frac{HP_{out}}{HP_{in}} \tag{40}$$

where

η_o = overall pump efficiency,

HP_{out} = horsepower output of the pump, and

HP_{in} = horsepower input of the pump.

Pump output was accurately determined by the flow and pressure measurements indicated in Chapter IV. Thus, the motor efficiency curve previously assumed appears as a logical source of error, particularly in lieu of the fact that only three known data points were available. In addition, the power requirements for which efficiency values were needed fell within the assumed portion of the curve.

Experimental error can almost entirely be attributed to the temperature measurement. Although the Minneapolis-Honeywell thermocouples are reportedly accurate to 4% of the total temperature measured, inspection of the thermocouple calibration curves in the Appendix B

indicate that the individual thermocouples read almost identical values. Therefore, it can be reasoned that the temperature differential measured was accurate, although the individual temperature measurements might well have been in error.

As stated in Chapter IV, the thermocouples were placed in the center of the flow passage in order to measure the bulk temperatures. It is possible that the sensing tip of the thermocouples were not located in the conduit centers, but the work of Hughes (17) indicates that the temperature profile for the fluid is essentially flat except for the region near the wall. Inspection of the test section indicated that probes remained near the center of the fluid passages and therefore probably measured the existing bulk temperatures.

The major source of error in the measurement of temperatures appears to be in the use of the millivolt potentiometer as a thermocouple output indicator. The potentiometer, although an extremely accurate instrument, was able to record only one emf output at a time by a manual balancing of the unit. Therefore, a period of 20-30 seconds elapsed before additional thermocouple readings were taken. Although steady-state conditions prevailed, the temperatures at the various stations were observed to fluctuate as much as 0.5 degrees indicating a possible accumulative error from point to point. Likelihood of slightly greater error existed at the higher pressure differentials due to the increased difficulty in maintaining steady-state operating conditions. Finally, the balancing dial on the potentiometer could be moved as much as 0.007 millivolt without

appreciably changing the zero balancing position. This movement corresponds to a 0.233 degree error or a total error of 0.466 degree between two successive stations.

The injected air was observed to remain in the upper portion of the suction line indicating that a uniform oil-air mixture did not exist at the pump inlet. Since the oil and air remained in so-called layers within the suction line, it is probable that the pump inlet thermocouple measurements were affected due to the air surrounding the thermocouple and thereby changing the film coefficient around the probe. As Schanzlin stated, entrained air does not immediately dissolve into the oil at the pump discharge, but often remains in globule form for some distance. Therefore, similar statements can be made concerning the pump discharge thermocouple. However, once equilibrium conditions were reached, this particular source of error should have been alleviated.

Due to the properties of the insulating materials and the small temperature differential (at most, 3-7 degrees) between the system temperature and the ambient temperature, the adiabatic assumption was valid because little heat was allowed to cross the system boundaries. A sample calculation is shown in Appendix A.

Although the experimental data did not correlate closely with the assumed theoretical values, the results obtained were promising. The addition of air increased the temperature rise for a given pressure differential as expected. The theoretical and experimental curves had almost identical shapes. The gradually decreasing slopes of the curves were due to the increased overall pump efficiency as the pump neared its

rated load.

The volumetric efficiencies for the test runs are shown in Figure 22, indicating the adverse effect of air entrainment. The overall efficiencies as determined from the assumed motor efficiency curve are shown in Figure 23, while those required to give the experimentally determined thermal increase are shown in Figure 24. In either case the overall efficiencies increase as the pump nears its rated operating condition.

The results of the valve tests are shown in Figures 25 through 37. Initially, the temperature differentials across the valve were determined by measuring the output of the two thermocouples on separate potentiometers. Tests V-1 through V-4 were performed in this manner, while the temperature differentials of the remaining valve tests were measured using one potentiometer and the switching circuit. As can be seen from Figures 25 through 30, runs V-1 through V-6 indicated temperature differentials slightly less than the expected theoretical values. However, runs V-7 through V-10 and VA-1 through VA-3 resulted in temperature differentials somewhat higher than expected. Air entrainment appeared to have no definite effect upon the heat generation capabilities of the needle valve.

All valve tests were run for a test section flow rate of 4.7 gallons per minute. Since a portion of the fluid was bypassed downstream of the pump, it was assumed that the air was divided in the same proportion as the fluid. This assumption implies that the air has had ample time to become mixed in the oil.

Many of the arguments previously made concerning temperature measurements can be applied in explaining the discrepancy between

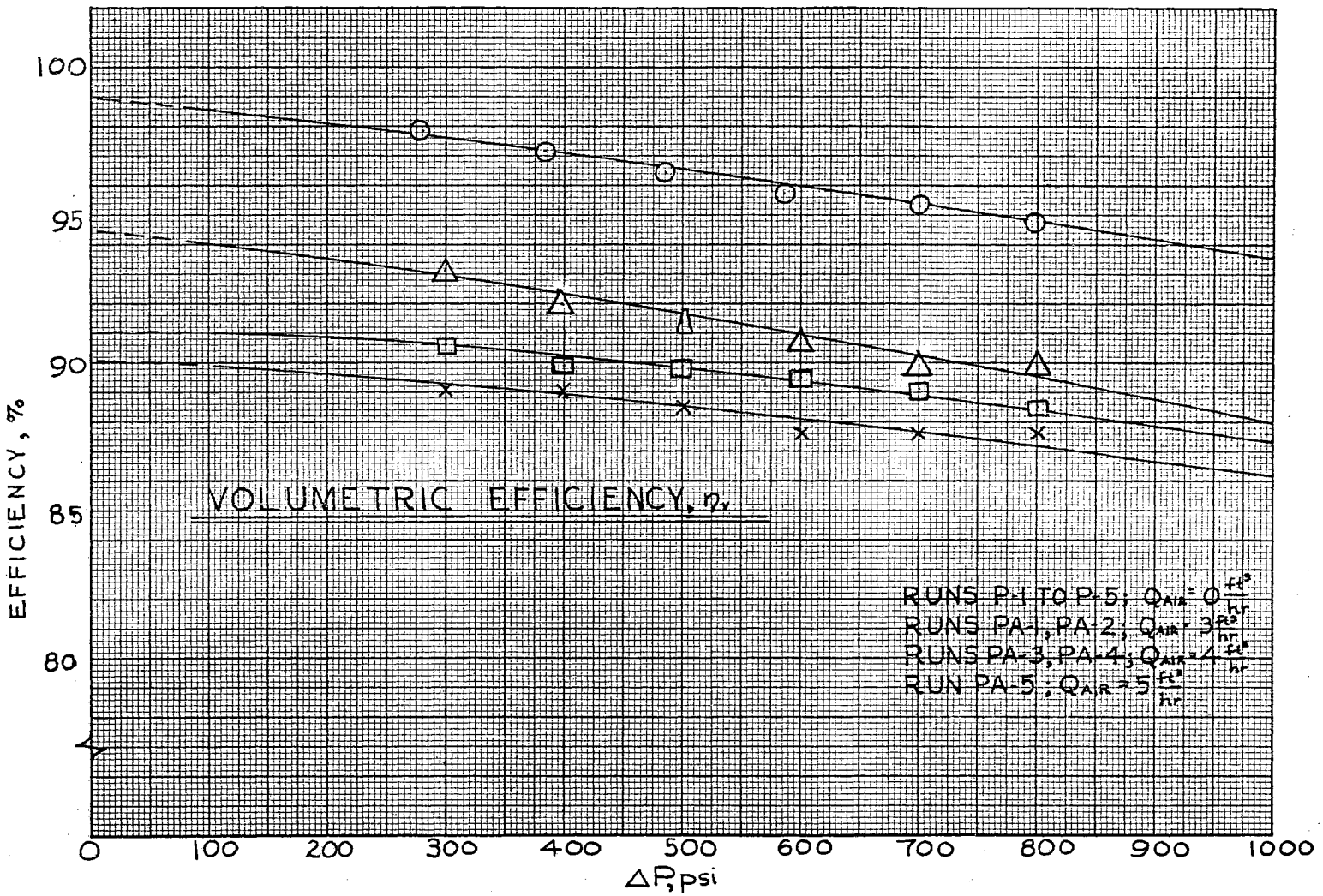

Figure 22. Experimental Variation of Volumetric Efficiency

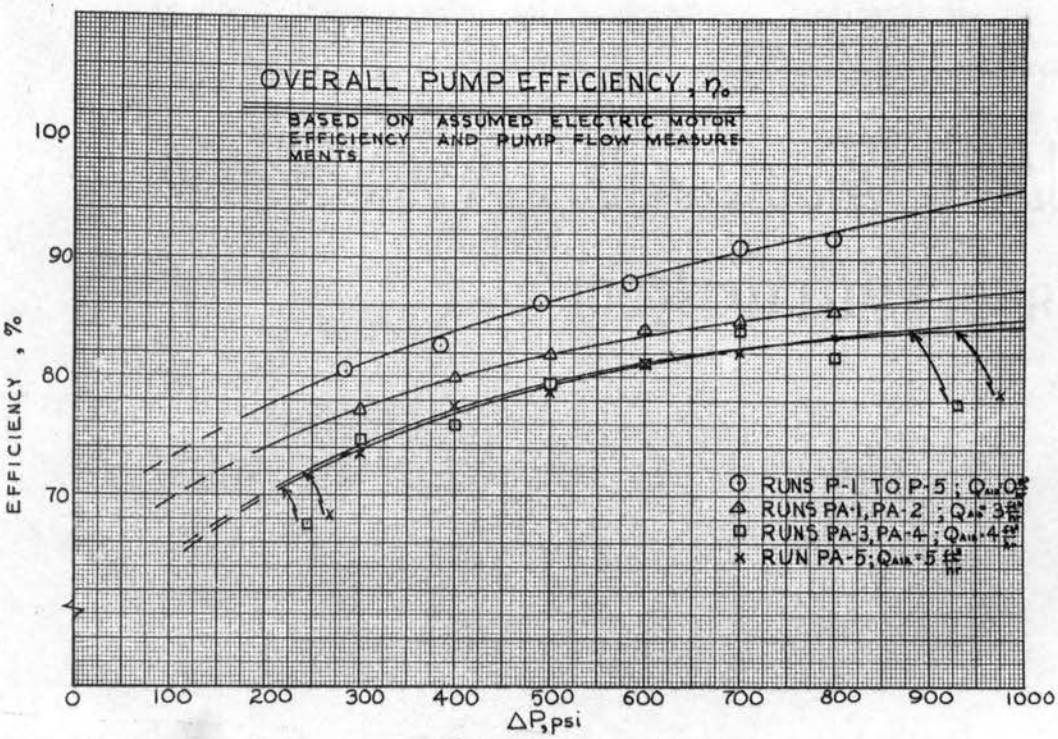

Figure 23. Theoretical Variation of Overall Pump Efficiency

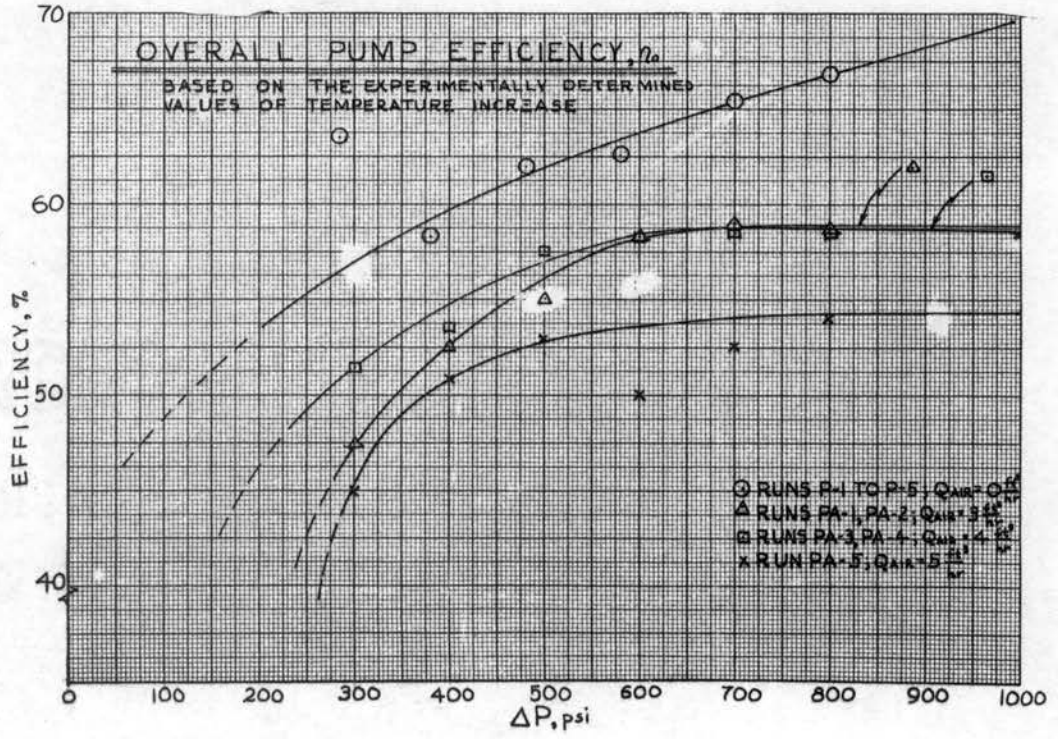

Figure 24. Experimental Variation of Overall Pump Efficiency

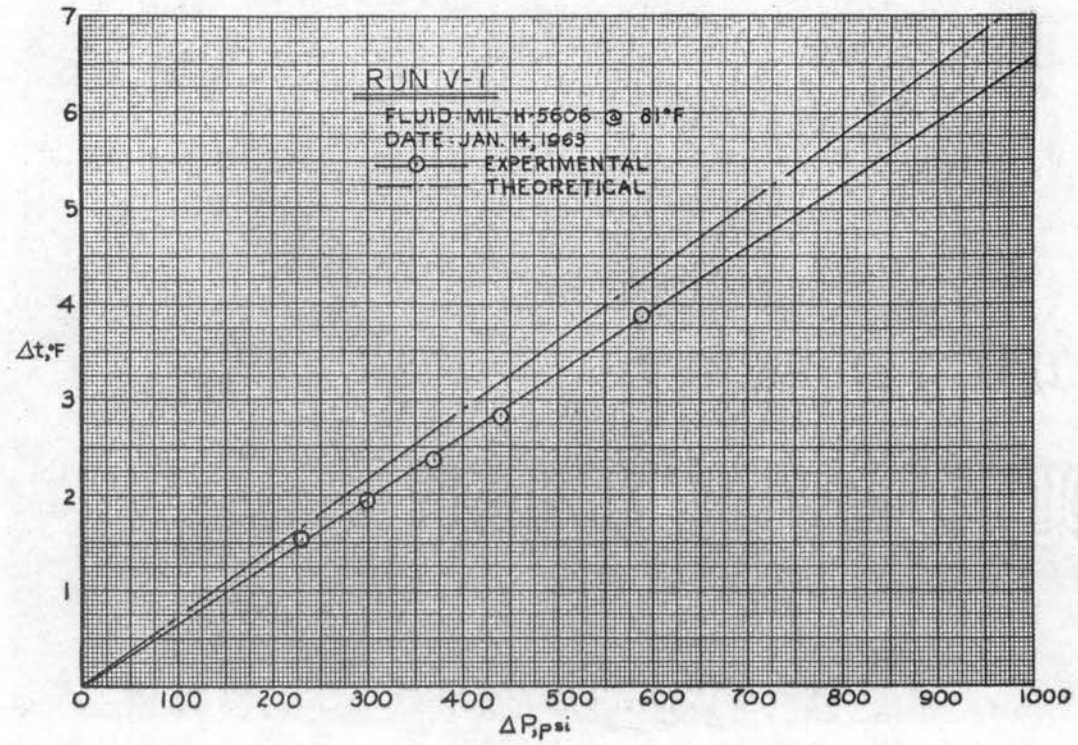

Figure 25. Run V-1

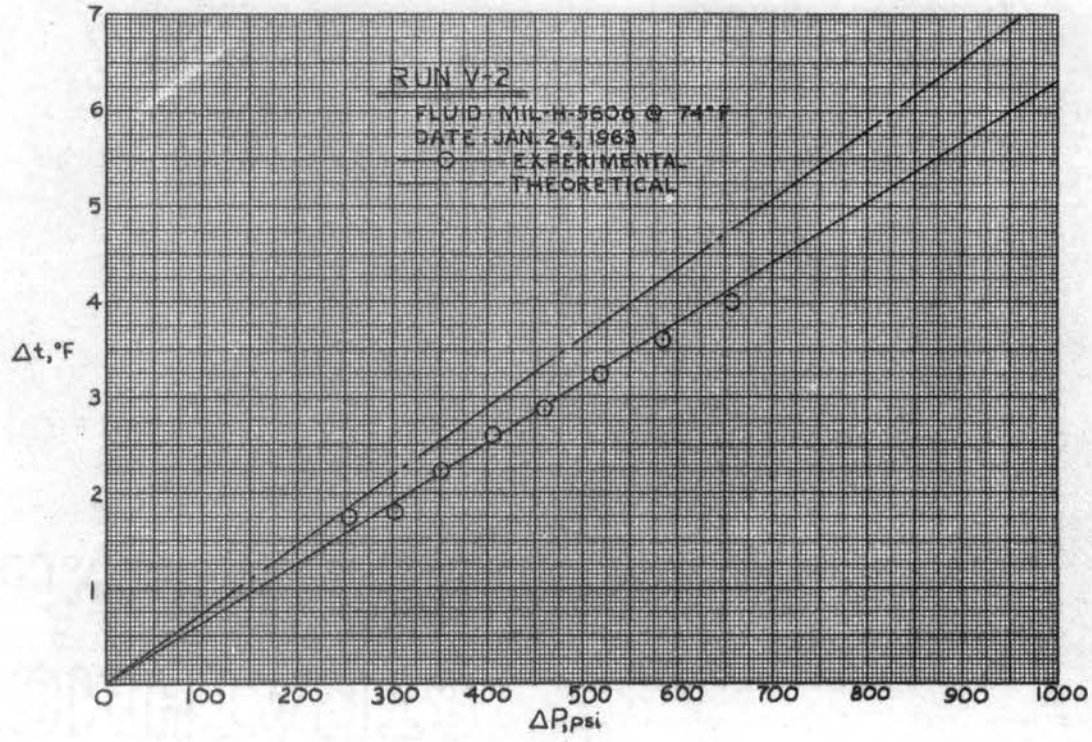

Figure 26. Run V-2

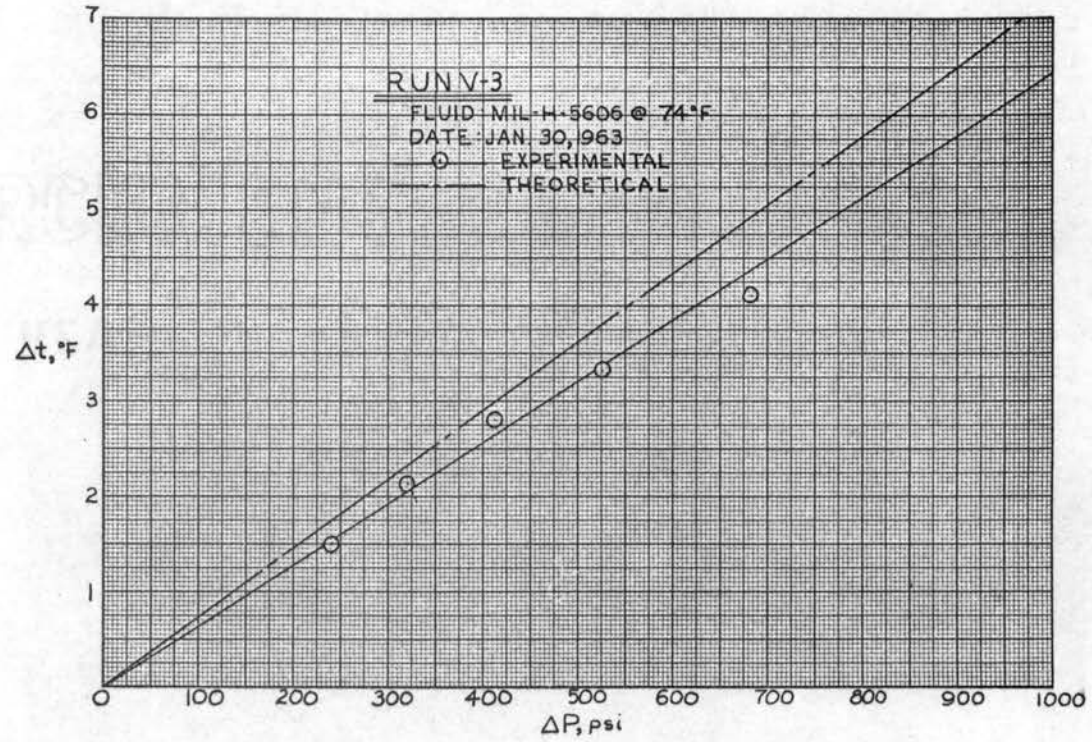

Figure 27. Run V-3

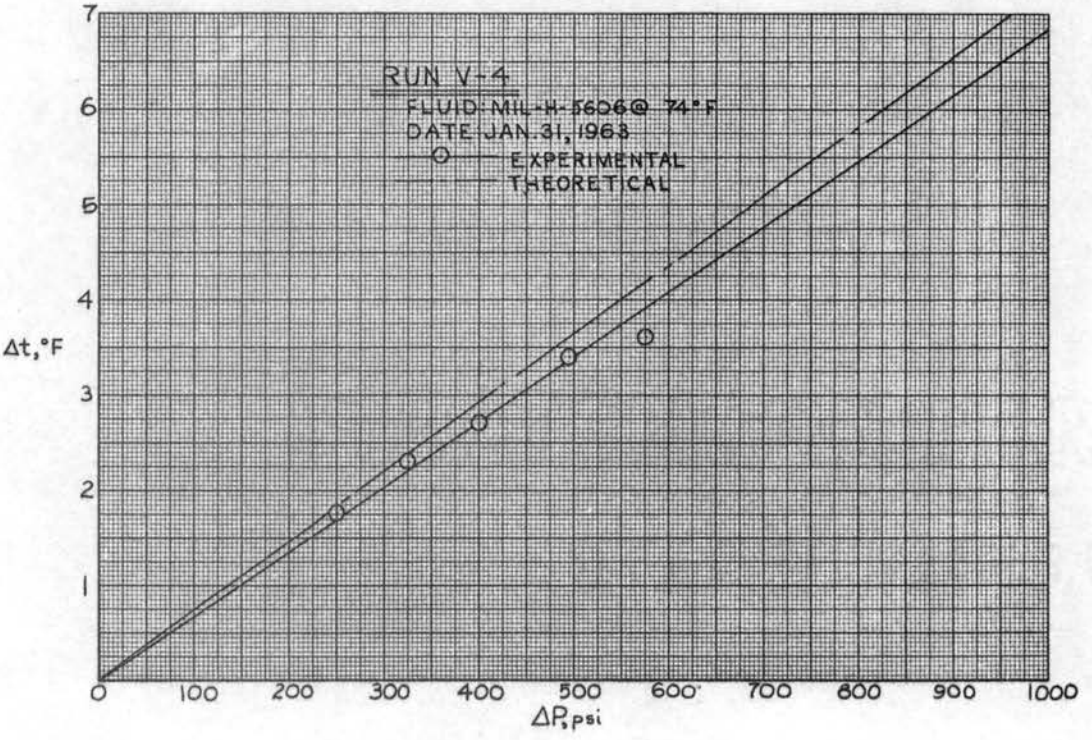

Figure 28. Run V-4

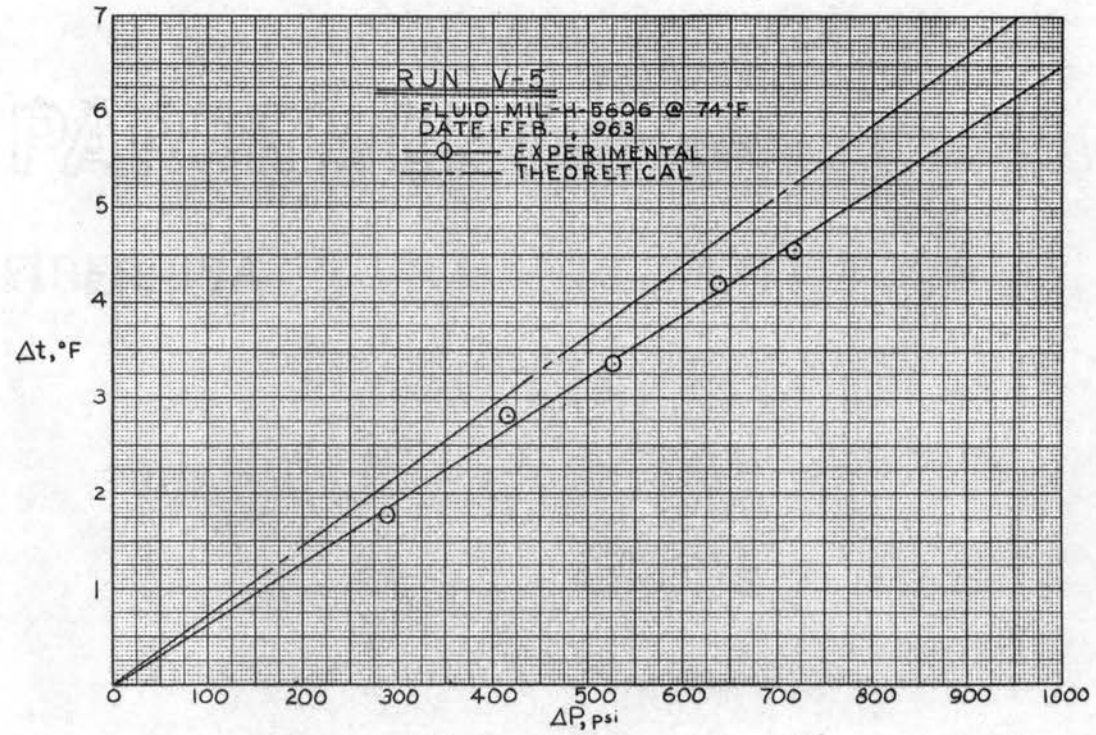

Figure 29. Run V-5

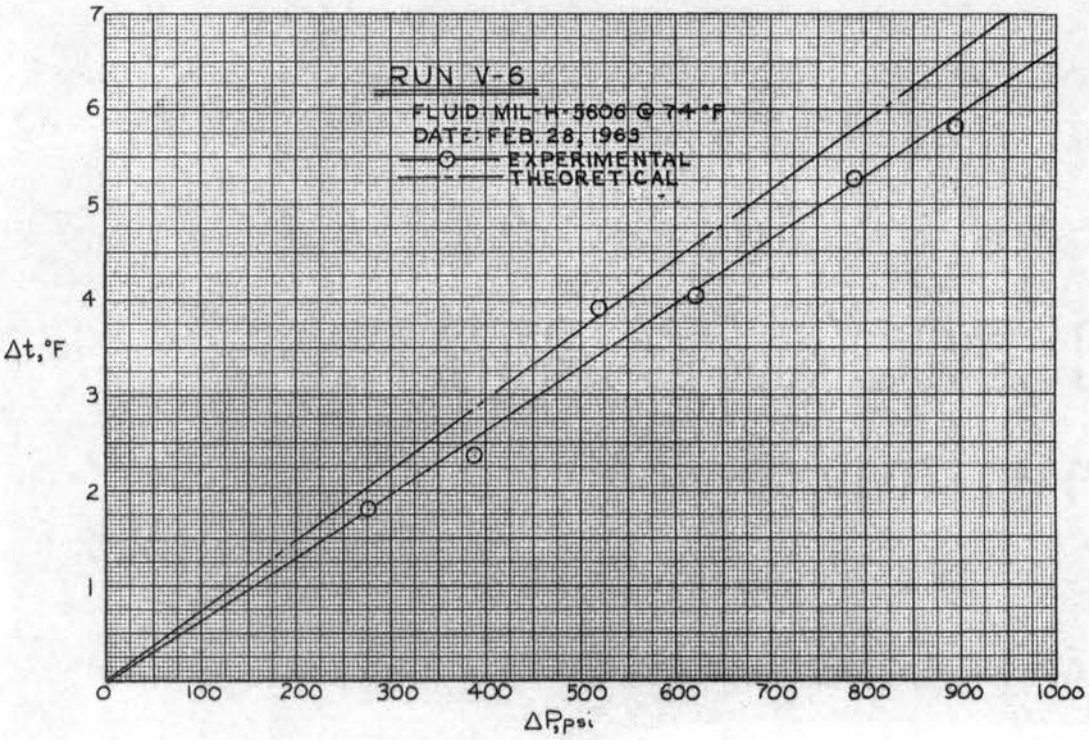

Run 30. Run V-6

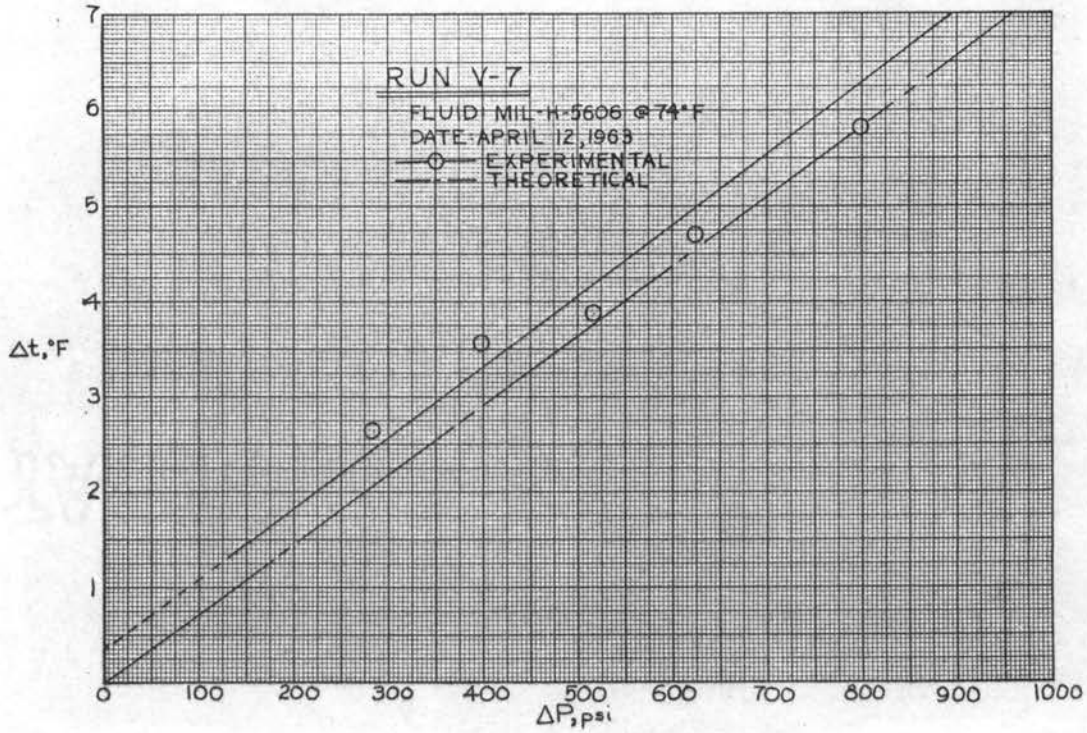

Figure 31. Run V-7

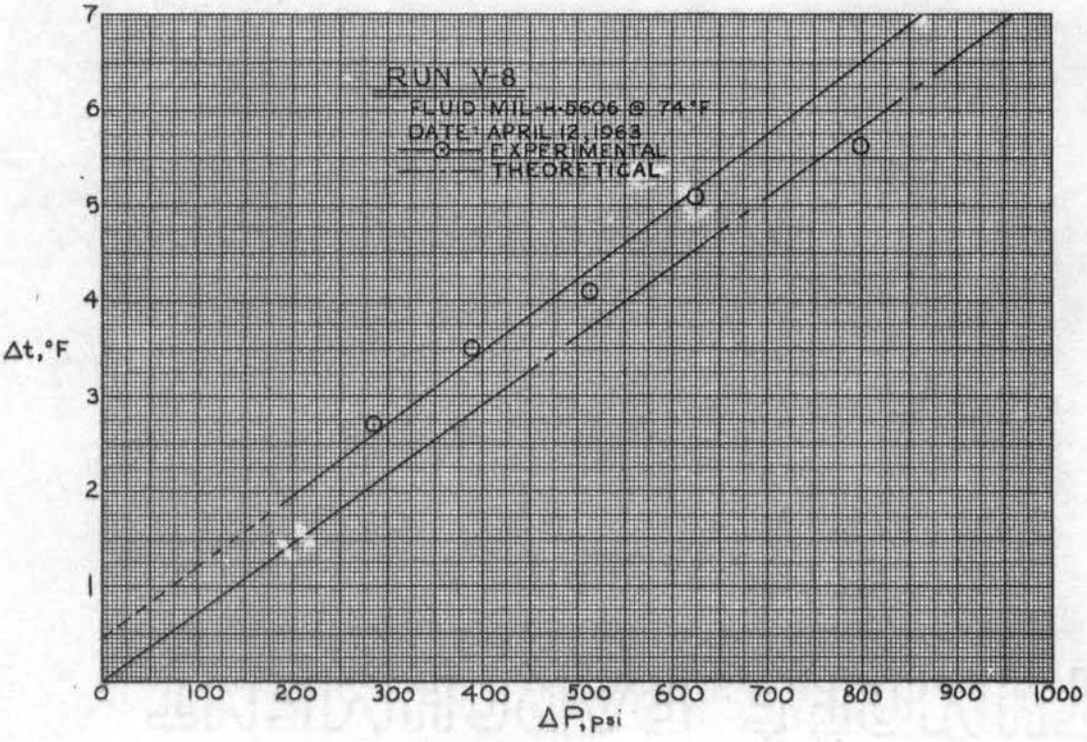

Figure 32. Run V-8

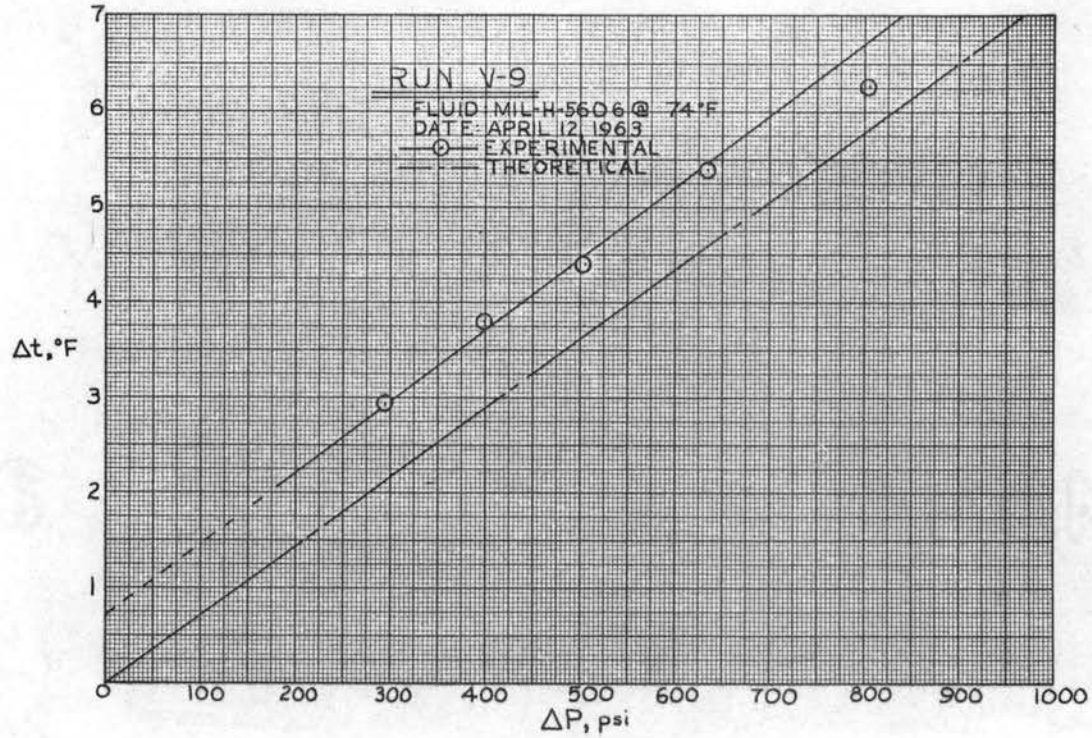

Figure 33. Run V-9

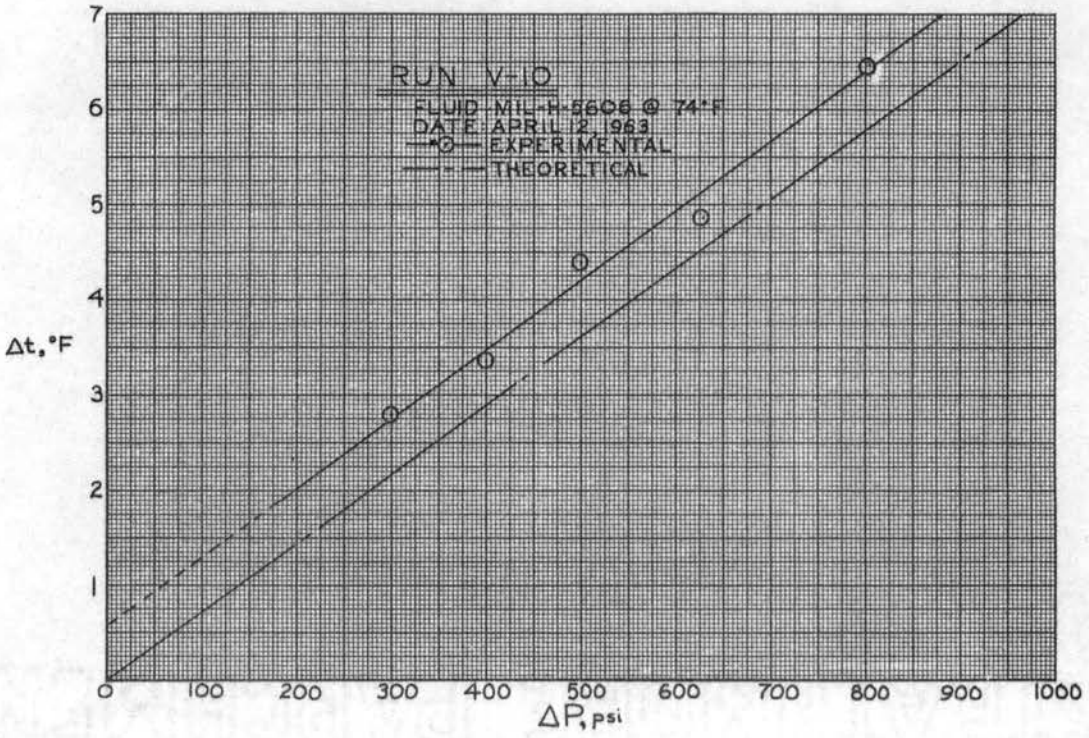

Figure 34. Run V-10

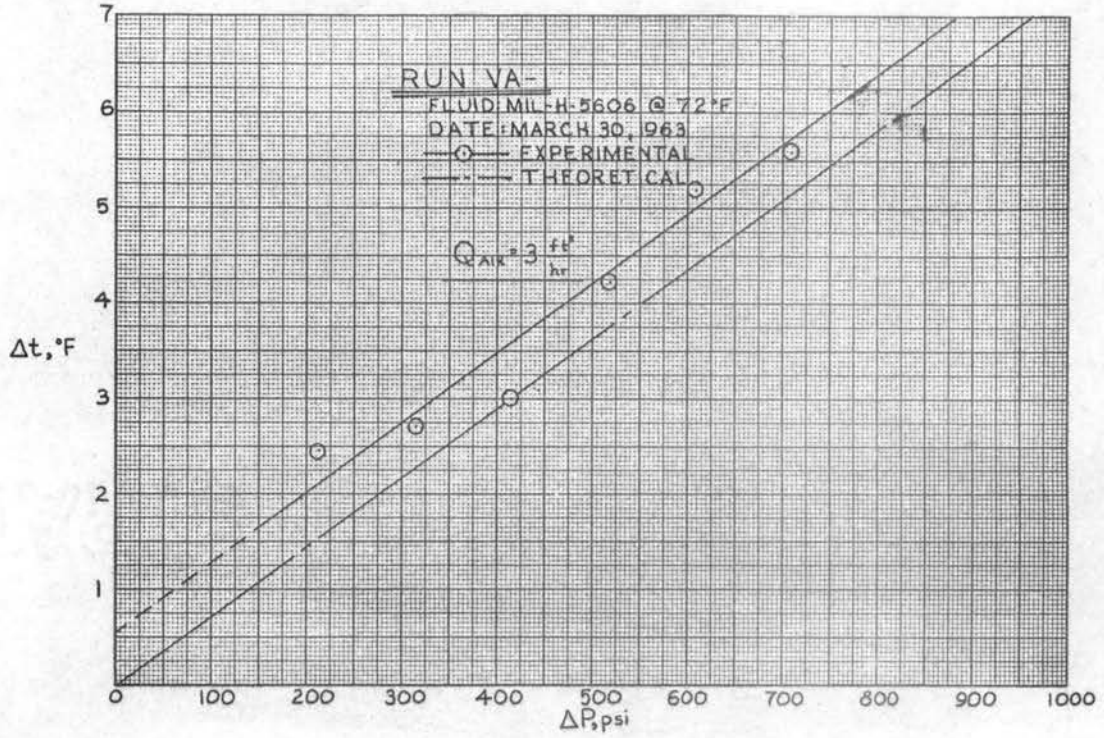

Figure 35. Run VA-1

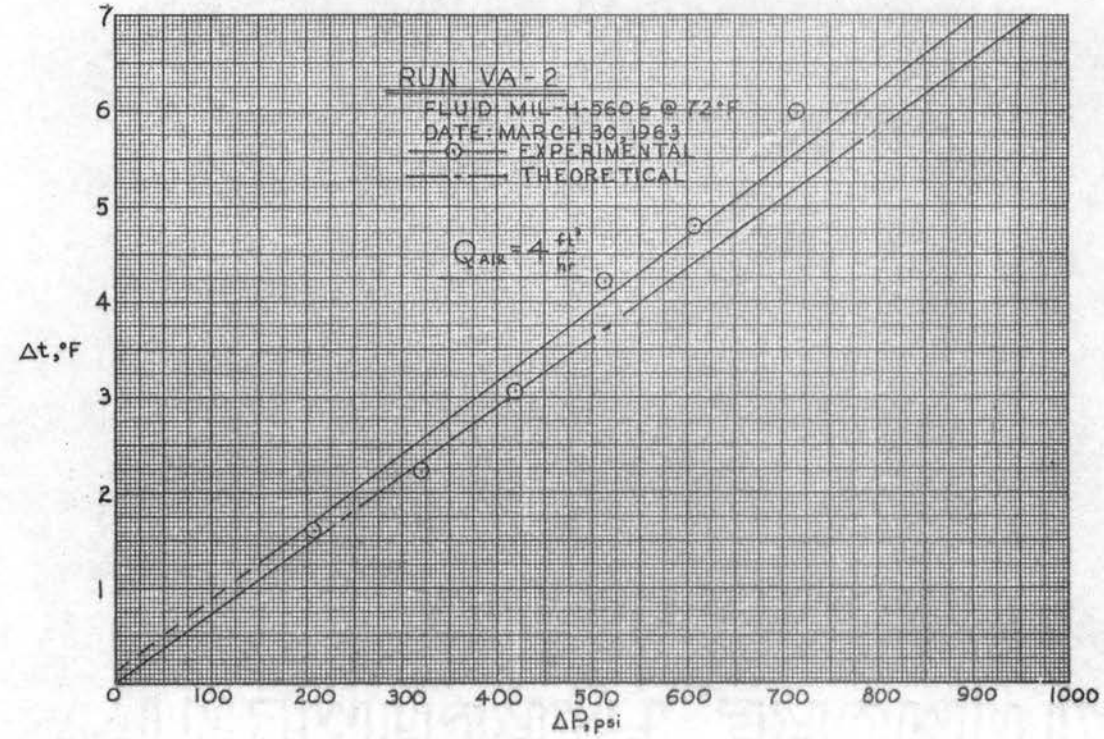

Figure 36. Run VA-2

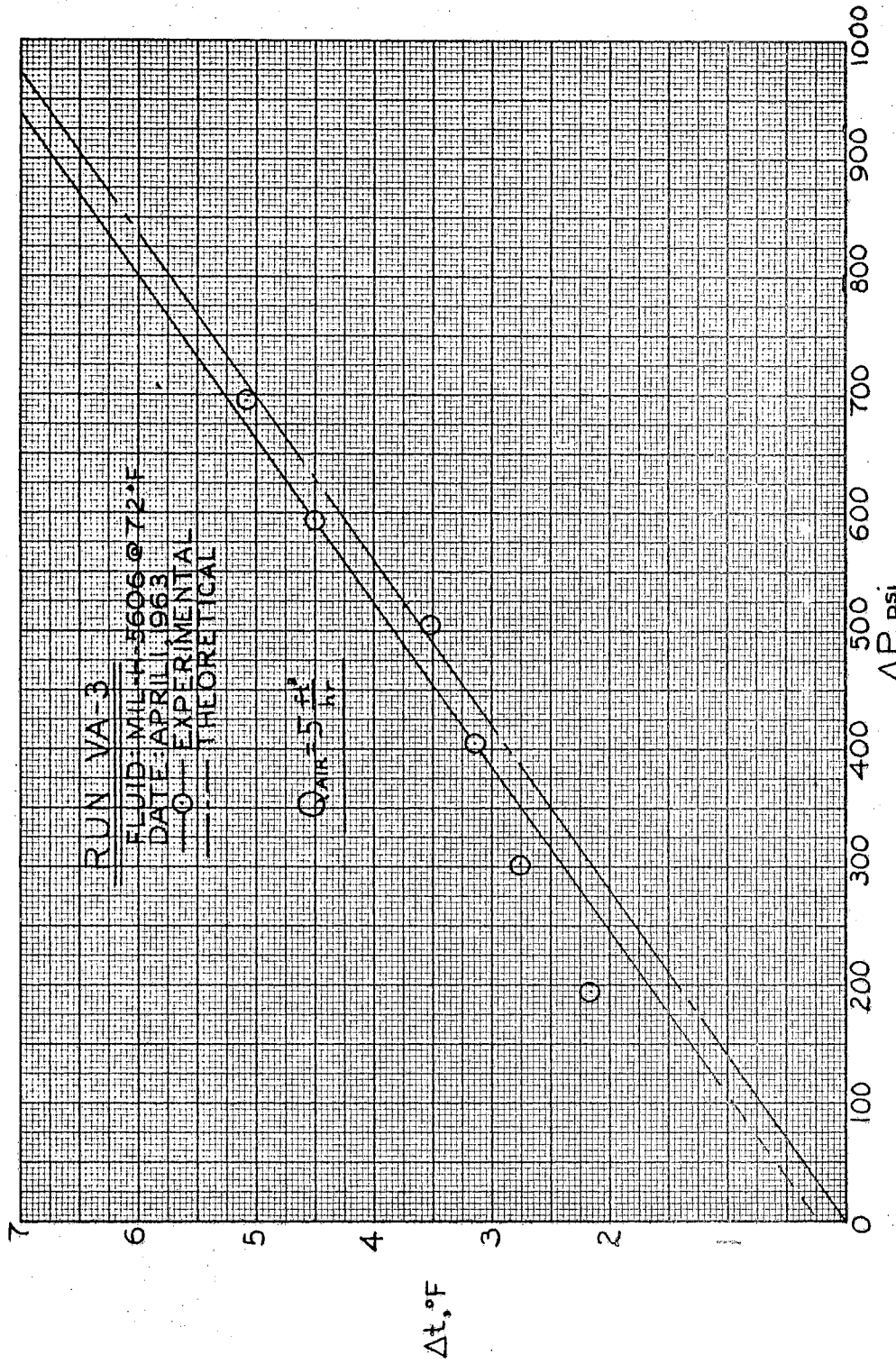

Figure 37. VA-3

experimental and theoretical results for the valve. The inability of the potentiometer to simultaneously measure both upstream and downstream temperatures appears as the most logical explanation although it does not adequately explain the large scattering of data. Again, the calibration curves for the thermocouples were almost identical indicating little error in a differential temperature measurement. When two potentiometer units were used, each unit was checked against the other, and both were found to read essentially the identical temperature.

Representative tabulations of the experimental results are shown in Table I and Table II of Appendix D.

CHAPTER VI

CONCLUSIONS AND RECOMMENDATIONS

The heat generation capabilities of the gear pump and needle valve were adequately described by the theoretical relationships in Equation 19 and Equation 27. The temperature increase due to pumping is a function of the overall pump efficiency for a given pressure differential and a given fluid. The effect of entrained air upon pump operation is to reduce the volumetric efficiency of the pump, thereby decreasing the overall pump efficiency and increasing the temperature differential at a given pressure level.

The temperature increase due to the throttling process of the needle valve is directly proportional to the pressure drop across the valve. Test results were inconclusive in determining the effect of entrained air upon the heat generation capabilities of the valve.

In review, the results obtained considered only adiabatic and steady-flow conditions, and only the common Mil-H-5606 petroleum base hydraulic oil was used as a fluid media.

In regard to future studies of this nature several recommendations can be made. Accurate and reliable temperature measurements could best be obtained through the use of a continuous reading, multi-channel recorder. Such an instrument would alleviate the problem of continually balancing the potentiometer and the errors introduced due to the time differential in measuring successive

temperatures.

The power stand should include adequate heat-exchanger capacity to maintain steady-state conditions at a desired reservoir temperature for system pressure differentials as high as 2000 psi. The various components should be tested at these high pressure levels to accurately determine the large heating effects as modern systems commonly operate in the 2000-3000 psi range.

A necessity in the pump testing is the accurate determination of input and output power in order to evaluate the overall pump efficiency.

Finally, air should be injected into the system in the form of finely divided bubbles in order to guarantee a uniform oil-air mixture. This could be accomplished by placing a separate screen at the point of air injection.

SELECTED BIBLIOGRAPHY

(1) Magnus, A.B. "Calculating Temperatures in Hydraulic Systems." Hydraulics and Pneumatics, November, 1962, 69-74.

(2) Wittren, R.A. "Techniques for Reducing Hydraulic System Overheating." Machine Design, July 5, 1962, 134-140.

(3) Douglas, J.K. "Heat--Its Generation and Natural Dissipation in Hydraulic Circuits." Bulletin 90030, The Oilgear Company, Milwaukee 4, Wisconsin, 1961, 4-8.

(4) "Temperature Control of Hydraulic Systems." Bulletin E23,02, Racine Hydraulics and Machinery, Inc., Racine, Wisconsin, June, 1959, 1-4.

(5) LeRoy, W. W., and R. L. Leslie. "Hydraulic Fluid Effects on System Performance." Machine Design, November, 1962, 186.

(6) MacKenzie, W.E., and J. Smith. "Measuring Air Solubility in Hydraulic Fluid." Hydraulic and Pneumatics, August, 1960, 80.

(7) Firth, Donald. "How to Measure Air Content in Hydraulic Fluids." Applied Hydraulics and Pneumatics, April, 1960, 88, 90.

(8) Bernd, L. H., R. L. Peeler, and L. H. Smith, Jr. "Hydraulic Fluid Bulk Modulus--Its Effect on System Performance and Techniques for Physical Measurement." National Conference on Industrial Hydraulics, October, 1960, 183-185.

(9) Louthan, G. W. "Hydraulic Noise Reduction by Fluid Conditioning." Product Engineering, April, 1952, 182-185.

(10) Pigott, R. J. S. "Cavitation in Reciprocating and Rotary Pumps," Sixth National Conference on Industrial Hydraulics, October, 1950, 49-51.

(11) Schanzlin, Ernest H. "Higher Speeds and Pressures for the Hydraulic Pump." Twelfth National Conference on Industrial Hydraulics, October, 1956, 38-40.

(12) Jones, James B. and George A. Hawkins, Engineering Thermodynamics, First Edition. New York: John Wiley and Sons, Inc., 1960, 54-77.

(13) Gray, Alexander, and G. A. Wallace. Principles and Practice of Electrical Engineering. Seventh Edition. New York: McGraw-Hill, Inc., 1955, 426.

(14) "Aeronautical Recommended Practice." ARP 24A, Society of Automotive Engineers, Inc., New York, 1958.

(15) Beckwith, T. G. and N. Lewis Buck. Mechanical Measurements. Second Edition. Reading, Massachusetts: Addison-Wesley Publishing Company, Inc., 1961, 384.

(16) Lembcke, R. K. "Investigation and Study of B-52H Hydraulic System Overheat Problems." Boeing Document Number T3-1292, Wichita 1, Kansas, July, 1962, 59-60.

(17) Hughes, J. Martin. "Experimental Determination of Transverse Temperature Profiles for Oil Flowing in a Circular Tube." M. S. Thesis, Oklahoma State University, 1962.

APPENDIX A

SAMPLE CALCULATIONS

Calculation 1:

As stated on page 16, the term

$$t\left(\frac{\partial v}{\partial t}\right)_p \left(p_2 - p_1\right)$$

was neglected in Equation 14. The fact that this term can be neglected is illustrated in the calculations based on the following assumptions:

1. Pressure differential of 800 psi and average temperature of 80° F.
2. A specific volume of 0.01925 $\frac{ft^3}{lb_m}$.
3. A volume expansivity of 0.39×10^{-3} $\frac{1}{°F}$.

   This is the value for a light oil and was used since no data of this type was available for Mil-H-5606.

Since the volume expansivity, β, is expressed as

$$\beta = \frac{1}{v}\left(\frac{\partial v}{\partial t}\right)_p \qquad \text{(A-1)}$$

then

$$\beta v = \left(\frac{\partial v}{\partial t}\right)_p \qquad \text{(A-2)}$$

Therefore, the neglected term is rewritten as

$t\beta v\ (p_2 - p_1)$. Thus,

$$t\beta v\ (p_2 - p_1) = (540)(.390 \times 10^{-3})\ (1.925 \times 10^{-2})$$

$$(800)(778/144) = 0.601\ \frac{btu}{lb_m} \tag{A-3}$$

If the latter term had not been neglected, the temperature rise across the pump could have been expressed as

$$t_2 - t_1 = \frac{(p_2 - p_1)}{62.4\ c_p\ \gamma} \left[\frac{1 - \eta_o\ (1 + t\beta)}{\eta_o}\right] \tag{A-4}$$

Calculation 2:

The $\frac{\dot{m}_a}{\dot{m}_o}$ term was neglected based on calculations made from actual test data. This ratio was determined using the largest air flow rate and the smallest oil flow rate. The oil flow rate was found to be

$$\dot{m}_o = 12.1\ gpm = 84.0\ \frac{lb_m}{min} \tag{A-5}$$

The air was injected at a vacuum of 2" Hg and a temperature of 75° F. considering the air as an ideal gas, then

$$\dot{m}_a = \frac{p\dot{V}}{Rt}\ \frac{(13.7)\ (144)\ (5)}{(53.3)\ (535)\ (60)} = 0.00576\ \frac{lb}{min} \tag{A-6}$$

where

$\dot{V}$ = volume flow rate
R = gas constant.

Thus,

$$\frac{\dot{m}_a}{\dot{m}_o} = \frac{5.76\ (10^{-3})}{8.40\ (10)} = 6.86\ (10^{-4}) \tag{A-7}$$

Calculation 3:

The pump and valve were considered as spheres having a thermal conductivity of

$25 \frac{btu}{hr\text{-}ft\text{-}^{o}F}$.

Since the conductivity was so high, it was assumed that no temperature gradients existed in the pump and valve housings and that the exterior temperatures for both were essentially the same temperature as the fluid passing through them. The additional assumptions were:

1. Room temperature = 72° F.
2. Pump temperature = 75° F.
3. Valve temperature = 79° F.
4. Thermal conductivity of insulation material = $0.22 \frac{btu}{hr\text{-}ft\text{-}^{o}F}$.
5. Outside radius of insulation on pump = 5 inches.
6. Inside radius of insulation on pump = 4.0 inches.
7. Outside radius of insulation on valve = 3.5 inches.
8. Inside radius of insulation on valve = 3.0 inches.

Using the relation for pure radial heat conduction

$$q = \frac{4\pi k r_1 r_2}{(r_2 - r_1)} (t_1 - t_2) \qquad (A\text{-}8)$$

in which K = thermal conductivity. The heat losses for the pump and valve are

$$q_p = \frac{4\pi(.22)(1/3)(5/12)}{(5/12 - 1/3)} (75 - 72) = 13.8 \frac{btu}{hr} \qquad (A\text{-}9)$$

$$q_v = \frac{4\pi(.22)(3.5/12)(1/4)}{(3.5/12 - 1/4)} (79 - 72) = 33.8 \frac{btu}{hr} . \qquad (A\text{-}10)$$

APPENDIX B

CALIBRATION DATA

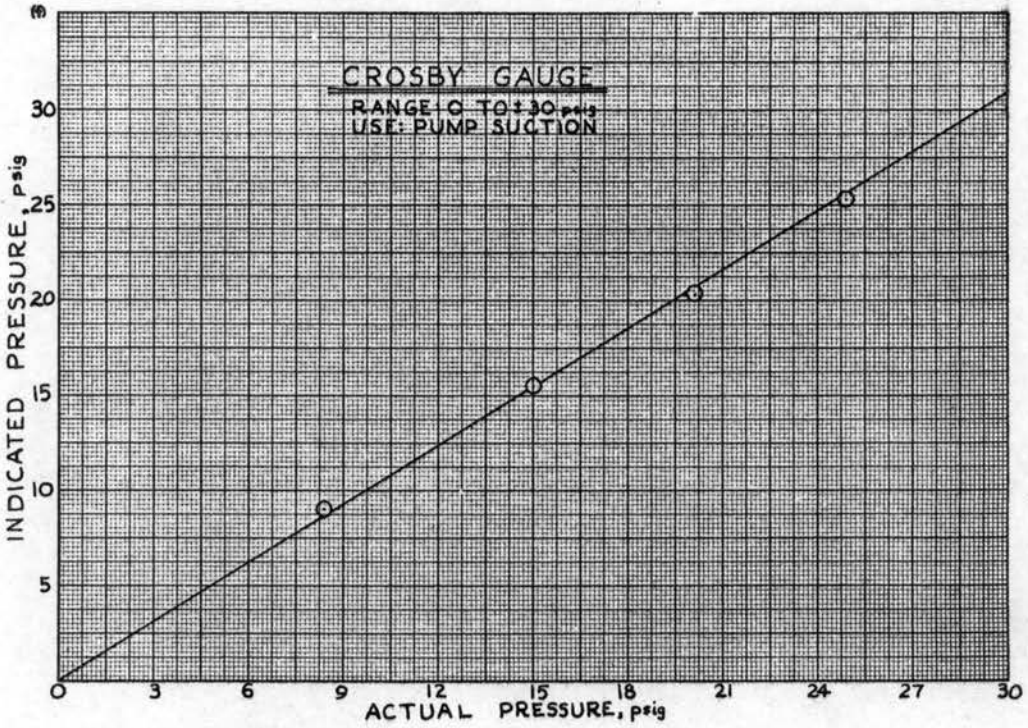

Figure 38. Crosby Gauge Calibration

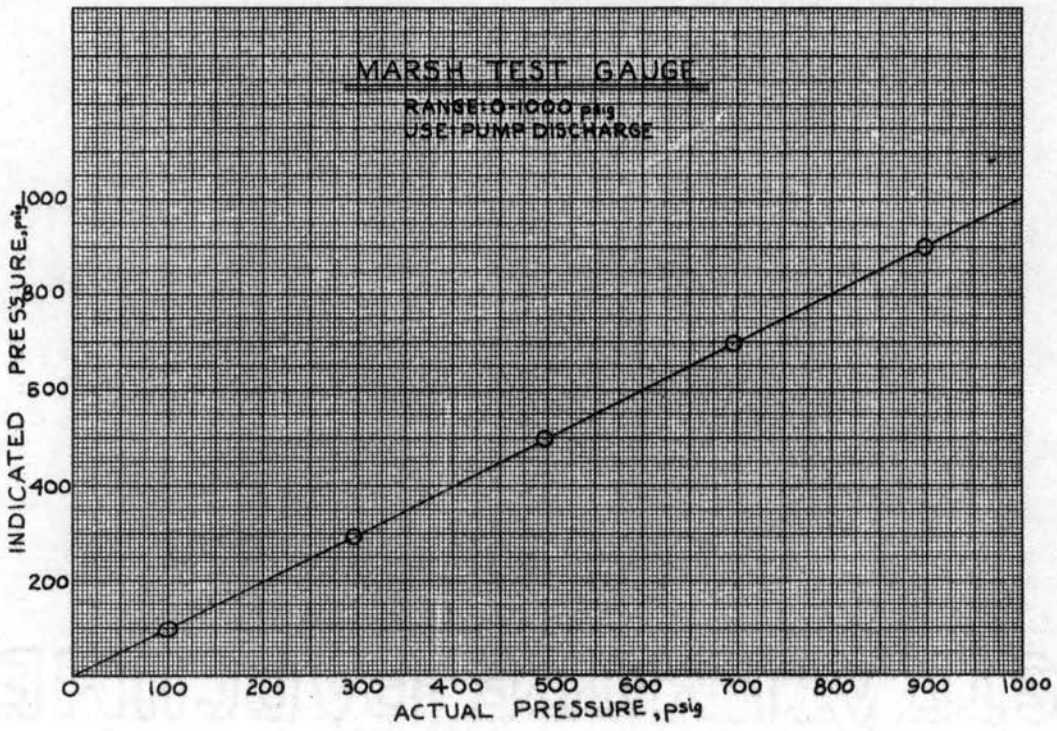

Figure 39. Marsh Test Gauge Calibration

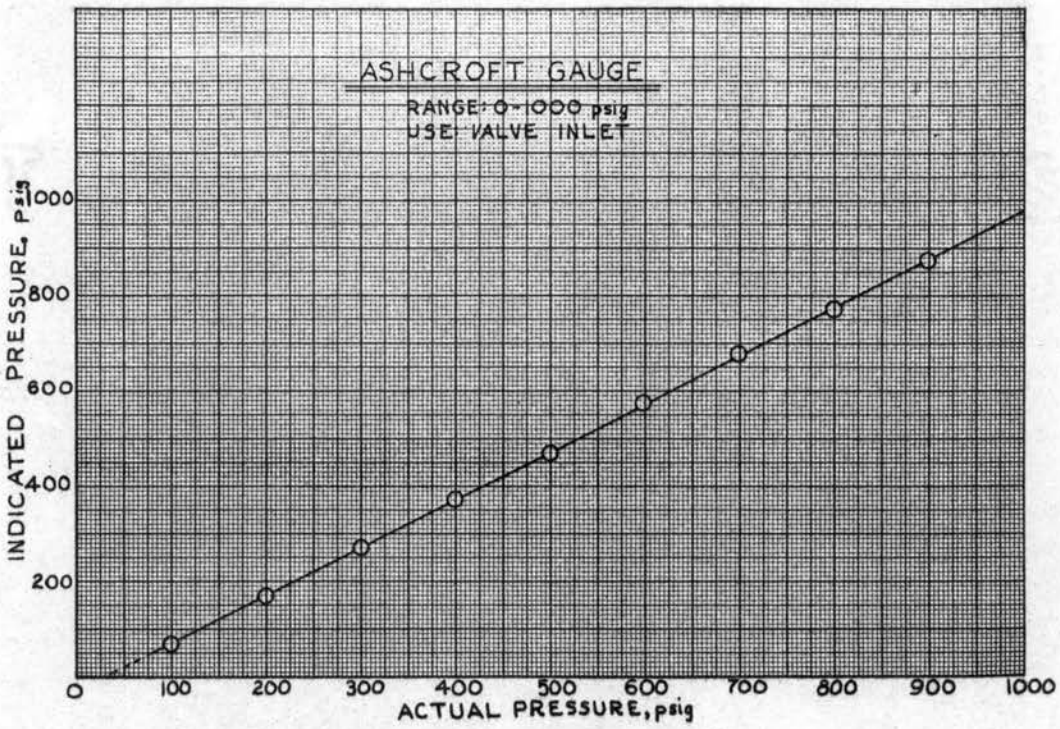

Figure 40. Ashcroft Gauge Calibration

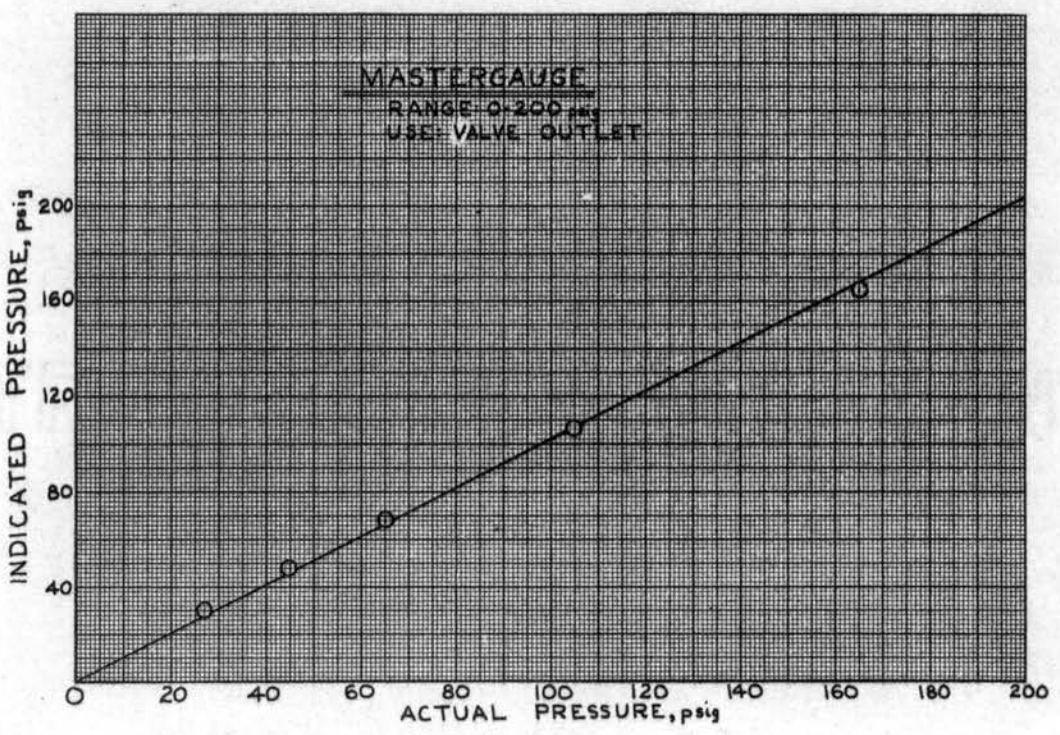

Figure 41. Mastergauge Calibration

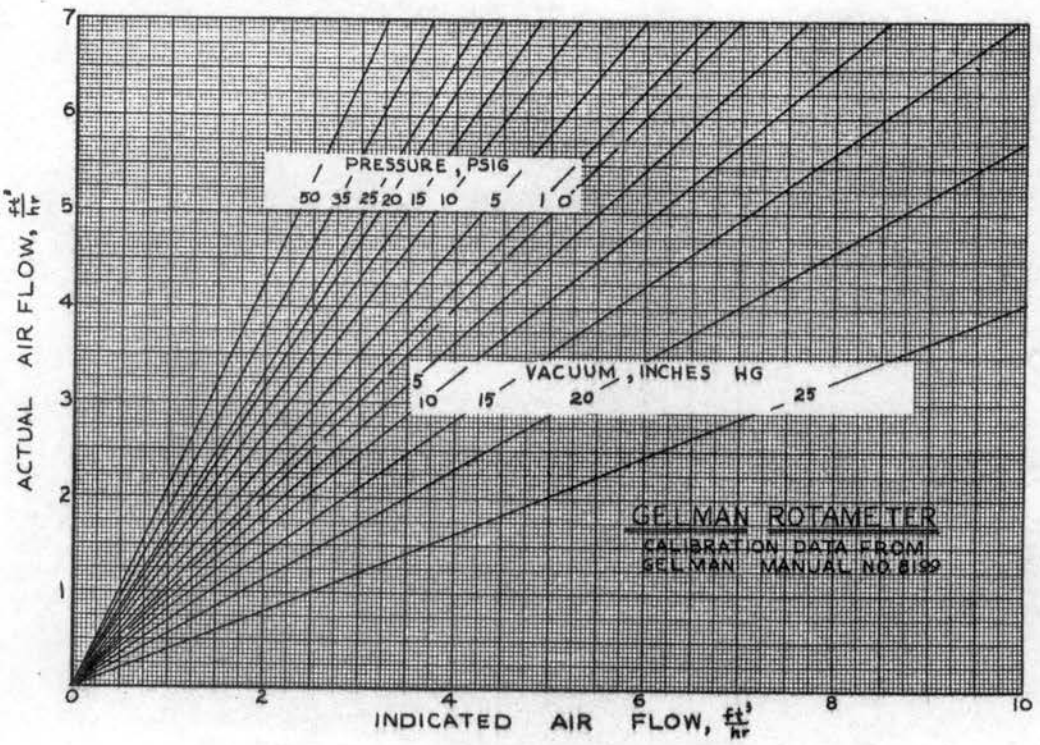

Figure 42. Rotameter Calibration

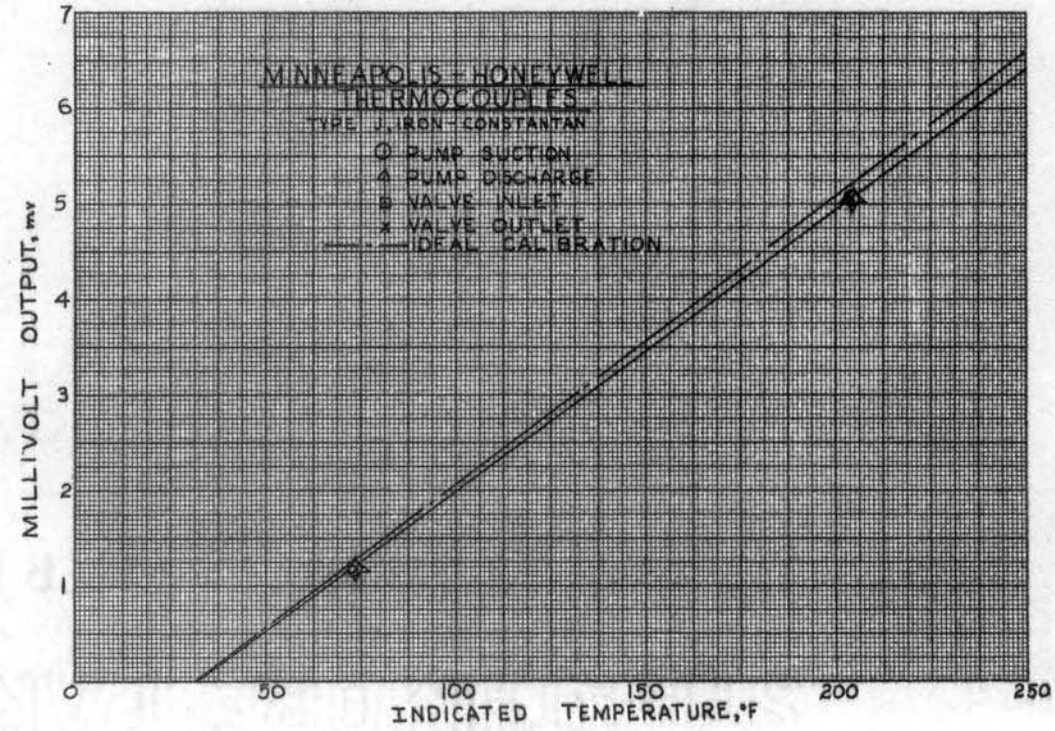

Figure 43. Thermocouple Calibration

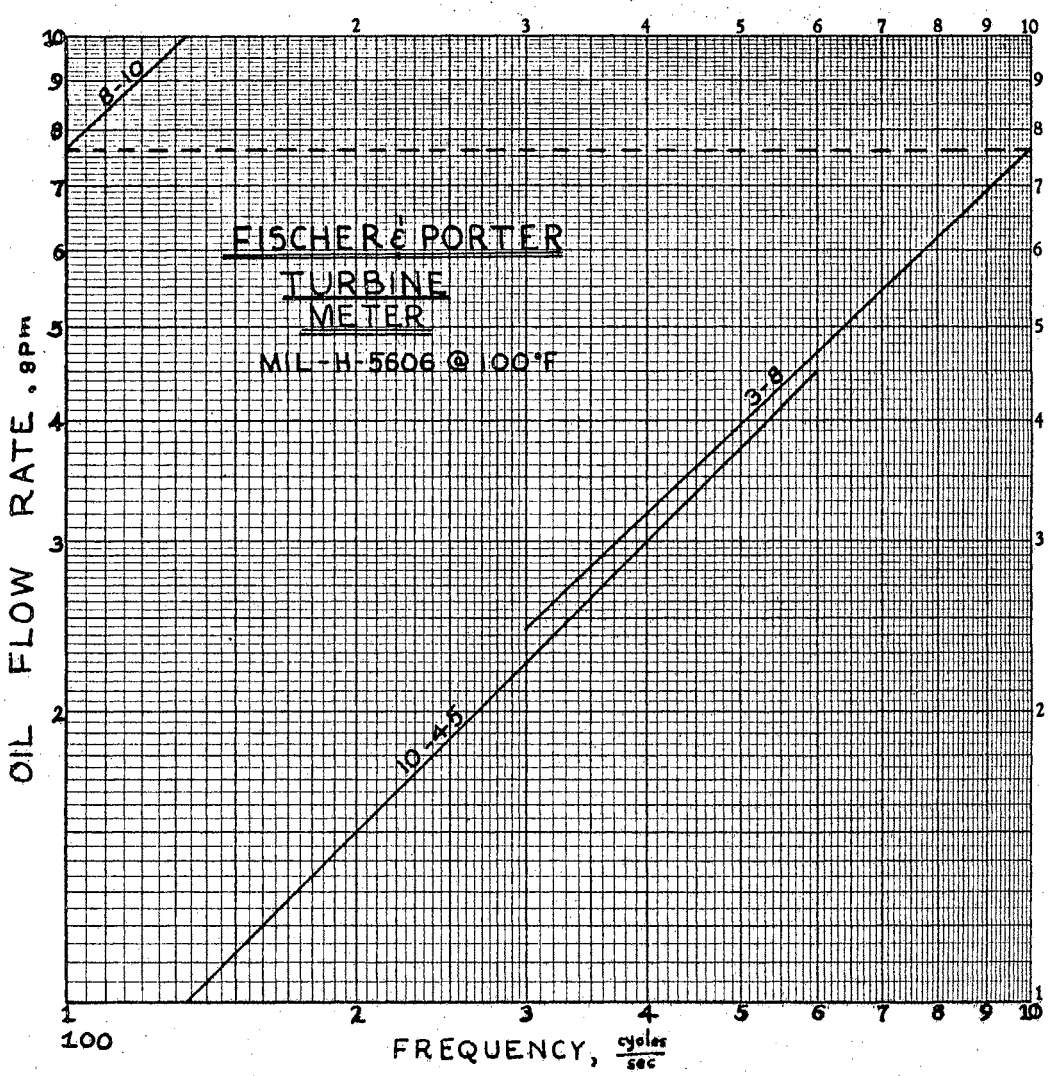

Figure 44. Turbine Meter Calibration

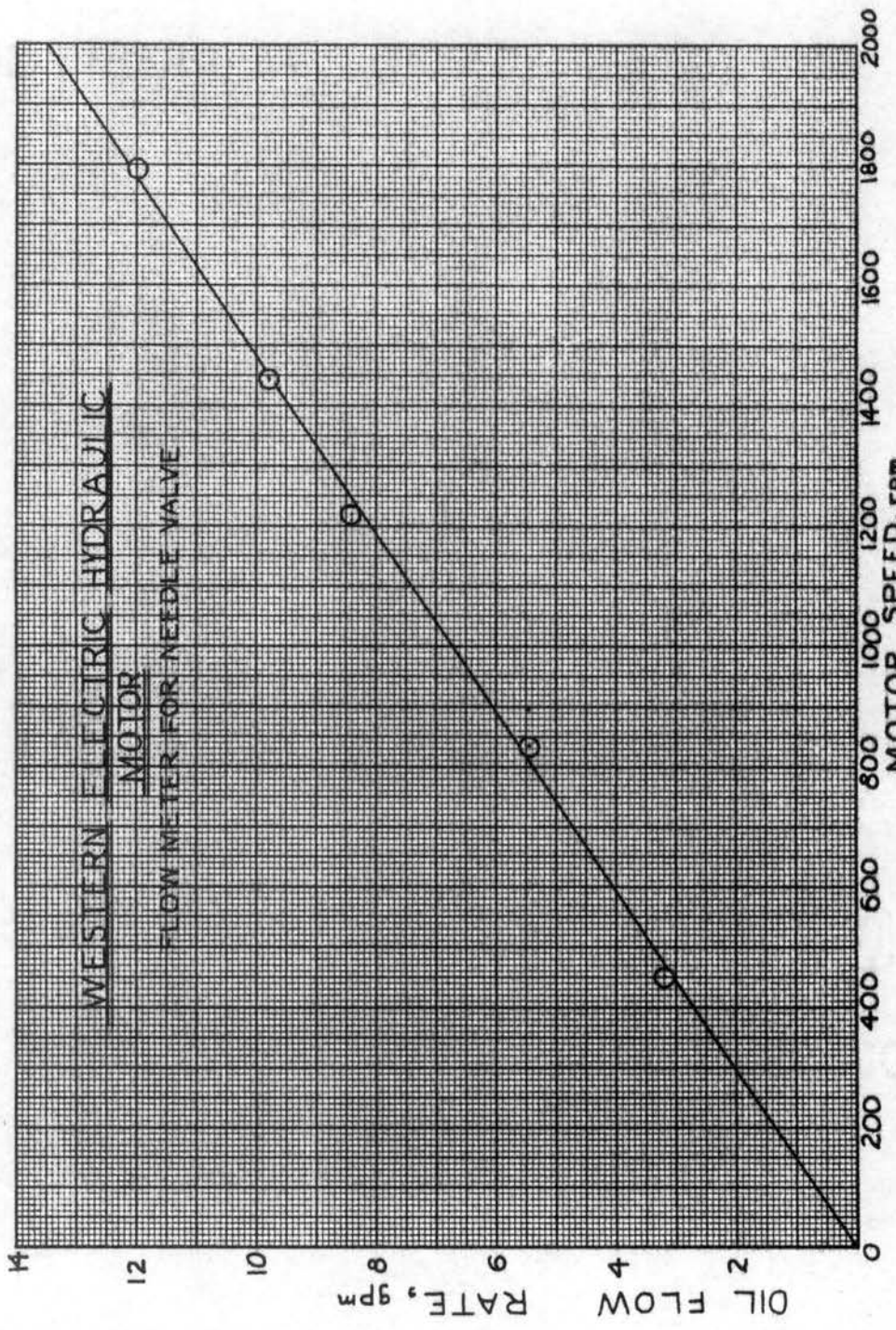

Figure 45. Hydraulic Motor Calibration

APPENDIX C

FLUID PROPERTIES

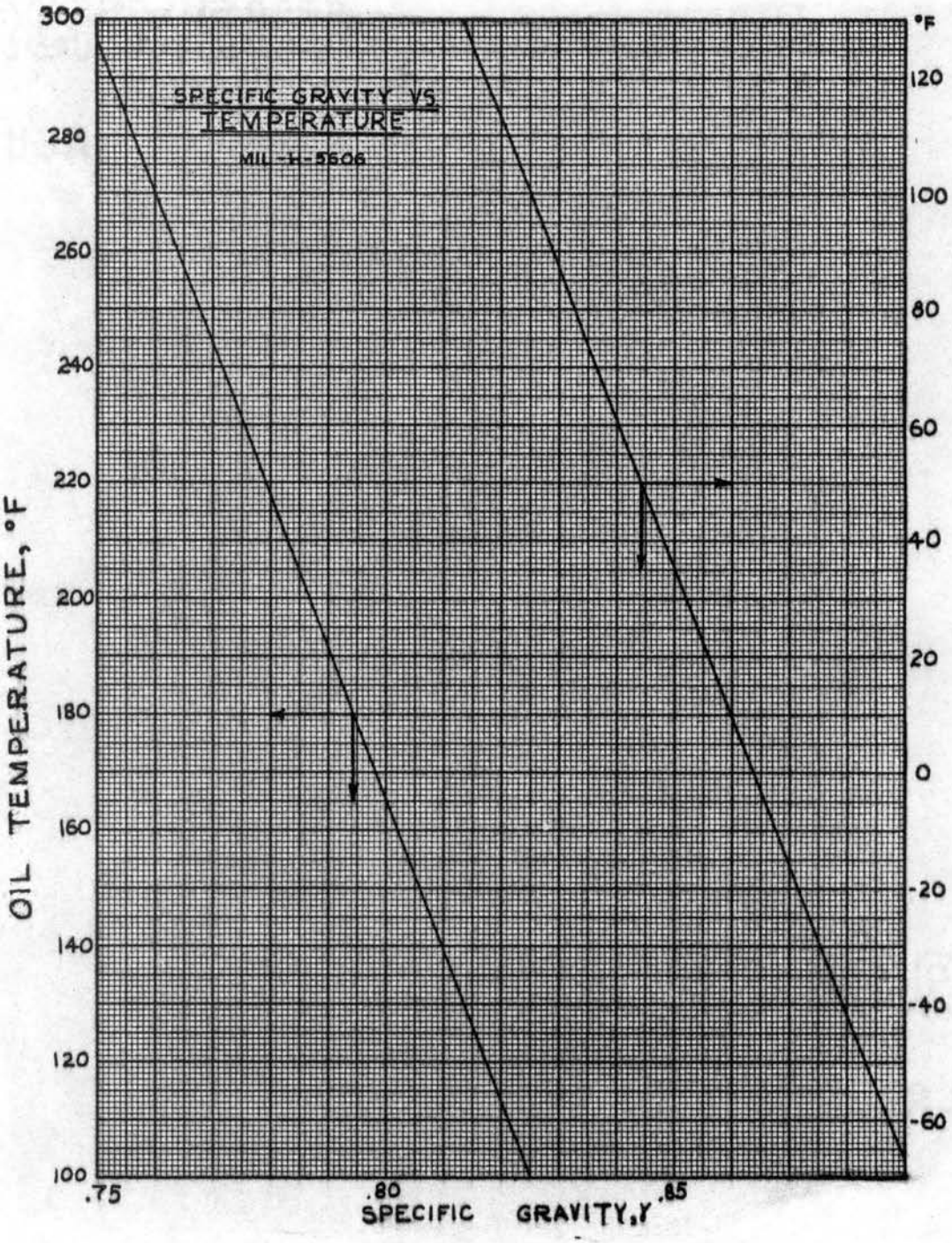

Figure 46. Specific Gravity Versus Temperature

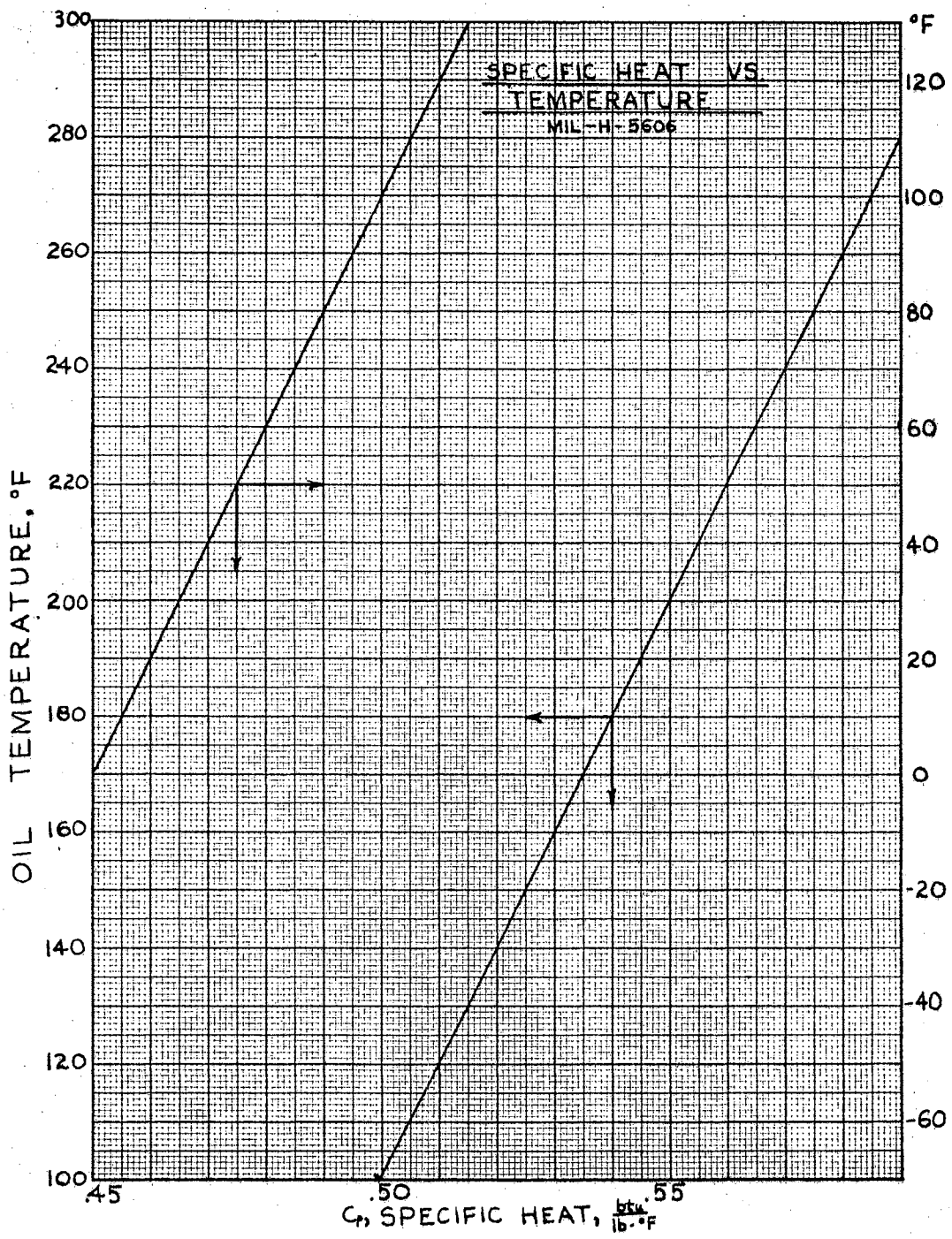

Figure 47. Specific Heat Versus Temperature

APPENDIX D

REPRESENTATIVE TABULATION OF DATA

TABLE I

RUN PA-3

EMF OUTPUT		PUMP FLOW				PUMP AND MOTOR POWER					PUMP EFF.		FLUID PARAMETERS					
Upstream	Downstream	CPS	RPM_{EM}	Q_{ACT}	Q_T	KW	PF	HP_{ACT}	HP_M	HP_P	η_v	η_o	P_{UP}	P_{DOWN}	ΔP	t_{UP}	Δt_A	Q_{air}
1.110	1.172	167	1875	12.5	13.8	3.00	.445 19.0 208	4.020	2.94	2.196	90.6	74.6	.983	300	301	71.33	2.07	4
1.106	1.182	166	1875	12.4	13.8	3.70	.515 19.8 209	4.960	3.80	2.196	89.9	75.8	.983	400	401	71.20	2.53	4
1.120	1.201	166	1875	12.4	13.8	4.35	.565 21.0 210	5.830	4.57	2.880	89.9	79.4	.983	500	501	71.67	2.70	4
1.107	1.201	165	1875	12.35	13.8	4.97	.610 22.2 209	6.660	5.33	3.630	89.5	81.3	.983	600	601	71.23	3.14	4
1.111	1.219	164	1875	12.3	13.8	5.57	.665 23.2 208	7.470	6.01	4.330	89.1	83.8	.983	700	701	71.37	3.60	4
1.120	1.244	163	1875	12.2	13.8	6.45	.700 24.8 208	8.640	7.03	5.035	88.5	81.4	.983	800	801	71.67	4.13	4

TABLE II

RUN V-2

EMF OUTPUT		VALVE FLUID PARAMETERS						
Downstream	Upstream	P_{up}	P_{down}	P	t_{up}	t_{down}	t	Q_{air}
1.299	1.256	299	42	257	76.2	77.95	1.875	0
1.294	1.247	348	45	303	75.9	77.7	2.205	0
1.310	1.253	400	49	351	76.10	78.33	2.56	0
1.299	1.239	400	49	351	75.63	77.95	2.56	0
1.314	1.246	462	49	413	75.866	78.466	3.00	0
1.335	1.259	513	52	461	76.3	79.17	3.36	0
1.342	1.255	573	52	521	76.17	79.40	3.80	0
1.372	1.274	635	50	585	76.80	80.40	4.25	0
1.386	1.276	708	49	659	76.87	80.87	4.80	0

APPENDIX E

EXPERIMENTAL APPARATUS

1. Hydraulic Power Stand:

   Designed and built by graduate research assistants at Oklahoma State University, Stillwater, Oklahoma.

2. Electric Motor:

   Manufacturer: Westinghouse Electric Corporation
   Type: CS, Serial No. 5308, Style 1071064, 3-phase inductor type, 20 hp., 220/440 volts, 24.5/49 amps., 60 cps.

3. External Gear Pump:

   Manufacturer: Cessna Aircraft Company
   Model L20106
   Pressure: 2000 psi
   Maximum Speed: 2750 rpm
   Displacement: 1.70 in^3 per revolutions.

4. Thermocouples:

   Manufacturer: Minneapolis-Honeywell Regulator Company
   Type J, Iron-Constantan
   Style: Megopak, Quik-Konnect.

5. Millivolt Potentiometer:

   Manufacturer: Leeds and Northrup Company
   Model 8686.

6. Thermocouple Switch:

   Manufacturer: C. J. Tagliabue Manufacturing Company
   12-position switch.

7. Industrial Analyzer:

Manufacturer: Weston Electric Instrument Corporation
Type 2, Serial No. 357, Model 639.

8. Turbine Meter:

Manufacturer: Fischer and Porter Company
Model 10C1505.

9. Turbine Frequency Counter:

Manufacturer: Fischer and Porter Company
Model S-44K.

10. Amplifier:

Manufacturer: Hewlett-Packard
Model 450A.

11. EPUT Meter:

Manufacturer: Beckman-Berkley Division
Model 5210D.

12. Hydraulic Motor:

Manufacturer: Webster Electric Company
Type 2HCSF-3, Serial No. 104725B4.

13. Hand Tachometer:

Manufacturer: James G. Biddle Company
Serial No. 104725B4.

14. Rotameter:

Manufacturer: Gelman Instrument Company
Range: 0-10 ft^3 per hr.

VITA

George Bruce Gibson

Candidate for the Degree of

Master of Science

Thesis: HEAT GENERATION CAPABILITIES OF AN EXTERNAL GEAR PUMP AND NEEDLE VALVE

Major Field: Mechanical Engineering

Biographical:

Personal Data: Born in Oklahoma City, Oklahoma, January 26, 1939, the son of George Earl and Allice Corinne Gibson.

Education: Graduated from Hillcrest High School of Dallas, Texas in 1957; received the Bachelor of Science degree from Texas Technological College with a major in Mechanical Engineering in May, 1962; completed the requirements for the Master of Science degree in May, 1963.

Experience: The writer has been employed as an Engineering Aid by Ling-Temco-Vought, Dallas, in the summers of 1958, 1959, and as an Associate Engineer during the Summer of 1962; employed by Texas Technological College, Lubbock, as a dormitory counselor, September-January, 1962, employed as a graduate assistant, Oklahoma State University, Stillwater, during the periods of January-May, 1962 and September, 1962-June, 1963.

Organizations, Honors, and Awards: American Society of Testing Materials, Pi Eta Sigma, Phi Kappa Phi, Tau Beta Pi, Graduated with Honors, 1962.